

การศึกษาหาขึ้นที่เป็นสาเหตุของภาวะด้านมไม่เจริญและเนื้อเยื่อชั้นนอกเจริญผิดปกติ



นางสาว สุรัสวดี อัครรัตน์

ศูนย์วิทยทรัพยากร
จุฬาลงกรณ์มหาวิทยาลัย

วิทยานิพนธ์นี้เป็นส่วนหนึ่งของการศึกษาตามหลักสูตรปริญญา วิทยาศาสตร์ดุขฎีบัณฑิต

สาขาวิชาชีวเวชศาสตร์ (สหสาขาวิชา)

บัณฑิตวิทยาลัย จุฬาลงกรณ์มหาวิทยาลัย

ปีการศึกษา 2552

ลิขสิทธิ์ของจุฬาลงกรณ์มหาวิทยาลัย

IDENTIFICATION OF A GENE RESPONSIBLE FOR
BILATERAL AMASTIA WITH ECTODERMAL DYSPLASIA

Miss Surasawa dee Ausavarat

ศูนย์วิทยทรัพยากร
จุฬาลงกรณ์มหาวิทยาลัย

A Dissertation Submitted in Partial Fulfillment of the Requirements
for the Degree of Doctor of Philosophy Program in Biomedical Sciences
(Interdisciplinary Program)

Graduate School

Chulalongkorn University

Academic Year 2009

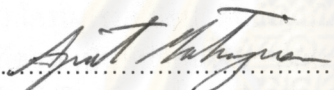
Copyright of Chulalongkorn University

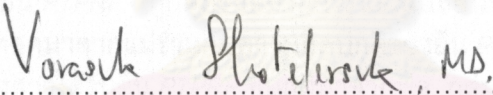
Thesis Title IDENTIFICATION OF A GENE RESPONSIBLE FOR BILATERAL
AMASTIA WITH ECTODERMAL DYSPLASIA
By Miss Surasawadee Ausavarat
Field of Study Biomedical Sciences
Thesis Advisor Professor Vorasuk Shotelersuk, M.D.
Thesis Co-advisor Assistant Professor Kanya Suphapeetiporn, M.D., Ph.D.
Thesis Co-advisor Verayuth Praphanphoj, M.D.

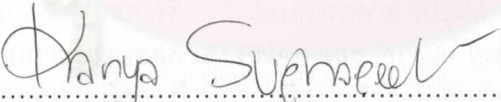
Accepted by the Graduate School, Chulalongkorn University in Partial Fulfillment of
the Requirements for the Doctoral Degree

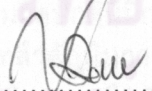
..... Dean of the Graduate School
(Associate Professor Pornpote Piumsomboon, Ph.D.)

THESIS COMMITTEE

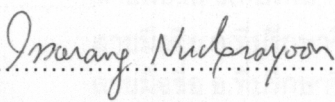
..... Chairman
(Professor Apiwat Mutirangura, M.D., Ph.D.)

..... Thesis Advisor
(Professor Vorasuk Shotelersuk, M.D.)

..... Thesis Co-Advisor
(Assistant Professor Kanya Suphapeetiporn, M.D., Ph.D.)

..... Thesis Co-Advisor
(Verayuth Praphanphoj, M.D.)

..... External Examiner
(Associate Professor Duangrurdee Wattanasirichaigoon, M.D.)

..... Examiner
(Associate Professor Issarang Nuchprayoon, M.D., Ph.D.)

สุรัสวดี อิศวรรณ์ : การศึกษาหาชิ้นที่เป็นสาเหตุของภาวะเต้านมไม่เจริญและเนื้อเยื่อ
ชั้นนอกเจริญผิดปกติ (Identification of a gene responsible for bilateral amastia with
ectodermal dysplasia) อ. ที่ปรึกษาวิทยานิพนธ์หลัก: ศ. นพ. วรศักดิ์ โชติเลอศักดิ์
อ.ที่ปรึกษาวิทยานิพนธ์ร่วม: ผศ.พญ.ดร.กัญญา สุภปีดิพร, อ.นพ.วีรยุทธ ประพันธ์พจน์,
103 หน้า

สิ่งหนึ่งที่ทำให้มนุษย์ซึ่งเป็นสัตว์เลี้ยงลูกด้วยนมต่างจากสัตว์อื่นคือ การมีเต้านม (breast and mammary glands) อย่างไรก็ตาม องค์ความรู้เกี่ยวกับการเจริญและพัฒนา (growth and differentiation) ของเต้านมมนุษย์ยังมีจำกัดมาก วิธีหนึ่งในการศึกษาคือ ศึกษาผู้ที่มีความผิดปกติของเต้านมตั้งแต่เกิด ภาวะเต้านมไม่เจริญร่วมกับเนื้อเยื่อชั้นนอกเจริญผิดปกติ (bilateral amastia with ectodermal dysplasia) เป็นภาวะที่เหมาะสมอย่างยิ่งในการศึกษาเพื่อหาปัจจัยที่จะมีผลต่อการเจริญเติบโตของเต้านม แต่ข้อจำกัดคือ ผู้ที่มีภาวะดังกล่าวนี้มีน้อยมาก จากรายงานทั่วโลกพบอุบัติการณ์การเกิดโรคเพียง 1 ราย ในทุกๆ 3 ปี และในประเทศไทยยังไม่เคยมีรายงานโรคนี้มาก่อน คณะผู้วิจัยได้ทำการศึกษารายกรณีในผู้ป่วยหญิงไทย 1 ราย พบว่าโครโมโซมมีลักษณะ 46,XX,t(1;20)(p34.1;q13.13) ซึ่งมีการแลกเปลี่ยนชิ้นส่วนของโครโมโซมระหว่าง 1p34.1 และ 20q13.13 โครโมโซมที่ผิดปกตินี้ยังพบในแม่ พี่สาว และน้องสาวซึ่งมีการเจริญของเต้านมที่ปกติ อย่างไรก็ตาม เป็นที่น่าสนใจว่าจุดตัดบนโครโมโซมที่ 1 นั้นตัดผ่านยีน *PTPRF* ในขณะที่จุดตัดบริเวณโครโมโซมที่ 20 นั้น ไม่มียีนใดอยู่เลย ผู้วิจัยตั้งสมมติฐานว่า ลักษณะที่พบในผู้ป่วยเกิดจากการที่ยีน *PTPRF* ถูกตัดขาดจากการแลกเปลี่ยนของโครโมโซมซึ่งโครโมโซมดังกล่าวได้รับการถ่ายทอดมาจากแม่ร่วมกับความผิดปกติของยีน *PTPRF* ที่ได้รับมาจากพ่อ ในขณะที่พี่สาวและน้องสาวได้รับยีน *PTPRF* ที่ปกติมาจากพ่อ กลุ่มผู้วิจัยได้ตรวจหาการกลายพันธุ์ของยีน *PTPRF* ในผู้ป่วยชาวไทยและผู้ป่วยต่างประเทศซึ่งมีการรายงานเกี่ยวกับลักษณะดังกล่าวมาก่อนหน้านี้อีก 2 ราย ผลการศึกษาไม่พบการกลายพันธุ์ที่สำคัญต่อการเกิดโรค อย่างไรก็ตาม การศึกษาเกี่ยวกับการแสดงออกของ RNA และ Protein ในผู้ป่วย พบว่า มีระดับลดลงอย่างเห็นได้ชัด เมื่อเทียบกับแม่ พี่สาว ซึ่งมีความผิดปกติของโครโมโซมแบบเดียวกัน ข้อมูลจากการศึกษา Haplotype สนับสนุนว่าผู้ป่วยได้รับ allele จากพ่อแตกต่างจากพี่น้องที่ปกติ ผลการศึกษานี้ทำให้ผู้วิจัยคาดว่าความผิดปกตินี้มีการถ่ายทอดแบบลักษณะด้อย การศึกษานี้ช่วยสนับสนุนว่ายีน *PTPRF* มีบทบาทสำคัญในการเจริญของเต้านมมนุษย์ ทั้งยังทำให้เกิดความเข้าใจเกี่ยวกับวิวัฒนาการของยีนที่มีบทบาทในสัตว์เลี้ยงลูกด้วยนมนอกจากนี้ การที่ยีน *PTPRF* เกี่ยวข้องกับกระบวนการเกิดมะเร็งเต้านม การศึกษาถึงหน้าที่ของยีนนี้อาจจะนำไปสู่ความเข้าใจในกระบวนการเกิดมะเร็งเต้านมอีกด้วย

สาขาวิชา ชีวเวชศาสตร์.....ลายมือชื่อนิสิต.....สุรัสวดี อิศวรรณ์
ปีการศึกษา 2552.....ลายมือชื่อ อ.ที่ปรึกษาวิทยานิพนธ์หลัก.....
ลายมือชื่อ อ.ที่ปรึกษาวิทยานิพนธ์ร่วม.....
ลายมือชื่อ อ.ที่ปรึกษาวิทยานิพนธ์ร่วม.....

4789698620: MAJOR BIOMEDICAL SCIENCES

KEYWORDS: amastia / athelia / development of breasts and nipples / ectodermal dysplasia / kidney agenesis / chromosomal balanced translocation / PTPRF / LAR.

SURASAWADEE AUSAVARAT: IDENTIFICATION OF A GENE RESPONSIBLE FOR BILATERAL AMASTIA WITH ECTODERMAL DYSPLASIA. THESIS ADVISOR: PROF. VORASUK SHOTELERSUK, M.D., THESIS CO-ADVISOR: ASST. PROF. KANYA SUPHAPEETIPORN, M.D., Ph.D., VERAYUTH PRAPHANPHOJ, M.D., 103 pp.

Although protein tyrosine phosphatase receptor type F (PTPRF) has been known to involve in human breast cancer and mouse mammary gland development, very little is known about its role in human mammary gland development. We identified a 18-year old Thai woman with bilateral absence of breasts and nipples, ectodermal dysplasia, and unilateral renal agenesis, who was found to have an inherited chromosomal balanced translocation, 46,XX,t(1;20)(p34.1;q13.13). High Density SNP-CGH Array analysis confirmed the normal DNA dosage. With fluorescent in situ hybridization analysis, the breakpoint on chromosome 1 was identified to interrupt the *PTPRF* gene. Although no apparent causative mutations or splicing defects were detected in the other allele of *PTPRF*, deficiency of its RNA and absence of its protein levels strongly suggest its involvement in the organs' development. The proband's unaffected mother and sisters, although harbored the same balanced translocated chromosome, did have a significant remaining level of PTPRF. Microsatellite analysis showed that the proband and her sisters inherited a different paternal chromosome. These findings suggest that the syndrome is inherited in an autosomal recessive manner. We, for the first time, present evidences that PTPRF plays an important role in human breast development. This finding could have implications on evolution of mammals, developmental biology of human mammary glands and malignancy of breast cancer.

Field of study: Biomedical Sciences Student's signature: Surasawadee Ausavarat
 Academic year: 2009 Advisor's signature: Vorasuk Shotelersuk
 Co-Advisor's signature: Kanya Suphapeetiporn
 Co-Advisor's signature: Verayuth Praphanphoj

ACKNOWLEDGEMENTS

I would like to express my deepest appreciation to my advisor, Professor Vorasuk Shotelersuk, my co-advisor Dr.Verayuth Praphanphoj and Assistant professor Kanya Suphapeetiporn for their guidance, understanding, patience, and most importantly, their invaluable supervisions during my graduate studies. They encouraged me to not only grow as an experimentalist but also as an instructor and an independent thinker.

Most importantly, special thanks are extended to the patient and her family for participation in this study. I am also grateful to Drs. Silvia Castillo Taucher, Guillermo Lay-Son and Prof.Dr.Frits A.Beemer for sending us their patients DNA and dealing with the patients included in this study. I really appreciate their great collaboration.

I would like to thank my entire research group at the Center of Excellence for Medical Genetics especially Ms.Siraprapa Tongkobpetch for their friendship, moral support, help and many advices. Special thanks to all members of Center for Medical Genetics Research at Rajanukul Institute. Thanks to Ms. Supranee Buranapraditkun for technical help in EBV-transformed cell line. Moreover, I would like to take this opportunity to thank Dr. William A Gahl, Dr.Thomas C. Markello, Dr.David Adams and members of his group at the National Human Genome Research Institute, National Institutes of Health in Bethesda, Maryland whose lab I worked for a short duration but with where I gained a lot of experiences, friendship and research inspiration.

I am as ever, especially indebted to my mother and aunt, Mrs Suwannee Ausavarat and Ms.Pranee Nantasenammat for their love and moral support throughout my life. Moreover, I thank my friend, Patra Yeetong, who endured and survived the experience of graduate school and provided me with unending encouragement and support.

Financial support was provided by the Royal Golden Jubilee Ph.D. program, Center of excellence for Medical Genetics, Chulalongkorn University, the 90th Anniversary of the Chulalongkorn University fund (Ratchadaphiseksomphot Endowment Fund), Biotech, and the Thailand Research Fund.

CONTENTS

	PAGE
ABSTRACT (THAI).....	IV
ABSTRACT (ENGLISH).....	V
ACKNOWLEDGEMENTS.....	VI
CONTENTS.....	VII
LIST OF TABLES.....	XI
LIST OF FIGURES.....	XIII
LIST OF ABBREVIATIONS.....	XVI
CHAPTER I: INTRODUCTION	1
Background and Rationale.....	1
Research Questions.....	3
Objectives.....	3
Hypotheses.....	3
Key Words.....	3
Expected Benefit.....	3

Research Methodology.....	4
Conceptual Framework.....	5
CHAPTER II: REVIEW OF RELATED LITERATURE.....	6
Embryonic mammary gland development.....	6
Hormone regulation of mammary cell fate.....	13
Review case reported with bilateral absence of breast.....	15
Chromosomal translocation; short cut to locate a disease gene.....	21
PTPRF; a candidate gene responsible for breast development.....	24
Functional significance of PTPRF (LAR) in development.....	26
CHAPTER III: MATERIALS AND METHODS.....	30
Subjects and clinical descriptions.....	30
Establishment of EBV-immortalization of human B-lymphocytes.....	32
Chromosome Analysis by Giemsa Staining.....	33
BAC/PAC clone preparation.....	34
Generation of subfragment probe by Long-template PCR.....	34

Probe Labeling by Nick Translation.....	35
Fluorescence in situ hybridization.....	36
DNA Extraction and RNA Extraction.....	40
Reverse Transcription PCR.....	41
Mutation Analysis.....	42
Detection of abnormal splicing fragment by amplification of cDNA.....	43
Quantitative Real-Time PCR.....	46
Western Blot Analysis.....	48
Haplotype Analysis.....	49
PTPRF Gene Phylogeny.....	51
Identification of other submicroscopic chromosomal imbalances.....	53
CHAPTER IV: RESULTS.....	54
Chromosomal translocation in the proband and family members.....	54
FISH analysis with breakpoint spanning clones.....	57
Schematic of the breakpoint and PTPRF gene.....	61

Quantitative RT-PCR of PTPRF expression.....	62
Absence protein expression in proband.....	63
Mutation analysis of the <i>PTPRF</i> gene.....	64
No overlapping chromosomal aberrations in three patients	67
Haplotype analysis.....	70
PTPRF gene phylogeny in mammals and non mammals	71
CHAPTER V: DISSCUSSION.....	74
REFERENCES.....	80
APPENDICES.....	93
Appendix A: Buffer and Reagents.....	94
Appendix B: Glossary.....	102
BIOGRAPHY.....	103

LIST OF TABLES

XI

TABLE	PAGE
1. Genetics pathways controlling mammary gland development.....	14
2. Review reported case with bilateral absence of breast	18
3. Example of disease associated balanced chromosomal rearrangements	23
4. Component for Nick translation	35
5. Component for probe precipitation.....	36
6. List of BAC/PAC clones for Fluorescence <i>in situ</i> hybridization	37
7. List of Primers for generation of fragmented probe	39
8. List of Primers for amplification of genomic DNA of PTPRF	44
9. List of Primers for amplification of complementary DNA of PTPRF	46
10. Real-Time PCR Components for PTPRF Gene	47
11. Real-Time PCR Components for GAPDH Gene	47
12. List of TaqMan Probes in Quantitative Real-Time experiment	47
13. Description of Taqman Probe for GAPDH in Quantitative RT-PCR	48
14. List of Microsatellite Markers selected from Mapviewer	50

TABLE	PAGE
15. List of Microsatellite Markers for chromosome 1	50
16. List of PTPRF cDNA sequence from NCBI and ensembl	52
17. Summary of FISH results from chromosome 1.....	59
18. Summary of FISH results from chromosome 20.....	60
19. Summary of FISH results from subfragment probe	61
20. Summary of polymorphisms found in three patients.....	65
21. Summary results of our patient, her family members and unrelated patients...	66



ศูนย์วิทยุทรัพยากร
จุฬาลงกรณ์มหาวิทยาลัย

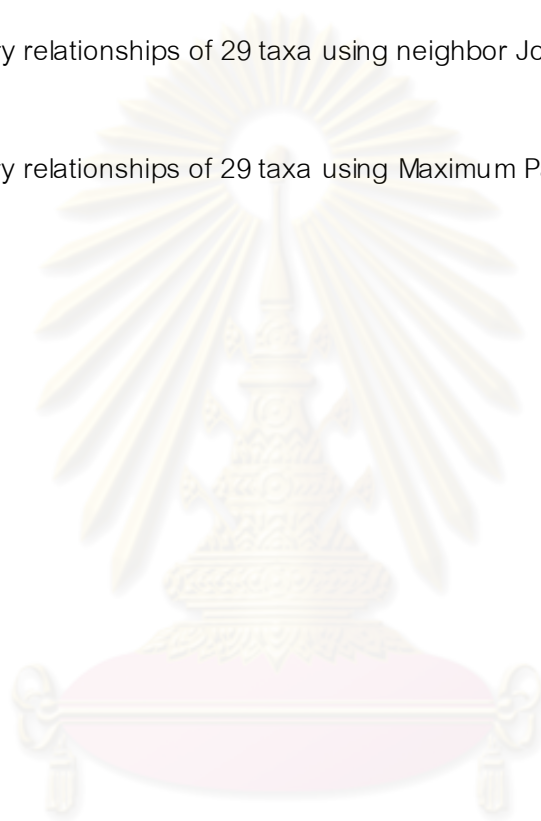
FIGURE	PAGE
1. Chromosome analysis of the proband	2
2. Signaling molecules that regulate mammary gland	7
3. Signaling molecules that regulate positioning of the mammary bud	9
4. Morphological stages in embryonic development of the mammary gland	11
5. Hormones and genes that control development of mammary gland.....	13
6. Main steps in positional cloning of genetic disorders	22
7. Relationship of PTPRF exon structure and protein domain	24
8. Proteolytic Cleavage of LAR-RPTP.....	25
9. Schematic of LAR alternatively spliced element	29
10. Clinical features of patient	30
11. Family pedigree	31
12. Clinical manifestation of patient from Chile	31
13. Clinical manifestation of patient from Netherland with AREDYLD	32
14. Chromosome analysis of the proband	54

FIGURE	PAGE
15. Chromosome analysis of the younger sister	55
16. Chromosome analysis of the elder sister	55
17. Chromosome analysis of the mother	56
18. Chromosome analysis of the elder brother	56
19. Pedigree of family members.....	57
20. FISH of RP5-1029K14 giving split signal from chromosome 1	58
21. FISH of RP5-991B18 giving split signal from chromosome 20	58
22. Schematic representation of the breakpoint and <i>PTPRF</i> on chromosome 1	61
23. Schematics of <i>PTPRF</i>	62
24. Quantitative real-time PCR Results.....	63
25. Western blot results.....	64
26. 1M SNP Array result of Thai Patient.	67
27. 1M SNP Array result of patient from Chile..	68
28. 1M SNP Array result of patient from Netherlands.....	69

29. Haplotype analysis of chromosome1 of family members carried balanced translocation.....70

30. Evolutionary relationships of 29 taxa using neighbor Joining model..... 71

31. Evolutionary relationships of 29 taxa using Maximum Parsimony model.....72



ศูนย์วิทยทรัพยากร
จุฬาลงกรณ์มหาวิทยาลัย

LIST OF ABBREVIATIONS

AD	Autosomal Dominant
ALMS1	Alstrom syndrome 1
AR	Autosomal Recessive
AREDYLD	Acral-renal-ectodermal-dysplasia-lipoatrophic-diabetes
BAC	Bacterial Artificial Chromosome
BCA	Bicinchoninic Acid
BLAST	Basic Local Alignment Search Tool
cDNA	Complementary DNA
CDS	Coding Sequence
CpG	cytosine and guanine separated by a phosphate
DNA	Deoxyribonucleic acid
EBV	Epstein-Barr Virus
FISH	Fluorescence <i>in situ</i> hybridization
GAPDH	Glyceraldehyde 3-phosphate dehydrogenase
HRP	Horseradish peroxidase
IgG	immunoglobulin G
LAR	Leukocyte-related common antigen receptor
MEM	Modified Eagle Medium
miRNA	microRNA
mRNA	Messenger RNA
PAC	P1 Artificial Chromosome
PBS	Phosphate Buffer Saline
PCR	Polymerase Chain Reaction
PTPRF	Protein Tyrosine Phosphatase Receptor Type F

PVDF	Polyvinylidene fluoride
RIPA	Radioimmunoprecipitation Assay
RNA	Ribonucleic Acid
ROX	6-Carboxyl-X-Rhodamine
rpm	Round per minute
RPMI	Roswell Park Memorial Institute
SDS-PAGE	Sodium Dodecyl Sulfate Polyacrylamide Gel Electrophoresis
SEM	Standard error of Measurement
SNP	Single Nucleotide Polymorphism
SSC	Saline Sodium Citrate Buffer
WAGR	Wilms Tumor, Aniridia, Genitourinary Anomalies, and Mental Retardation Syndrome



ศูนย์วิทยทรัพยากร
จุฬาลงกรณ์มหาวิทยาลัย

CHAPTER I

INTRODUCTION

Background and Rationale

Mammary gland makes mammals different from other organisms. Although excellent progress has recently been made in defining the signaling pathways that are involved in the mammary gland development in mice, current knowledge about human mammary gland development is very restricted and still has to be elucidated. Patients with aberrant breast development are the most suitable and valuable to identify a gene involved in human breast development. Amastia is the complete absence of breast which is the result of complete failure of mammary ridge to develop at about 6 weeks in utero (1). This condition is a very rare congenital anomaly with a wide range of associated features. It is inherited as either autosomal dominant or recessive pattern. Amastia is characterized by the absence of the breast and nipple-areolar complex at birth. In addition, there is a lack of breast development during puberty whereas other secondary sexual characters and fertility are normal (1, 2). In 1965 Trier (2) reviewed the literature and found 43 cases of congenital breast absence and classified them into three groups as follows;

- (i) Bilateral absence of breast associated with congenital ectodermal defect.
- (ii) Unilateral absence of the breast associated with the absence of pectoralis major muscles called Poland syndrome.
- (iii) Bilateral absence of breast with variable associated defects.

Amastia may be isolated, syndromic, familial or embryopathic. The syndromes described with amastia are as follows;

- Ectodermal dysplasia, Trichoodontoonychial type (3, 4)
- Congenital amastia with polywhorls and webbed fingers (5)
- Acral-renal-ectodermal-dysplasia-lipoatrophic-diabetes (AREDYLD syndrome) (6, 7)
- Bilateral amastia with ureteral triplication and dysmorphism (8)
- Amastia with vaginal agenesis (9)
- Scalp-ear-nipple syndrome, Finlay-Marks syndrome (10-18)

In familial cases, both autosomal dominant and autosomal recessive inheritances have been reported. Embryopathic amastia has been reported in a girl infant born to a woman treated with methimazole and propranolol (19). The treatment of amastia requires total breast reconstruction. The cause of this condition is still unknown.

Here we reported a 29-year-old female who had complete absence of both breasts and nipples along with other defects, including ectodermal dysplasia and unilateral renal agenesis. Conventional cytogenetic analysis revealed an apparently reciprocal balanced translocation, 46, XX, t(1;20)(p34.1;q13.13).

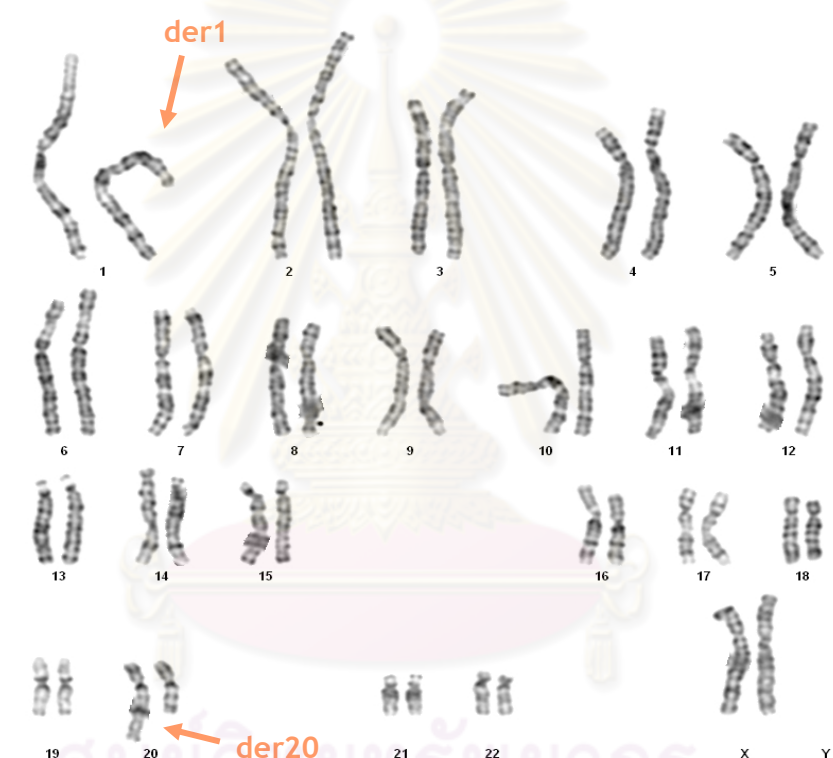


Figure 1. Chromosome analysis of the proband showing apparently reciprocal balanced translocation, 46XX, t(1,20)(p34.1;q13.13)

Balanced translocation chromosome region(s) have been used to identify a disease-associated gene due to disruption or otherwise inactivation of a gene(s) in the breakpoint. We hypothesized that a gene was interrupted by one of the breakpoints which caused the phenotype. Here we performed the clinical, cytogenetic and molecular characterization of the patient with bilateral amastia and ectodermal dysplasia

who had balanced translocation. We mapped the breakpoint and identified the responsible gene. The expression of that gene from the patient was determined.

Research question

1. Which gene(s) is interrupted by the breakpoints?
2. Is the identified gene responsible for the disorder in our patient?
3. Is the identified gene responsible for amastia in other unrelated patients?

Objective

1. To identify the gene responsible for bilateral amastia with ectodermal dysplasia.
2. To provide supporting evidence that the gene identified has an important role in breast development.

Hypotheses

1. One of the chromosome breakpoints causes the disease.
2. Both of the breakpoints associate with the disease.
3. The finding is coincidental. No gene is interrupted by any of the breakpoints.
4. The expression of the adjacent gene(s) could be altered due to a putative position effect caused by the translocation.

Research design

Descriptive and *in vitro* studies

Key words

Amastia, athelia, development of breasts and nipples, ectodermal dysplasia, kidney agenesis, chromosomal balanced translocation, PTPRF, LAR

Ethical consideration

The local Ethics Committee has approved this study. Written informed consent was obtained from all patients or their parents who participated in this experiment.

Expected benefit

1. To further elucidate the genes and pathways involved in breast development.
2. To provide accurate information and appropriate counseling for families with the disease.

Research methodology

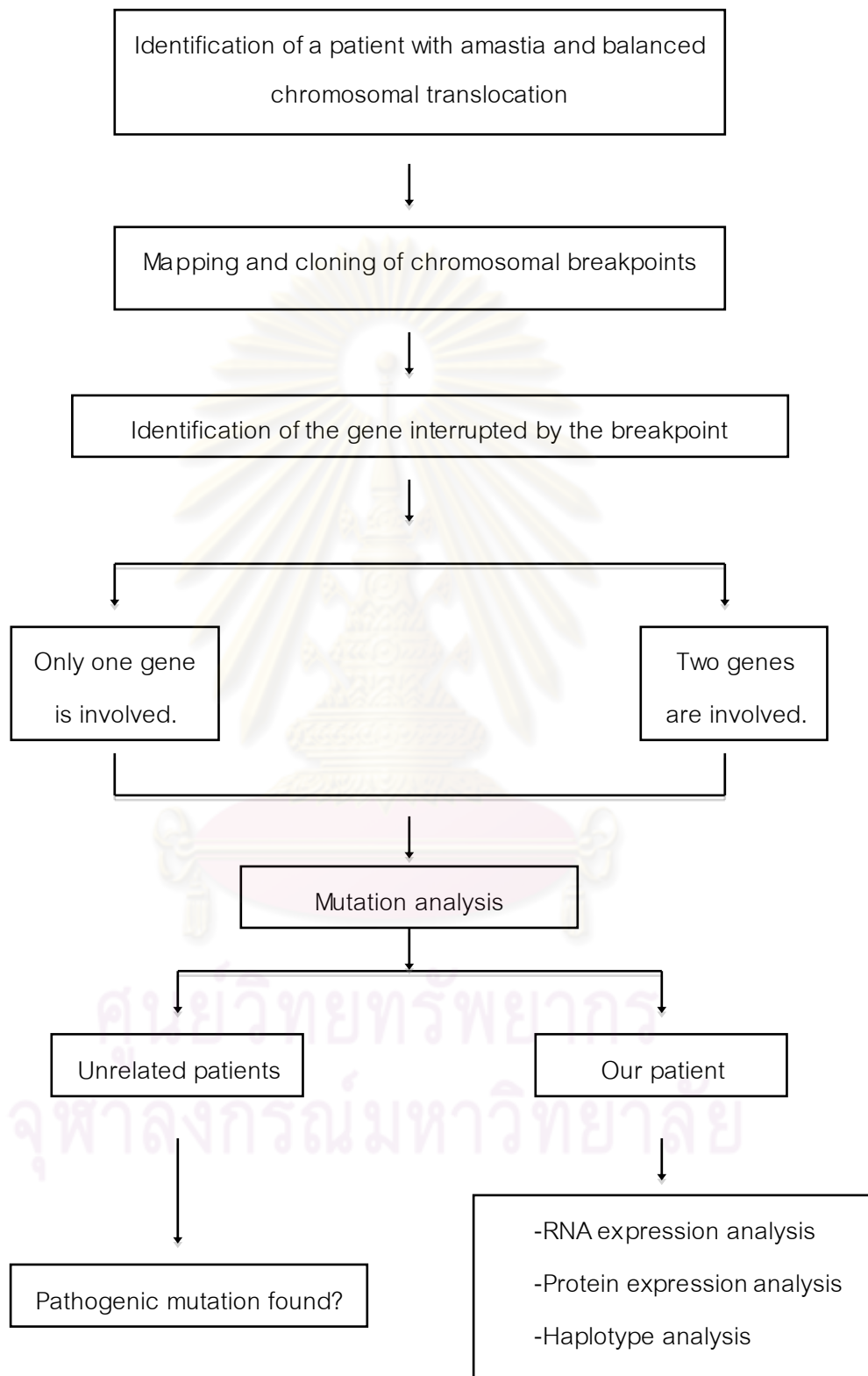
To map the balanced translocation of t(1;20)(p34.1;q13.13) in the patient, we used both molecular genetic and cytogenetic techniques to characterize the breakpoints. BAC and PAC clones were obtained from the BACPAC Resources Center (BPRC). In order to amplify larger (approximately 10-20 kb) BAC/PAC subfragments, the long template PCR system was used. A series of primer pairs were chosen from the genomic sequence of breakpoint-spanning clones. Genomic BAC/PAC DNAs and their long-range PCR products were labeled with spectrum orange dUTP by standard nick translation. FISH was performed on metaphase spreads using standard molecular cytogenetic techniques.

From cytogenetic investigation, we were able to narrow down the breakpoint on chromosome 1 into 10 kb. This 10 kb critical region interrupts the gene called protein tyrosine phosphatase, receptor type, F (*PTPRF*) while the breakpoint of chromosome 20 does not disrupt any known gene. *PTPRF* is a member of the protein tyrosine phosphatase (PTP) family.

To validate *PTPRF* as a candidate gene for bilateral amastia, we established EBV-transformed lymphoblastoid cell cultures for quantitative Real-time PCR and western blot analysis. Peripheral blood lymphocytes (B-lymphocytes) were immortalized successfully by infecting them with Epstein Barr Virus (EBV). These cells could then be used as a source of DNA or RNA for studying genomic structures and expression, respectively.

We then attempted to find the pathogenic mutation in the *PTPRF*. We performed mutation screening of the *PTPRF* gene in our patient and two other unrelated patients from Netherlands (6) and Chile (20). We screened the mutations in the promoter, coding sequences and proximal intronic sequences by PCR-direct sequencing. DNA sequence analysis was performed using the genome BLAST program. To identify other submicroscopic chromosomal imbalances, such as duplications, deletion or copy-neutral variants, we used 1M SNP Array to search for such alterations in three unrelated patients. We also performed haplotype analysis using a set of microsatellite markers to study the allele segregation in our Thai family.

Conceptual framework



CHAPTER II

REVIEW OF RELATED LITERATURE

Embryonic mammary gland development

A number of recent studies using human and mouse genetics, in particular targeted gene deletion and transgenic expression, have identified some of the signals that control specific steps in development. Most of the genes were obtained from the studies of mouse models. Studying these defects in mouse models will provide a better understanding of the aetiology of the corresponding human syndromes.

Mammary glands are highly modified sweat glands. Development of mammary glands begins in embryogenesis and continues well into adult life, when functional development and differentiation occur. The embryonic phase of mammary gland development involve in regulatory mechanisms that are also found in other skin appendages. In contrast to embryonic phase, mammary gland developments in adult stages are nearly controlled by hormones. Breast embryogenesis takes place in several stages including milk line initiation, placode formation, bud formation and rudimentary ductal tree. Each stage is relatively flexible and some of the stages may overlap.

In most mammals the first step in mammary gland development is marked by a lateral ectodermal thickening that protrudes slightly from the body wall. The mammary ridges develop at fourth week on the ventral body of embryos and extend from the axillary to the inguinal regions bilaterally. The formation of bilateral milk lines in the mouse occurs embryonic day (E) 10.5. In mouse studies, specification of the mammary line is dependent on canonical Wnt signaling (wingless-related MMTV integration site) (21). One of the earliest described markers of the mammary line is the expression of a Wnt responsive β -galactosidase (TOPGAL) transgene in cells between the limb buds of E10.5 TOPGAL transgenic embryos. Following this, several Wnt genes become expressed within the mammary line between E11.25 and E11.5, including Wnt10b, Wnt10a, and Wnt6 (21-23). These findings suggest that specification of the mammary line requires an early Wnt signaling event that is then responsible for inducing a cascade of further Wnt gene expression and Wnt signaling within the milk line and placodes.

Studies of fibroblast growth factor (FGF) indicated that FGF signaling pathway may also contribute to mammary line specification. Knockout of the *Fgf10* and *Fgfr2b* genes in mice has been shown to disrupt the formation of four out of the five mammary placodes (24). Between E10.5 and E11.5, *Fgf10* is expressed in the most ventral-lateral reaches of the dermatomyotome of the somites adjacent to the developing mammary line.

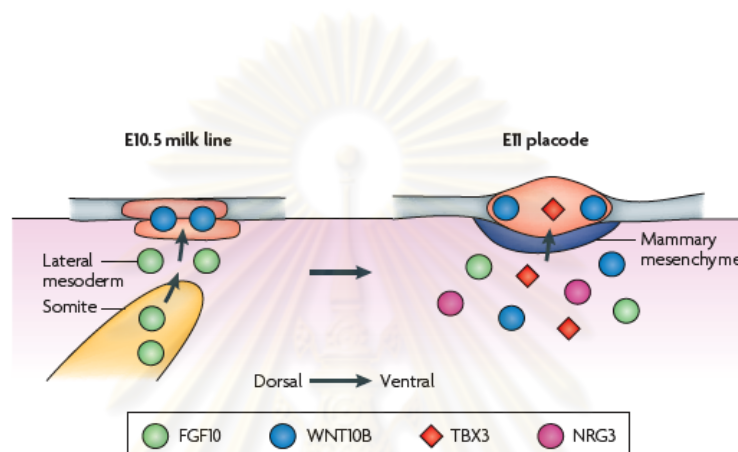


Figure 2. Signaling molecules that regulate mammary line initiation and placode formation. The proteins are expressed during formation of milk line (left) and placode (right) (25)

It has been shown that inhibition of Wnt signaling does not alter expression of FGF10 or FGFR1 signaling (21, 22). These data suggest that FGF signaling is important to the earliest stages of mammary development and acts in parallel to Wnt signaling, rather than downstream of it. Mammary gland aplasia or hypoplasia is a prominent feature of the mammary-ulnar syndrome, caused by mutations in the *TBX3* gene, which encodes a T-box transcription factor (26, 27). *Tbx3*^{-/-} mice exhibit no morphologic evidence of mammary placodes and do not show evidence of Wnt10b or lymphoid enhancing factor (*Lef*) 1 expression, two molecular markers of mammary placodes (27). So, it is evident that *TBX3* is important for placode formation.

A working model that combines these findings is shown in Figure 2 (25). Specification of the mammary line would be the result of FGF signals from the somite acting together with canonical Wnt signaling initiated by generally expressed Wnts in the

ectoderm and causes the stratification of the ectoderm to form a placode. FGF, WNT and NRG3 (neuregulin 3) signals from the lateral mesoderm induce expression of *Tbx3* (T-box 3) in the epithelium of the placode. This dual signal would activate TBX3 expression, which in turn initiates the expression of other Wnt and FGF pathway genes necessary for mammary line development and the transition to placode formation. In this manner TBX3 would be both downstream and upstream of Wnt and FGF signaling, which is a known paradigm for T-box transcription factors.

The second stage occurs by E11.5, when five pairs of lens shaped placodes form at specific locations along the mammary line. Placodes are thought to arise from the migration of cells within the mammary line, although this has yet to be formally documented. Individual placodes form in a characteristic sequence; pair 3 is first, followed by pairs 4, 1 and 5, and finally by pair 2. The same signaling pathways that have been implicated in the specification of the mammary line are also important for the development of the mammary placodes. TOPGAL transgene expression and Wnt10b expression have been reported to become discontinuous within the mammary line and localize to the forming placodes (21, 22).

The placodes are thought to form from cell movements within the mammary line, and in TOPGAL embryos individual drifting β -galactosidase positive cells can be seen clustering around the developing placodes (21). In cultured embryos, activation of Wnt signaling using lithium chloride or Wnt3a results in the accelerated formation of enlarged mammary placodes (21). Finally, *Lef1*^{-/-} embryos form smaller placodes that then degenerate (28, 29). Wnt signaling is known to modulate cell adhesion and promote cell migration in other settings, and so it is attractive to postulate that Wnts might be involved in promoting the cell migration and invagination necessary for the formation of placodes.

As noted in the section above, the Fgf receptor, FGFR2b is expressed within the developing mammary placodes, and disruption of this gene in mice inhibits the development of four pairs of placodes (24). In addition, Fgf4, Fgf8, Fgf9, and Fgf17 are all expressed within the developing placodes, as is another Fgf receptor, FGFR1 (22). In cultured embryos, beads soaked with Fgf8 have been shown to induce the ectopic expression of placodal markers when placed along the mammary line, and an FGFR1

inhibitor has been shown to inhibit the development of placodes from the mammary line (22). Thus, it is likely that FGF signaling participates in regulating this process. TBX3 and the related T-box family member TBX2 are both expressed at E11.5 in developing placodes (27). However, the phenotype of the *Tbx3* knockout mice suggests that TBX2 and TBX3 have nonoverlapping functions. Interestingly, TBX2 has been shown to regulate adhesion molecules such as cadherins and integrins (30), and so it is possible that TBX2 may contribute to the migration and invagination of the mammary epithelial cells during placode formation.

More recently, *TBX3* has been shown to determine the dorso-ventral position of mammary buds together with bone morphogenetic protein 4 (*BMP4*) (31). At E10.5 TBX3 and BMP4 are expressed in strips that run between the limb buds in partially overlapping and complementary patterns. Inhibition of BMP signaling through application of bead soaked with the inhibitor Noggin extinguishes *Lef1* expression. These observations suggest a model for positioning of placodes along the dorso-ventral axis in which TBX3 and BMP4 interact in regulating localized expression of *Lef1*.

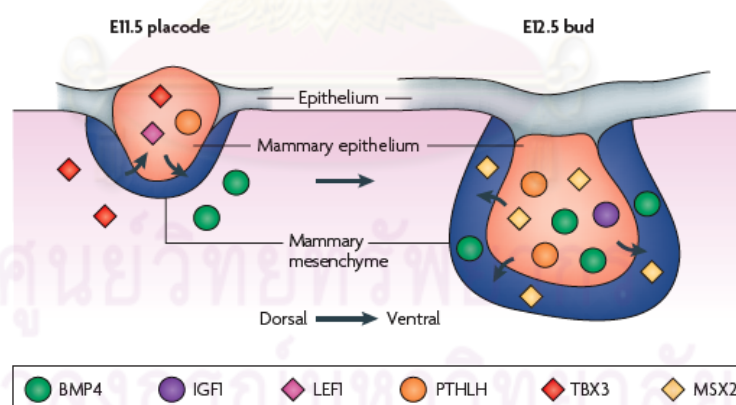


Figure 3. Signaling molecules that regulate dorso-lateral positioning of the mammary bud and formation of the dense mammary mesenchyme (25).

The third stage involves the invagination of cells within the placode into the underlying mesenchyme to form the typical bulb-shaped mammary buds and occurs between E11.5 and E12.5 (Figure 3). Part of this process involves the condensation and

differentiation of the underlying mesenchyme into specialized, dense mammary mesenchyme arrayed radially around the epithelial bud. A growing number of signaling molecules have been described as being expressed within either the epithelial or mesenchymal cells of the mammary bud.

The homeodomain-containing transcription factors MSX1 and MSX2 are both expressed in the mammary buds, and MSX2 is also expressed in the underlying mesenchyme (32, 33). Knockout of either *Msx1* or *Msx2* alone has no effects on mammary bud formation, although knockout of *Msx2* does affect the next phase of mammary development. However, when both genes are disrupted, placodes form but do not develop into mammary buds (33). Thus, MSX1 and MSX2 appear to have necessary but redundant functions during the formation of the buds. One of the molecules expressed by the mammary epithelial bud as it starts to invaginate into the mesenchyme is parathyroid hormone-related protein (PTHrP). Its receptor, PTH1R, is expressed in the mesenchyme underlying the developing bud (34, 35). If either PTHrP or the PTH1R is disrupted in mice, then morphologically normal mammary buds form but they degenerate and never grow out to form ductal trees (34, 35). This is because PTHrP is necessary for the mesenchyme to acquire a specialized mammary fate. When this does not occur, the mammary epithelial cells take on an epidermal fate, undergo squamous differentiation and morphogenesis fails. Another consequence is the loss of sexual dimorphism, because PTHrP is the epithelial factor that induces androgen receptor expression within the mammary mesenchyme (36). PTHrP signaling is also necessary for the mammary mesenchyme to induce the overlying epidermis to form the nipple. Thus, in *PTHrP* knockout mice, no nipples were formed, and when PTHrP was overexpressed in the epidermis, the entire ventral surface of the embryo was transformed into nipple skin (34-36).

In female embryos, the buds remain morphologically quiescent until the final stages of embryonic development begin at E15.5–E16.5. At this point, the mammary epithelial cells begin to proliferate, and the bud sprouts down out of the dense mesenchyme and into the developing mammary fat pad located within the dermis. Concurrent with this process, epidermal cells overlying the bud differentiate into nipple

skin. Once the mammary sprout has reached the fat pad, it begins a process of ductal branching morphogenesis that gives rise to the rudimentary ductal tree, consisting of a primary duct and 15–20 secondary branches, which is present at birth (37).

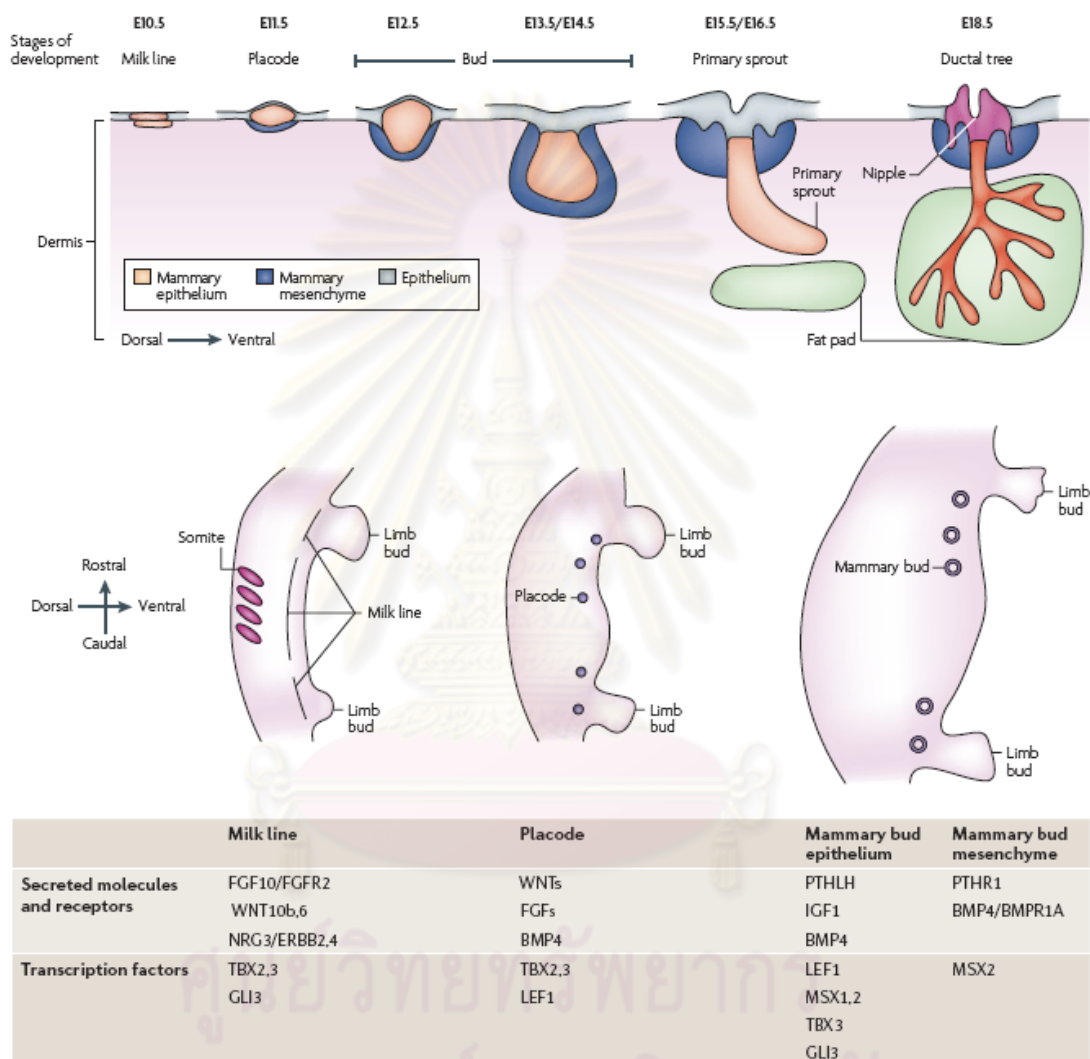


Figure 4. Morphological stages in embryonic development of the mammary gland (25).

The initial branching morphogenesis of the embryonic mammary gland is hormone independent because mice that are deficient in either estrogen receptor (α or β), the prolactin receptor, the growth hormone receptor, or the progesterone receptor have no obvious embryonic mammary phenotype (38, 39). Likewise, the initial outgrowth of the bud occurs in the absence of growth factor receptors such as the insulin-like

growth factor-1 receptor and the epidermal growth factor receptor, which are thought to be important to the regulation of hormone dependant branching morphogenesis during puberty (39).

A function in mammary mesenchyme induction and ductal growth has also been found for RASGRF1 (Ras protein-specific guanine-releasing factor 1; also known as p190 B RhoGAP), a negative regulator of the Rho pathway (40). A role for RASGRF1 in mammary biology was first postulated when the gene that encodes it was identified as being highly up regulated in terminal end buds, the structures that show highest proliferative activity in the ductal tree at puberty (41). *Rasgrf1*^{-/-} embryos have much smaller epithelial buds at E14.5 (40). The epithelial cells are disorganized and the cells in the mammary mesenchyme lack expression of steroid receptors. Absence of insulin receptor substrate 1 (IRS1) and IRS2, which are downstream mediators of the insulin-like growth factor 1 receptor (IGF1R), results in the same defects as seen in *Rasgrf1*^{-/-} embryos. This suggests that insulin-like growth factor 1 (IGF1) signalling through RASGRF1 is important for the formation of a normal-sized mammary bud and the induction of mammary mesenchyme cell identity. As the rate of cell proliferation is low during this developmental phase, it seems that the inhibition of bud growth is due to a migration defect in cells that form the epithelial bud. It is unclear whether the defect in the mesenchyme is cell autonomous or is an indirect effect of perturbed epithelial differentiation. It will also be interesting to see if PTHLH and IGF1 function in the same or parallel pathways.

Four genetic models develop mammary buds but subsequently have defects in ductal outgrowth. These are *Pthrp*^{-/-}, *Pth1r*^{-/-}, *Msx2*^{-/-} and *p190-B*^{-/-} mice (33, 35, 41). In the case of PTHrP and its receptor, the failure of bud outgrowth is the result of defects in the mammary mesenchyme (34-36). A similar mesenchymal defect might also hold for the *Msx2*^{-/-} mice, because expression of this transcription factor is limited to the mesenchyme at this stage (32, 33). The mechanisms underlying the failure of transplanted *p190-B*^{-/-} buds to grow are currently under investigation (41).

Hormone regulation of mammary cell fate

Systemic hormones are key regulators of postnatal mammary gland development and play an important role in the etiology and treatment of breast cancer. Mammary ductal morphogenesis is controlled by circulating hormones, and these same hormones are also critical mediators of mammary stem cell fate decisions.

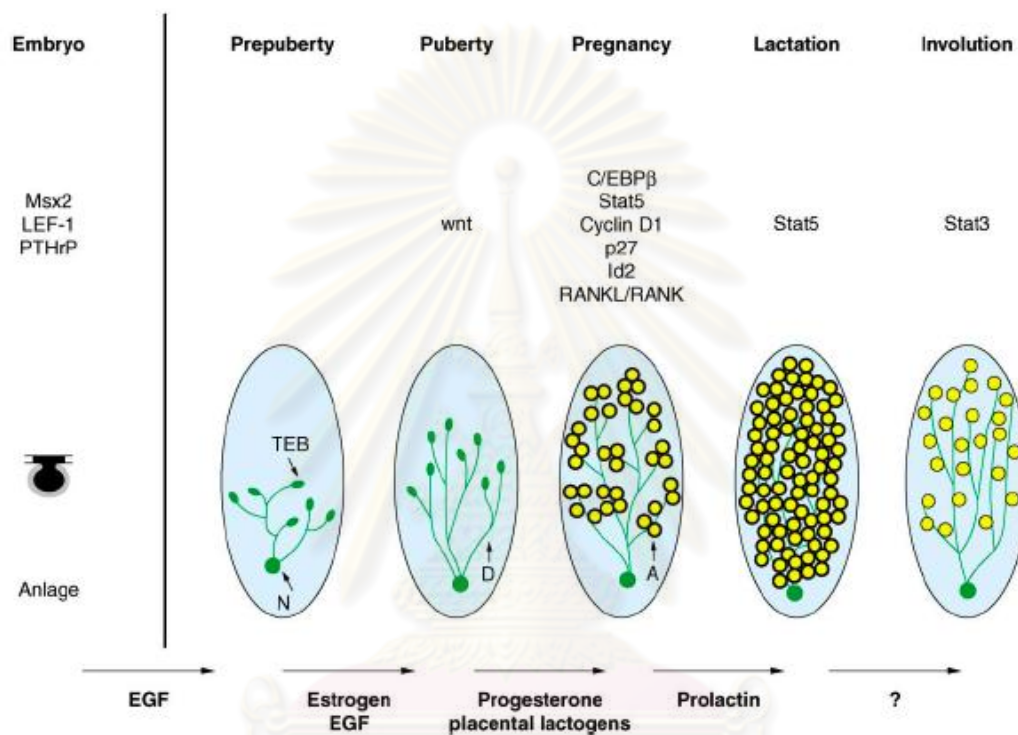


Figure 5. Hormones and genes that control development of mammary gland (38).

From Figure 5, the anlage is composed of epithelium (dark knob) and stroma (gray surrounding). The oval shown in the postnatal stages depicts the mammary fat pad (stroma). The solid green circle represents the nipple (N) from which the ducts originate. The ends of growing ducts form terminal end buds (TEB) during puberty. Mammary ducts (D) are shown as solid lines and the lobuloalveolar structures are presented as yellow circles (A). The hormones that control distinct developmental windows are shown below the arrows. The genes that have been implicated genetically in developmental processes are listed above the respective stages. Epidermal growth factor (EGF) signals through the stroma and controls early ductal outgrowth. Together with estrogen, it also controls ductal elongation and branching during puberty. Progesterone, placental lactogens, prolactin, and the osteoclast differentiation factor

signal alveolar proliferation and differentiation during pregnancy and possibly lactation. The signals inducing tissue remodeling during involution have not been defined. The genes that control distinct stages of mammary development are shown. Ductal elongation and branching during puberty is controlled by inhibin β B, CSF-1, the progesterone receptor, and wnt. Proliferation and differentiation of mammary alveolar cells is controlled by the prolactin receptor, Stat5, RANKL, cyclinD1, p27, Id2, and C/EBP β . Mammary function during lactation is controlled by prolactin through Stat5, and tissue remodeling and cell death during involution by Stat3, bax, and bcl-x (38). The genetic pathways controlling mammary gland development are summarized in Table 1.

Table 1. Genetic pathways controlling mammary gland development

Signalling pathways	Mammary defects	Reproductive system
Estrogen receptor α	Absence of ductal outgrowth	Infertile
Progesterone receptor	Impaired alveolar development	Infertile
SRC-1, SRC-3	Reduced ductal branching	Fertile
Prolactin	Reduced ductal branching	Infertile
Prolactin receptor	Reduced ductal branching, impaired alveolar development	Non functional corpus luteum
Stat3	Delay involution	Not described
Stat5a	Impaired differentiation	None
Stat5b	None	Non functional corpus luteum
Stat5a/b	Not described	Non functional corpus luteum
Bcl-x	Not described	Loss of primordial germ cells
RANKL or RANK	Impaired alveolar development	Not described
PTHrP or PPR1	Lack of embryonic mesenchyme and prim sprout outgrowth	Not described

Review of cases with bilateral absence of breast

Congenital absence of the breast is a rare genetic condition. Several terms have been used to classify the different defects found in this condition. Although strictly speaking, athelia refers to absence of the nipple, and amastia refers to absence of the breast, these terms have been used interchangeably (13). The term congenital absence of the breast is a separate entity from hypoplasia of the breast. Complete breast absence is defined by the absence of the nipple, whereas nipples are present in hypoplasia of the breast (2). Complete absence of breasts is the complete failure of mammary ridge to develop at about 6 weeks in utero (1). This condition is a very rare congenital anomaly with a wide range of associated features. It is inherited as either autosomal dominant or recessive pattern. In 1965 Trier (2) reviewed the literature and found 43 cases of congenital breast absence and classified them into three groups which are different in their mode of inheritance and associated deficits.

1. Bilateral amastia with congenital Ectodermal Defect; In 1886, Hutchinson first described absence of the breast associated with congenital ectodermal defect (2). Seven such cases of affected boys were added by Trier (2). It is inherited as sex-linked recessive with a 50 percent chance of transmission from mother to son (2). Heterozygous girls showed 10 percent to 30 percent of less manifestations than in boys(42). Ectodermal dysplasia was also presented in the skin and its appendages (such as hair, eccrine, and sebaceous glands), the teeth, and nails are mainly affected (42). Additional features, including cleft lip and palate, microphthalmia, and corneal dysplasia, have been observed (42). Burck and Held (42) described the first case of a female infant who presented with complete absence of the breast associated with congenital ectodermal defect. Her mother, maternal aunt, and grandmother had hypodontia, sparse hair, and small breasts associated with mamillary hypoplasia (42). In this female infant, pedigree analysis suggested either autosomal or sex-linked dominant inheritance and excluded homozygosity for an X chromosome-linked recessive gene (42).

2. Unilateral absence of the breast which frequently associated with the absence of pectoralis major muscles called "Poland syndrome". It is identified by absence of the

breast or hypoplastic breast unilaterally associated with absent pectoral muscles and other musculoskeletal defects ipsilaterally (43). Trier (2) reported 20 cases of this defect, with 9 people missing the right breast and 11 people missing the left breast. Milder forms of Poland syndrome occur more frequently than severe forms and may be unrecognized (44).

3. Bilateral absence of the breast with variable associated defects.; Bilateral absence of the breast was first described by Gilly in 1882 (2). Trier (2) documented 16 cases of bilateral absence of the breast. Ten of the women had no anomalies other than absence of both breasts and nipples. Many other defects have been reported with bilateral amastia. Syndromes associated with the absence of breast and nipple include ectodermal dysplasia of the tricho-odonto-onychial type (3), congenital amastia with polywhorls and webbed fingers (5), acral-renal-ectodermal-dysplasia-lipoatrophic-diabetes (AREDYLD syndrome) (6, 7), bilateral amastia with ureteral triplication and dysmorphism (8), amastia with vaginal agenesis (9) and the scalp-ear-nipple syndrome (SEN or Finlay-Marks syndrome) (10, 11, 13-18). The latter is the most associated syndrome. Additionally, renal involvement has been reported in some cases of scalp-ear-nipple syndrome (16, 17). The structural ear malformation is presented in this disorder but not all patients had hearing impairments. However, this condition has also been associated with cleft palate, high-arched palate, scant axillary and pubic hair, absence of a finger, and "lobster claw" deformity of the hands and feet (2). Amastia may be isolated, syndromic, familial or embryopathic. Fraser reported a three-generation family in which seven members had bilateral absence of the breast without any other abnormalities (a man, three of his four daughters, and three of his granddaughters) (2). Goldenring and Crelin described a mother and daughter with bilateral absence of the breast with sparse body hair, a "saddle nose" deformity, hypertelorism, high arched palate, and no other musculoskeletal defect (2). Ferene described a family in which a mother with one absent and one hypoplastic breast had a daughter with bilateral absence of the breast. Since Trier's review, many additional reports of bilateral amastia have been added to the literature. Tawil and Najjar (45) reported the case of a 12-year-old girl with complete absence of the nipples and breasts, lowest ears with abnormal

pinnae and a hearing deficit, large mouth and macrognathia, high-arched palate, cubitus valgus, and malrotated kidneys. Mathews (46) described an 8-year-old girl with congenital bilateral absence of the breast as well as spasticity, growth failure, profound motor and mental retardation, microcephaly, micrognathia, strabismus, abnormal fingers and toes, puffiness of the dorsum of the hands and feet, bilateral simian creases, and a single dorsal crease on the fingers. Nelson and Cooper (5) described a family in which the father and two of his three daughters had bilateral absence or hypoplasia of the breasts associated with webbing of the fingers and a whorled scalp hair pattern. Wilson et al. (43) described a family in which absent or hypoplastic breasts were inherited from mother to daughter in three generations and from mother to son in the fourth generation. In these families, the pattern of inheritance seemed to be autosomal dominant. Kowlessar and Orti (47) reported complete absence of both breasts in a brother and sister who had no other abnormalities and normal findings on chromosome analysis. The parents of these siblings had normal breasts and were first cousins, suggesting that their genetic defect was autosomal recessive (47).

4. Teratogens; A case of athelia and choanal atresia was reported in a girl infant born to a woman treated for hyperthyroidism throughout the pregnancy with methimazole and propranolol. Her family history revealed no skin or breast abnormalities, and the patient had no evidence of congenital ectodermal defects. Her chest examination revealed symmetrical absence of both nipples, but both pectoralis muscles were determined to be present by palpation (19).

The treatment of amastia requires total breast reconstruction. The cause of this condition is not known. The previously reported cases with bilateral absence of breast are summarized in Table 2.

Table 2. Review of reported cases with bilateral absence of breast

Number of cases	Nipple	Ectodermal defect	Other anomalies	Year/Author
23	Two cases were hypoplasia and others were absence of breasts	Yes	Deformity of hand and foot Cleft palate Absence of a finger Saddle-nose Hypertelorism	1965, Trier WC.(2)
2	Absent	No	-	1968, Kowlessar M, Orti E.(47)
1	Absent	No	Hearing defect Malrotated kidneys	1968, Tawil HM, Najjar SS.(45)
1	Absent	No	Spasticity, growth failure Mental retardation Strabismus Bilateral simian creases	1974, Mathews J.(46)
1	Absent	Yes	-	1981, Burck U, Held KR.(42)
1	Hypoplastic	No	Webbed fingers and polywhorls	1982, Nelson MM, Cooper CK.(5)
2	Absent			
1	N/A	Yes	AREDYLD	1983, Pinheiro M, et al.(7)

2	Absent	YES	Hypotrichosis Hyperpigmentation	1986, Tsakalakos N, et al.(3)
1	Absent	No	Ureteral triplication hypertelorism	1987, Rich MA, et al.(8)
1	Absent	-	Choanal atresia	1987, Greenberg F.(19)
1	N/A	Yes	AREDYLD	1992, Breslau-Siderius EJ, et al.(6)
2	Aplastic	Yes	Scalp-ear-nipple syndrome hypertension	1994, Edwards MJ, et al.(14)
1	Absent	Yes	Scalp-ear-nipple syndrome Renal hypoplasia Cataract Coloboma of the iris	1997, Plessis G, et al.(17)
1	Absent	No	Vaginal agenesis	1999, Amesse L, et al.(9)
2	Absent	Yes	Scalp-ear-nipple syndrome renal and urinary tract anomalies	1999, Picard C, et al.(16)

2	Absent	Yes	Sensorineural hearing deficit Dentinogenesis imperfecta Renal hypoplasia Branchio-oto renal syndrome	2000, Lin KY, et al.(48)
1	Absent	Yes	-	2003, Iamin MT, Kumar VP.(49)
1	Hypoplasia	No	Cardiovertebral alteration and absence of axillary hair	2004, Martinez-Chequer JC, et al. (50)
1	Absent	Yes	-	2005, Ligia Aranibar D, et al.(20)
1	rudimentary	Yes	Scalp-ear-nipple syndrome	2005, Baris H, et al.(13)
1	Absent	Yes	Scalp-ear-nipple syndrome Coloboma of the iris	2006, Sobreira NL, et al.(10)
2	Hypoplastic	Yes	Scalp-ear-nipple syndrome	2007, Al-Gazali, L, et al.(18)
1	Absent	Yes	-	2009, Klinger M, et al.(4)

N/A= not available

Chromosomal translocation; short cut to locate a disease gene

The first successful mapping of a mendelian disorder by chromosome rearrangements was that of the Duchenne muscular dystrophy locus to Xp21. Since then, chromosome aberrations which delete, truncate, or otherwise rearrange and mutate specific genes have not only helped in the mapping of other disease loci, but have turned out to be key elements for the rapid isolation of disease genes by positional cloning strategies (51).

Disease-associated balanced chromosome rearrangements (DBCRs) truncating or otherwise inactivating genes form a visible bridge between human phenotypes and genotypes. Therefore, systematic breakpoint mapping and cloning in patients with balanced chromosome rearrangements has been proposed as an efficient strategy for elucidating the molecular causes of hereditary disease (51-53). De novo DBCRs can be identified by conventional karyotyping, and, with an incidence of 1 in 2,000, they are not rare (54). About 6% of these are associated with clinical abnormalities such as mental retardation with or without multiple congenital abnormalities (MCA), which is seen in almost half of these cases. In general, breakage events that give rise to DBCRs are not mediated by nonallelic homologous recombination (55), and they seem to occur everywhere in the human genome. An advantage of this approach is that breakpoints can be precisely mapped. Cytogenetically visible de novo translocations, small deletions and duplications are rare, but have led to the identification of candidate genes in a number of disorders such as Duchenne muscular dystrophy (56), familial adenomatous polyposis (57), retinoblastoma (58) and WAGR syndrome (59).

Specific chromosome rearrangements have predominantly been described in autosomal dominant (AD) and in X linked conditions. Of the 625 chromosomally mapped loci associated with genetic disorders, 54 (8.6%) are X linked (60). However, more than one third of the approximately 70 mendelian disorders associated with a specific chromosome rearrangement are X linked. This excess can be explained by almost routine application of cytogenetic analysis in two particular groups of patients: females affected with X linked diseases, suggesting X;autosome translocations, and males suffering from two or more X linked disorders, suggesting a contiguous gene syndrome.

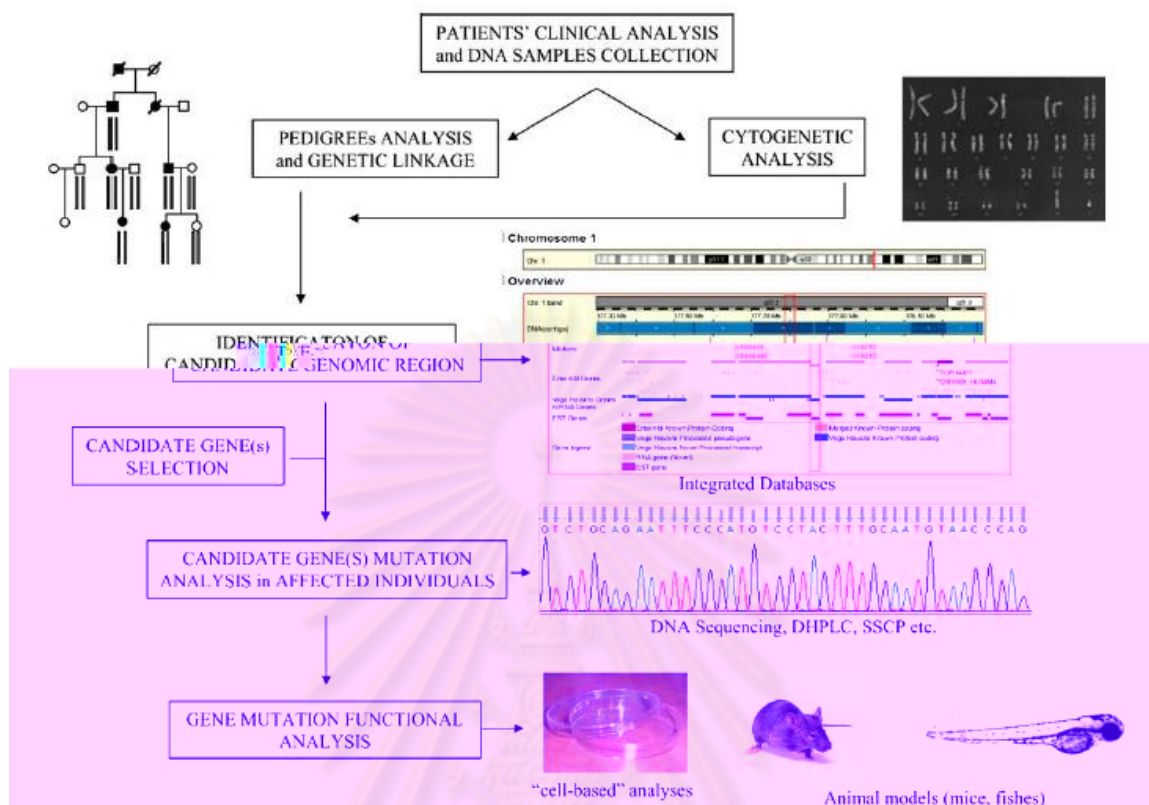


Figure 6. Main steps in positional cloning of genetic disorders (61)

Since there are no a priori reasons to believe that chromosome rearrangements should be less frequent in AD than in X linked disorders, the underrepresentation in AD disorders is probably because of ascertainment bias. The cytogenetic data in autosomal recessive (AR) disorders are so scanty that reliable statements regarding their frequency cannot be made. In only one AR disorder (Zellweger syndrome) has more than one chromosome rearrangements being described, a de novo deletion and a de novo inversion (62, 63). A specific chromosome mutation will only show an AR locus if the other allele happens to be mutated (unmasking of heterozygosity) (64), and this will be a rare occurrence as the gene frequencies for even the most common AR disorders do not exceed 1/25 to 1/50. Owing to the number of recessive traits, and the relatively high frequency of familial translocations and inversions in man (51), some of these breakpoints may affect recessive loci. The risk of unmasking of heterozygosity by a transmissible chromosome rearrangement will increase with the number of individuals

that receive the rearrangement. In addition, familial translocations may predispose to the formation of uniparental disomy, whereby AR mutations can be reduced to homozygosity (65). The occasional occurrence of an inherited balanced translocation or inversion would therefore not be unexpected in AR disorders (66).

However, the first example of a gene responsible for an autosomal recessive disorder identified by a chromosomal balanced translocation was *ALMS1* gene for Alström syndrome (67). The author postulated that this individual was a compound heterozygote, carrying one copy of a gene disrupted by the translocation and the other copy disrupted by an intragenic mutation. The disorders associated with balanced chromosomal rearrangements are summarized in Table 3.

Table 3. Example of diseases associated with balanced chromosomal rearrangements (53)

MIM No	Phenotype	Karyotype
<i>(1) Disorders with proven candidate regions/genes (indicated in bold)</i>		
175700	Greig cephalopolysyndactyly syndrome	46,XY,t(3;7)(p21.1;p13)pat ¹⁵
161200	Nail-patella syndrome	46,XY,t(1;9)(q41;q34)unknown ²⁸
190350	Trichorhinophalangeal syndrome type I	46,XX,t(7;13;8)(p21;q21;q24.1)de novo ²²
130650	Beckwith-Wiedemann syndrome	46,XX,t(2;11)(q14;p15.4)mat
130650	Beckwith-Wiedemann syndrome	46,XX,t(9;11)(p11.2;p15.4)mat ¹⁰
176270	Prader-Willi syndrome	46,XY,t(9;15)(q21.2;q13.1)de novo ²³
176270	Prader-Willi syndrome	46,XX,t(15;18)(q13;q23)de novo
205900	Blackfan-Diamond anaemia	46,X,t(X;19)(p11;q11)de novo ²¹
11010	BPES	46,XY,t(2;3)(q22;q24)de novo ²⁰
310200	Duchenne muscular dystrophy	46,X,t(X;9)(p21;q13)de novo ¹⁶
310200	Duchenne muscular dystrophy	46,X,t(X;11)(p21;q23)de novo
<i>(2) Disorders with suspected candidate regions/genes (indicated in bold)</i>		
163950	Noonan syndrome	46,XX,t(4;12)(q26;21.3)unknown
269200	Smidt syndrome	46,XX,t(6;14)(p22.3;q12)mat (concordant)
	Aplasia of ulna	46,XX,t(2;10)(q24.3;q23.3)de novo
	Atypical cerebellar ataxia	46,XX,t(8;20)(p22;q13)mat (concordant)
	Polydactyly and syndactyli	46,XX,inv(7)(p14.3p22)de novo
<i>(3) Phenotypes considered not to be associated with the cytogenetic aberration</i>		
104050	Williams syndrome	46,XX,inv(8)(p12q23)unknown
201910	Adrenogenital syndrome	46,XX,t(13;18)(q31;p11.2)de novo ¹⁴
312750	Rett syndrome	46,XX,inv(2)(p21q11)de novo (Nielsen <i>et al</i> , in preparation)
<i>(4) Miscellaneous</i>		
122470	Cornelia de Lange syndrome	46,XX,inv(12)(p13q13)unknown
122470	Cornelia de Lange syndrome	46,XY,inv(12)(p11.23p13.33)mat
157900	Moebius syndrome	46,XY,t(7;8;11;13)(q21.1;q21.3;p14.3;q21.2)de novo ³⁵
248770	Marfanoid syndrome	46,XX,t(12;21)(q22;q22.1)de novo

PTPRF (*LAR*); a candidate gene responsible for breast development

The human protein tyrosine phosphatase receptor type F (*PTPRF*) gene or leukocyte common antigen-related molecule (*LAR*) (68), is composed of 33 exons spanning over 85 kb. Exon 2 encodes the signal sequence and the first 4 amino acids in the mature *LAR* protein. The 3 immunoglobulin-like domains are encoded by exons 3 to 7, and the 8 fibronectin type III (FN-III) domains are encoded by exons 8 to 17. Exons 18 to 22 encode the juxtamembrane and transmembrane domains, and exons 23 to 33 encode the 2 conserved tyrosine phosphatase domains and the entire 3-prime untranslated region (Figure 7). Alternative splicing of *LAR* mRNA was revealed by RT-PCR analysis. The human *LAR* mRNA in which exon 13 is spliced-out is the major mRNA species (68). Further alternative splicing of *LAR* mRNA is involved the FN-III domains 4, 5, 6 and 7 in various combinations (68).

The *LAR* protein has a broad tissue distribution and is expressed on cells of many different lineages including epithelial cells, smooth cells, and cardiac myocytes (69).

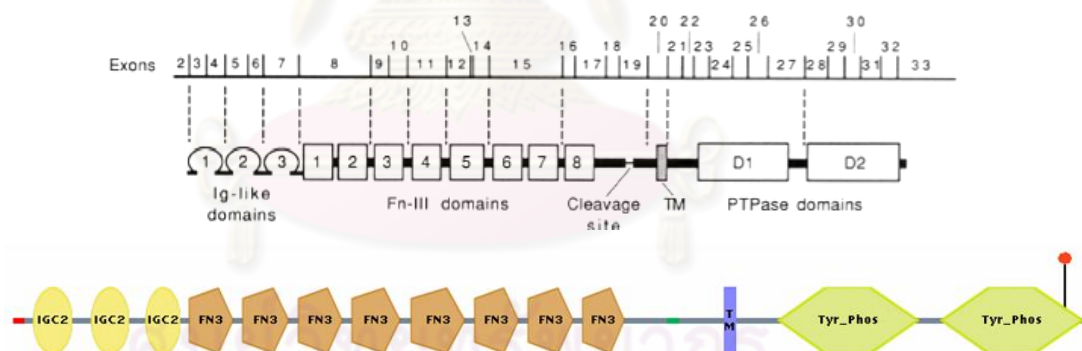


Figure 7. Relationship of *PTPRF* exon structure and protein domains. The exon organization of the *LAR* protein Ig-like domains, Fn-III domains, transmembrane region, and tandem PTPase domains are shown. In each case the exon/intron structure is indicated on top with the corresponding *LAR* protein domains shown schematically below (68).

LAR-RTPs are expressed as a 200-kDa proprotein and span the plasma membrane once with an extracellular amino-terminus. The cleaved proprotein consists of a 150-kDa extracellular domain (E-subunit) noncovalently bound to an 85-kDa

intracellular tandem phosphatase domains (P-subunit). These subunits remain non-covalently associated (70). This first proteolytic cleavage step is mediated by furin-like endoproteases that recognize a critical penta-arginine sequence at the C-terminus of the extracellular domain. A second, non-sequence-specific, calcium-dependent proteolytic cleavage step promotes extracellular domain shedding (71) and internalization of the P-subunit (72) (Figure 8).

Notably, the function of the proteolytic cleavage and shedding is still unknown. Similar to all PTPs, the 280 amino acid PTP catalytic domain contains an invariable signature motif ([I/V]HCXAGXXR[S/T]G) including an essential cysteine that catalyzes the nucleophilic attack on the phosphoryl group of its target substrate leading to its dephosphorylation (73).

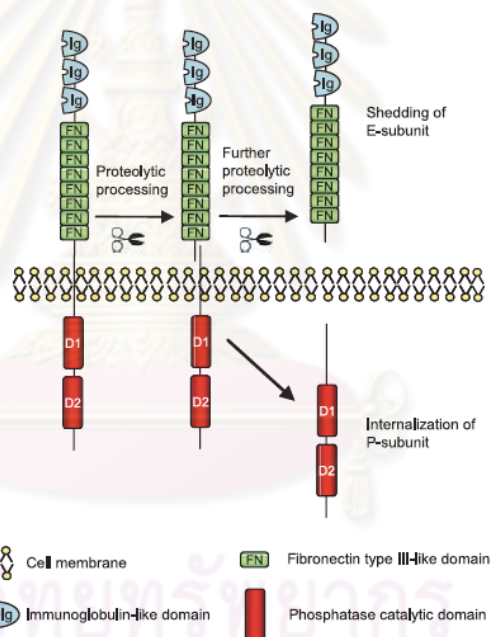


Figure 8. LAR-RPTPs are initially expressed as a ~200-kDa proprotein, which is then proteolytically cleaved by a furin-like endoprotease to generate a 150-kDa E-subunit and a noncovalently attached 85-kDa P-subunit. Further cleavage results in shedding of the E-subunit and internalization of the P-subunit (70).

The D1 domains have robust catalytic activity, while the D2 domains have weak, if any, catalytic activity against a variety of substrates (74). This suggests that D2 serves as a regulatory rather than a catalytic role. The three members of the LAR-RPTPs also share additional posttranslational modifications such as glycosylation (75) and

phosphorylation (76). All of these modifications, including proteolytic cleavages, may contribute to the regulation of LAR-RPTP activity.

Like most transmembrane PTPs, LAR has two tandem phosphatase domains which dominate its intracellular sequence. While the physiological substrates for LAR have not been definitively identified, some data suggest that β -catenin and plakoglobin, which are in a complex with the cadherin family of cell adhesion proteins, may be substrates (77).

The extracellular sequence of LAR may be equally important to its physiological function and its potential tumorigenic role. LAR has both immunoglobulin-like domains and fibronectin-type III domains in its extracellular E-subunit (78). These domains are expressed in many cell surface adhesion molecules and suggest an interaction of this PTP with extracellular ligands, perhaps adjacent cell surfaces or extracellular matrix. Recently, a LAR isoform has been shown to bind to the matrix protein laminin-nidogen (79). However, no data indicate regulation of PTP activity through extracellular domain binding interactions. Consistent with its structural domains and its potential substrates, LAR has been shown to localize to focal adhesions (80) and cadherin-containing complexes (72, 81).

Other reports link LAR to regulation of tyrosine kinase receptor autophosphorylation and signal transduction (82, 83). Each of these potential substrates is relevant to cell proliferation, differentiation and malignant transformation and could provide a link between LAR and breast cancer tumorigenesis.

Functional significance of PTPRF (LAR) in development

Role of PTPRF (LAR) in breast development

In 1997, Schaapveld et al. used gene targeting in mouse embryonic stem cells to generate mice lacking sequences encoding both LAR phosphatase domains. Homozygous mutant mice develop and grow normally. However, mammary glands of homozygous *Lar*-deficient females were incapable of delivering milk due to an impaired terminal differentiation of alveoli at late pregnancy. The authors concluded that LAR-mediated signaling may play an important role in mammary gland development and

function. Perhaps the most relevant observation relating LAR expression and activity to mammary epithelium and mammary tumors is the work of Schaapveld and coworkers (84). They have characterized a *Lar* knockout mouse and reported that the most apparent phenotype of this mouse was impaired terminal mammary gland development. At parturition, the number and size of alveoli in *Lar*^{-/-} were decreased, and premature involution of alveolar structures was observed. Secretory epithelial cells were morphologically abnormal with increased intracellular storage of secretion products in contrast to intraluminal secretion in wild-type glands. Expression of milk protein genes appeared to be unaffected. Also in this report, *Lar* mRNA expression levels were shown to be developmentally regulated in mammary epithelium, being relatively low until rising to maximum levels at gestational days 14–16. The specific role played by LAR in the complex hormonal synchrony of terminal mammary gland development and lactation is not known. LAR is clearly important in mammary gland development and is apparently elevated in breast cancer (85). With developing benign and malignant breast epithelium sharing features (invasion and migration), a role for LAR in breast cancer is an intriguing possibility. The current studies have been conducted to explore LAR as a possible prognostic marker in human breast cancer and its relationship to other established prognostic markers.

Role of PTPRF (LAR) in cancers

Compelling evidence implicated associated members of the PTP family with various congenital diseases (86) and led to the recognition that PTPs control many physiological processes. For example, Jirik et al. mapped *LAR*, a putative tumor suppressor gene, to 1p32, a region frequently deleted in human neuroblastoma and pheochromocytoma (87). Harder et al. found that coamplification of the *PTPRF* gene and the *MYCL1* gene in a small cell lung cancer line supported close linkage of the 2 genes (88). Moreover, *PTPRF* is known to be a tumor suppressor gene. In 2004, Wang et al. performed mutation analysis of protein tyrosine phosphates genes and identified *PTPRF* somatic mutations in 9 % of breast cancers (89). LAR expression was significantly increased in thyroid carcinomas (90) and breast cancers (85). Although more research

is needed, expression of LAR might correlate with breast cancer metastatic prognosis (91).

Role of PTPRF (LAR) in metabolic diseases

Several studies have implicated the receptor PTP in insulin signaling (92-95). Overexpression of LAR showed that it negatively regulated insulin signaling (83, 96). Subsequently, a role for LAR in insulin signaling has been muddled by conflicting results from *Lar*-deficient mice. In one study, in which *Lar* was disrupted in transgenic mice, “secondary” defects in glucose homeostasis were observed (97). For a phosphatase implicated in the negative regulation of insulin signaling, sensitivity to insulin would be expected in its absence rather than the resistance to insulin-stimulated glucose uptake that was observed. From that study, the role of LAR would not be directly on insulin receptor per se but downstream of the receptor, if indeed it influences the signaling pathway. A recent study seems to support this notion. When LAR was overexpressed in the skeletal muscle of mice, whole body insulin resistance was observed (98). The effect of the PTP was proposed to be most likely on downstream targets such as IRS-1. An alternate LAR disruption study in mice has been reported. The effects observed in these knockout mice were different from those observed in the transgenic null mice. The phenotypic defects were primarily observed in mammary gland development and function (84). Hence, it is still not clear what contribution LAR plays in insulin signaling.

Role of PTPRF (LAR) in nerve regeneration

The discoveries that LAR is expressed by mammalian neurons and that its expression is regulated during neural development by NGF (99, 100) suggested that LAR might modulate mammalian neuronal survival and/or neurite outgrowth. This hypothesis was supported by studies showing reduced size of basal forebrain cholinergic neurons and loss of cholinergic innervation of the dentate gyrus in *Lar*-deficient transgenic mice (101) and aberrant motor neuron pathfinding in *Drosophila Lar* loss-of-function mutants (102). *Lar*-deficient transgenic mice have also been found to have impaired outgrowth of sensory fibers during sciatic nerve regeneration (103).

The proximal membrane region of LAR contains two alternatively LAR Alternatively Spliced Element (LASE). First, LASE-a, a 33 bp alternatively spliced exon encoding an 11 amino acid segment insert located in the proximal membrane region 41 residues downstream from the transmembrane domain and 44 residues upstream from PTP-1. Second, LASE-c, a 27 bp alternatively spliced exon encoding a 9 amino acid segment located in the fifth FNIII domain (Figure 9). Measurement of the ratio of LAR RT-PCR products with and without the LASE-a insert in cortical, cerebellar and nonneuronal tissues showed that LASE-a splicing occurred preferentially in the nervous system and that the proportion of LAR transcripts containing LASE-a decreased during development (104).

Another evidence of LAR in nerve regeneration is generation of specific compounds that selectively inhibit RPTP-sigma but not the highly similar subfamily members LAR and RPTP-delta, which have opposite effects on regeneration (105, 106) and neurite outgrowth (107). All the studies showed an important novel potential mechanism regulating LAR-type tyrosine phosphatase receptor function in the nervous system. LAR-RPTPs represent great potential for the discovery of new nervous system treatment, an area of therapeutics that has provided very few answers thus far.

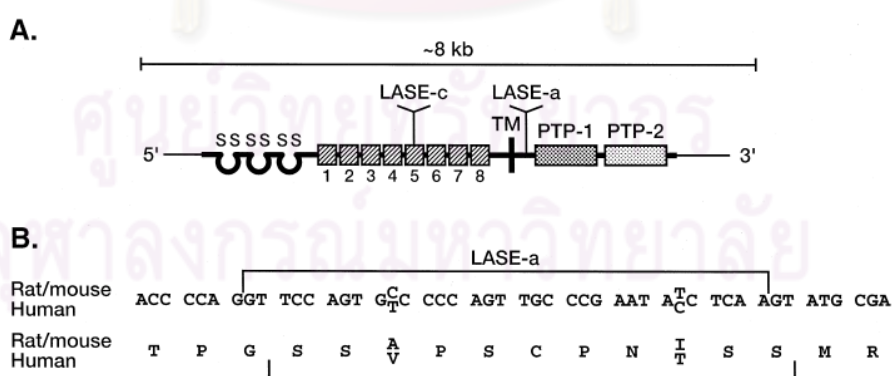


Figure 9. Schematic of LAR alternatively spliced element. (A) LASE-a and (B) LASE-c (104)

CHAPTER III

MATERIALS AND METHODS

Subjects and clinical descriptions

We identified an 18-year-old Thai woman who came to see plastic surgeons for total breast reconstruction. Her menarche was at 14 years of age and her menstruation had been regular. She had been generally healthy with normal intelligence. Physical examination showed normal height (157 cm, 50th percentile), mild hypertension with blood pressure of 140/90 mmHg., no eyebrows, epicanthal folds, small and cup-shaped pinnae, absence of all four upper incisors after extraction at age 15 years (they were small, brown and easily decayed) (Figure 10), bilateral absence of breasts and nipples, normal pectoralis muscles, brittle nails and normal external genitalia (by pelvic examination). Ultrasonography and computed tomography revealed absence of the left kidney and absence of left artery yet normal right kidney and uterus. She was the third child with an elder brother, an elder sister and a younger sister. The pedigree is shown in Figure 11. Her father passed away. None of the other family members were affected.

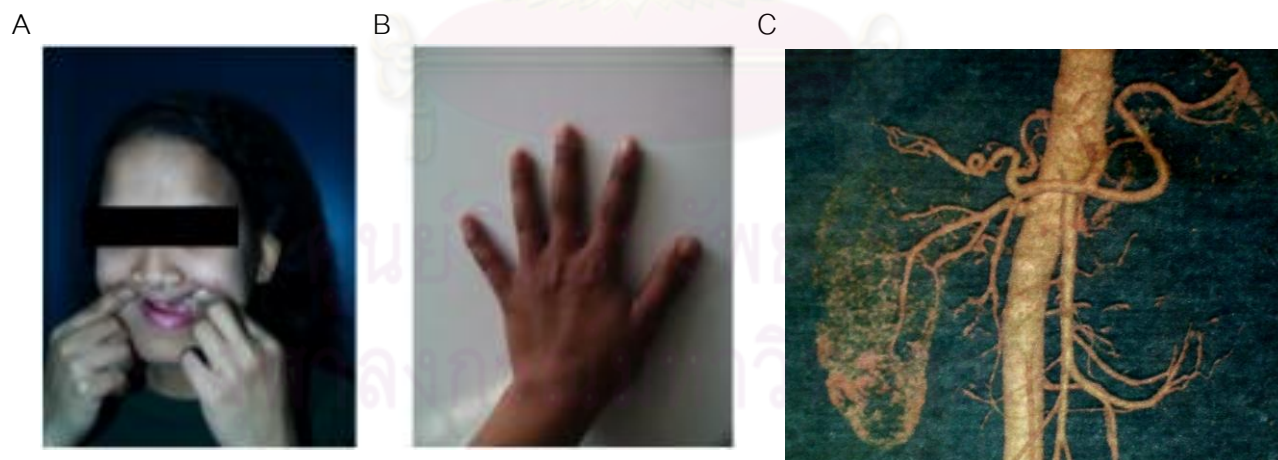


Figure 10. Clinical features of the patient presented with absence of breasts and ectodermal dysplasia. (A) Abnormal facial feature and dentinogenesis imperfecta. (B) Brittle nails. (C) Unilateral renal agenesis.

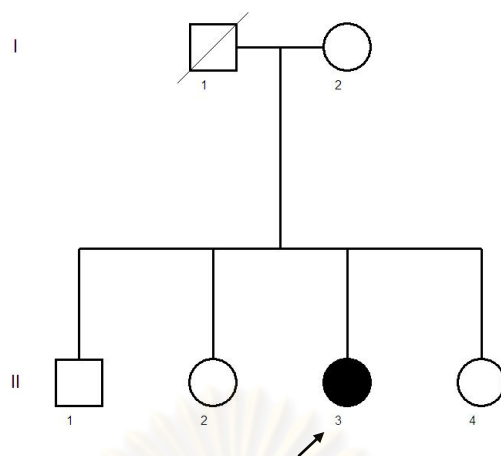


Figure 11. Family pedigree; they had four children and the proband was the third child. No other family members were affected.

After informed consent was received, peripheral blood (3 ml) was obtained from the patient and genomic DNA was extracted by standard methods. Controls were healthy volunteers unaffected with amastia and had no family history of amastia. Heparinized blood was used for transformation of lymphoblastoid cell lines. These transformed lymphoblastoid cell lines were used for RNA and protein extraction. DNA from the patients' family members who were at risk was also investigated.

To confirm a disease causing gene, mutation analysis was performed in the other two unrelated patients presented with bilateral amastia (Figures 12-13).



Figure 12. Clinical manifestation of the patient from Chile who presented with bilateral amastia. (A) Thin eyebrows and eyelashes, fine line wrinkles around the eyes and mouth, small teeth, broad nasal bridge and long philtrum. (B) Spindle fingers with erythema,

desquamation of the distal third of fingers, hypoplastic brittle nails and syndactyly (C)

Bilateral amastia (20)

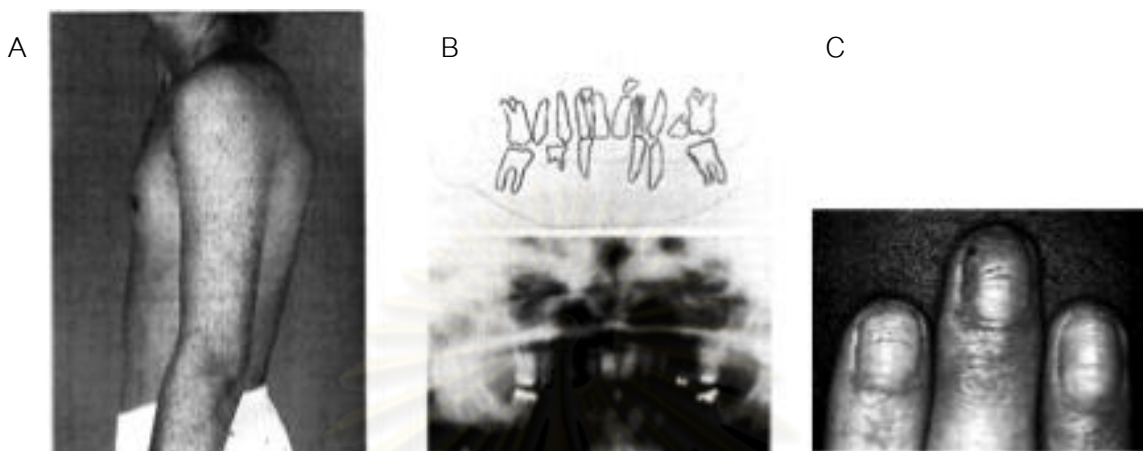


Figure 13. Clinical manifestation of the patient from Netherlands with AREDYLD (6) (A) Bilateral amastia. (B) X-ray of the upper and lower jaws. (C) Nails of the propoita showing transverse as well as longitudinal grooves (6).

Establishment of Epstein-Barr virus immortalization of human B-lymphocytes

Peripheral blood lymphocytes (B-lymphocytes) were immortalized successfully by infecting them with Epstein Barr Virus (EBV). These cells can then be used as a source of DNA or RNA to study genes and their transcripts. We isolated Peripheral Blood Mononuclear Cells (PBMCs) by carefully overlaying 3 ml to 6 ml fresh heparinized blood on the top of 4 ml ficoll, using blood to ficoll ratio of 1:1. Try not to mix blood and lower ficoll. Centrifuge for 30 min at 1,500 rpm at room temperature, leave the centrifuge break-off during this step. After centrifugation, an opaque lymphocyte layer will be seen just above the ficoll layer. Remove the plasma and transfer the PBMCs into a new 15-ml tube. Cell pellets were washed twice with 10 ml RPMI 1640 medium (Gibco), and centrifuged at 1,000 x g for 10 minutes. Resuspend cell pellets to reach 1×10^6 cells/ml and immortalization was achieved by mixing the cells with 1 ml of active EBV supernatant. Incubate at 37°C with 5% CO₂ for 30 minutes. This EBV supernatant was prepared using the EBV-transformed B95-8 marmoset cell line, the cells were grown in RPMI 1640 medium, supplemented with 10%

fetal bovine serum (FBS). These cultures were maintained for 12–15 days. After centrifugation for 10 min at 1,000 x g, the supernatant was filtered through a 0.22- μ m and stored at 4 °C until use.

The human immortalized cells were seeded with the primary culture medium (RPMI1640 with 20% fetal bovine serum, 100 units/ml of penicillin-streptomycin) in the 24-well plate to reach 1×10^5 cells/well. Add 10 μ g/ml cyclosporin A to suppress the growth of the T cells present in the preparation. Culture the cells in 37°C with 5% CO₂. Each week half of the supernatant was replaced by complete medium. No additional cyclosporine A was added. When large clumps appeared (usually 2 to 3 weeks after starting the culture), transfer cell clumps into the 25-cm³ flask and the cells were fed with 10 ml complete medium. Then subculturing, freezing and harvesting the cells were carried out according to the need.

Chromosome Analysis by Giemsa Staining

Heparinized blood of 0.5 ml was cultured at 37°C for 72 hours in 10 ml MEM medium with 0.3 ml phytohemagglutinin. Cells were synchronized with 0.1 ml methotrexate and incubated at 37°C for 17 hours. Centrifuge cells at 1,200 rpm for 10 minutes. Remove supernatant and gently wash the cells in 10 ml Hanks' solution and centrifuge cells at 1,200 rpm for 10 minutes. Remove supernatant and add 10 ml MEM medium. Release cells by adding 0.1 ml thymidine at 37°C for 3 hours. Add 0.1 ml ethidium bromide to prevent chromosome contraction and incubate for 1 hour 45 minute. Cells were harvested by adding 0.2 ml colcemid and incubated for 15 min. Centrifuge cells at 1,200 rpm for 10 minutes. Remove supernatant and slowly add 0.075 M KCl dropwise to 10 ml, incubate at 37°C for 15 min. Followed by fixation step, slowly add 3 ml of freshly prepared fixative mixture of 3:1 methanol:acetic acid. Centrifuge cells at 1,200 rpm for 10 minutes. Remove supernatant and slowly add 10 ml fixative dropwise. Repeat this step once. The cells can be stored at -20°C. To prepare metaphase spread, use a small amount of cell mixtures containing metaphase chromosomes and drop the cell mixtures from about 18 inches high onto the angled, humidified microscope slides a few times. Air-dry the slides at least 10

minutes. The slides were stable for a long time. GTG-banding was performed by incubating the glass slides in a 0.05% trypsin solution at 37°C for 7 seconds, followed by rinsing the slides in phosphate-buffered saline buffer and staining in a 5% giemsa stain for 5 min. The slides were rinsed with water and air-dried.

BAC/PAC clone preparation

BAC and PAC clones were selected from the Mapviewer NCBI, and obtained from the BACPAC Resources Center (BPRC) (Table 6). Streak bacterial clone stock and stab culture to single colonies on a LB agar plate with appropriate antibiotic (containing 12.5 µg/ml chloramphenicol for BAC clones and 25 µg/ml kanamycin for PAC clones). Pick a single colony from a freshly streaked selective plate and inoculate a culture of 5 ml LB medium containing the appropriate selective antibiotic. Incubate for 12–16 h at 37°C with vigorous shaking. Harvest bacterial cells by centrifugation at 8,000 rpm (6800 x g) for 10 minute at room temperature. Discard supernatants and resuspend pelleted bacterial cells in 100 µl P1 solution. Add 200 µl P2 solution and gently shake each tube to mix the contents. Let the tube sit at room temperature for 5 min. Slowly add 250 µl P3 solution to each tube and gently shake during addition. After adding P3 solution to every tube, place the tubes on ice for at least 5 min. Spin in cold centrifuge at full speed (20,000 x g; 14,000 rpm) for 5 minutes. Transfer supernatants to a new tube. Precipitate DNA by adding 900 µl of ethanol (96–100%) and centrifuge at full speed (20,000 x g; 14,000 rpm) for 5 minutes. Decant and drain pellets. Wash DNA pellets by adding 500 µl of 70% ethanol and centrifuge at 13,400 rpm for 5 minutes. Air dry pellets at room temperature and resuspend pellets in 50 µl water or desired volume.

Generation of subfragment probes by long-template PCR

In order to refine the critical region, we generate BAC/PAC subfragments of approximately 10 kb using long template PCR system. A series of primer pairs (Table 7) were chosen from the genomic sequence of breakpoint-spanning clones (RP5-1029K14 and RP11-347D21). Each subfragment probe was overlapped and used for subsequent

FISH analysis. We used 200 ng of plasmid DNA, 1X Amplibuffer C (Vivantis), 160 mM $(\text{NH}_4)_2\text{SO}_4$, 500 mM Tris-HCl, 17.5 mM MgCl_2 and stabilizers, 0.4 mM dNTPs, 0.4 μM of each primer and 2.5 U Perpetual OptiTaq DNA polymerase (Vivantis) in a total volume of 50 μl . The PCR amplification was performed as follows: initial denaturation at 95°C for 15 minutes, followed by 40 cycles of denaturation at 95°C for 30 seconds. The annealing step was performed at optimal annealing temperature (T_a) for each specific primer (Table 7) for 30 seconds. The extension was at 72°C for 11 minutes and the final extension was at 72°C for 10 minutes.

Probe Labeling by Nick Translation

Genomic BAC/PAC DNAs and their long-template PCR products were labeled with spectrum dUTP using nick translation kit (Vysis). Pipette the following components to the microcentrifuge tube (Table 4).

Table 4. Components for Nick translation

Component	Volume/Reaction
1 ug DNA	X μl
Nuclease-free water	(17.5-X) μl
0.2 mM SpectrumGreen or SpectrumOrange dUTP	2.5 μl
0.1 mM dTTP	5.0 μl
0.1 mM of each dCTP, dGTP, dATP Mix	10.0 μl
10X nick translation buffer	5.0 μl
0.5 (U/ μl) Nick translation enzyme	10.0 μl

Centrifuge briefly in a centrifuge to bring liquid to the bottom of the tube. Incubate at 15°C for 16 hours in a PCR machine. Stop the reaction by heating at 75°C for 10 minutes. Chill on ice. Check the size of the labeled probes by gel electrophoresis in 0.7~2% agarose gel and look for the peak size between 50 – 500 bp (or 100-300 bp) of the DNA fragments. To precipitate the labeling probe, the following components were combined, and the mixture was then incubated at -80°C for at least 15 minutes (Table 5).

Table 5. Components for probe precipitation

Component	Volume/Reaction
DNA labeled (Nick reaction)	5.0 μ l
COT-1	1.0 μ l
Human placental DNA	2.0 μ l
Purified water (ddH ₂ O)	4.0 μ l
3M Sodium acetate (NaOAc)	1.2 μ l
Absolute ethanol	30.0 μ l

Centrifuge the mixture at maximum speed at 4°C. Discard the supernatant, then vacuum dry for about 10 minutes. Resuspend the probes in 10 μ l hybridization solution. Store the DNA probe at -20°C until use.

Fluorescence in situ hybridization (FISH)

FISH was performed on metaphase spreads using standard molecular cytogenetic techniques. Fixed cell suspension from the chromosome analysis was used for preparation of metaphase on the slides. Drop metaphases a few drops angled on the microscope slide. Air-dry the slides and leave them overnight. If the slides are not dry enough, dehydrate the slide by immersing the slides into 100% ethanol for 1 min. Air dry. Wash slides with 2X SSC /0.05% Tween 20 at 37°C for 1 hour. Dehydrate the slides with 70%, 90%, and 100% ethanol for 1-2 min each and allow to air dry. During incubation, denature probes for hybridization at 75°C for 5 minutes. Apply 10 μ l of denatured probes to the slide. Immediately apply a coverslip and seal with rubber cement. Incubate slides with probe for 2 minutes at 72°C in hybridization tower. Keep the slides in a moist chamber at 37°C overnight. Remove rubber cement by using forceps. Remove coverslips by gently tipping them off. Wash the slides with 0.4X SSC at 68°C for 2 minutes. Washing the slides in 2X SSC at room temperature for 2 minutes. Apply 10-20 μ l of DAPI counterstain and a coverslip to hybridization location. Examine using a fluorescence microscope with appropriate filters.

Table 6. List of BAC/PAC clones for Fluorescence *in situ* hybridization

Clone	Type	Accession	Sequence Length (bp)	Position	Chromosome Band
RP11-329N22	BAC Library	AL513479	193826	38.5 M	1p34.3
RP5-1066H13	PAC Library	AC119677	170397	41.0 M	1p34.2
RP11-282K6	BAC Library	AC093420	193766	43.4 M	1p34.2
RP1-92O14	PAC Library	AL139289	90433	43.5 M	1p34.2-1p34.1
RP11-506B15	BAC Library	AL583862	167444	43.6 M	1p34.1
RP5-1029K14	PAC Library	AC092815	126651	43.8 M	1p34.1
RP11-184I16	BAC Library	AL451062	141866	43.9 M	1p34.1
RP11-570P14	BAC Library	AL356653	16184	44.25 M	1p34.1
RP11-30D7	BAC Library	AL596225	148750	44.7 M	1p34.1
RP11-69J16	BAC Library	AL359473	79340	45.2 M	1p34.1
RP11-291L19	BAC Library	AL451136	137143	45.6 M	1p34.1
RP11-322N21	BAC Library	AL672043	87234	46.35 M	1p34.1
RP11-49P4	BAC Library	AL136373	121112	46.8 M	1p33.0
RP11-346M5	BAC Library	AL731892	123921	47.1 M	1p33.0
RP11-330M19	BAC Library	AC096541	200368	48.0 M	1p33.0
RP11-329A14	BAC Library	AL356968	173373	48.6M	1p33.0
RP11-428D12	BAC Library	AC097062	185700	49.0 M	1p33.0
RP11-296A18	BAC Library	AL162430	211791	51.4 M	1p32.3
RP11-334A14	BAC Library	AL445183	193774	53.2 M	1p32.3

Clone	Type	Accession	Sequence Length (bp)	Position	Chromosome Band
RP11-109I2	BAC Library	AC091609	183521	55.3 M	1p32.3
RP11-243M12	BAC Library	AL359739	170284	57.7 M	1p32.2
RP11-470E16	BAC Library	AC093425	179499	59.3 M	1p32.1
RP11-32I17	BAC Library	AC096534	195270	61.2 M	1p31.3
RP4-614O4	PAC Library	AL121753	150728	33.3 M	20q11.22
RP11-425M5	BAC Library	AL109614	194433	35.6 M	20q11.23
RP5-1123D4	PAC Library	AL049691	169243	38.5 M	20q12
RP4-753D4	PAC Library	AL031676	126635	41.0 M	20q13.11
RP1-47A22	PAC Library	AL117374	84000	41.1 M	20q13.11
RP3-453C12	PAC Library	AL021578	147620	43.4 M	20q13.12
RP5-1050K3	PAC Library	AL121776	143981	45.1 M	20q13.12
RP4-569M23	PAC Library	AL031666	116370	45.4 M	20q13.13
RP1-73E16	PAC Library	Z95330	43922	45.9 M	20q13.13
RP11-347D21	BAC Library	AL357558	63227	46.0 M	20q13.13
RP1-66N13	PAC Library	AL137078	80725	46.4 M	20q13.13
RP5-991B18	PAC Library	AL049541	129874	46.6 M	20q13.13
RP5-1164I10	PAC Library	AL049537	110028	47.0 M	20q13.13
RP4-791K14	PAC Library	AL035685	155318	47.5 M	20q13.13
RP5-1114A1	PAC Library	AL035684	148845	49.7 M	20q13.2
RP11-80K6	BAC Library	AL121902	170740	51.0 M	20q13.2

Clone	Type	Accession	Sequence Length (bp)	Position	Chromosome Band
RP4-749H19	PAC Library	AL117380	178473	55.0 M	20q13.31
RP5-1018E9	PAC Library	AL035455	148667	56.4 M	20q13.32
RP4-719C8	PAC Library	AL121908	150985	57.7 M	20q13.32
RP11-157P1	BAC Library	AL354836	141056	60.3 M	20q13.33

Table 7. List of primers for generation of fragmented probes from BAC/PAC clones

Primer Name	Primer sequence (5'-3')	Annealing temperature (°C)	Amplicon size (bp)
RP5-1029K14-F1	GAG TGC GAT GAA GAT GAG GA	59	8850
RP5-1029K14-R2	TCA GAC TGG TCT TGA ACT CC		
RP5-1029K14-F2	CCT GCT GCT GAC CTT GTG AC	59	10050
RP5-1029K14-R3	CTG AGC ATC CAT CCA TAT GC		
RP5-1029K14-F3	CCT ATA GGA CCC AGT CAG GA	57	8540
RP5-1029K14-R4	GTC ACA AGG TAA GCA GCA GG		
RP11-347D21-F2	GGA TGC CTC AGG AAA CTT AC	57	9910
RP11-347D21-R1	AGA GCT GTT GAA CCT GGG TG		
RP11-347D21-F3	CTG TGT TAG CCA GGA TGG TC	57	9860
RP11-347D21-R2	ACC TGT CCA GGC AGG AAT TC		
RP11-347D21-F4	ACC TCT CGC TCT CTG GGC TT	57	11260
RP11-347D21-R3	CTC TCC CTG CCT AGT TTC CA		
RP11-347D21-F5	GCT GAA CAG GGA GTA AGG AG	57	10467
RP11-347D21-R4	AAG GAG TGG CTC TCA GAC AG		
RP11-347D21-F6	GCT CAC TAC CCC TCA GAC AG	57	10529
RP11-347D21-R5	CCA CGC ATC TCT CAC TCA TC		

DNA Extraction

Total DNA extraction was performed according to Qiagen kit protocol. Buffy coat from 3-5 ml of EDTA blood was separated by centrifugation at 1,000 x g for 10 minutes. Remove plasma and transfer buffy coat to a new 15-ml tube. Add 10 ml cold lysis buffer I and mix thoroughly. Centrifuge at 1,000 x g for 5 min, discard supernatant and then repeat this step once. Add 200 μ l Buffer AL to the sample and 20 μ l proteinase K. Mix by pulse-vortexing for 15 s. Incubate at 56°C for 10 min. Add 200 μ l ethanol (96–100%) to the sample, and mix again by pulse-vortexing for 15 s. After mixing, briefly centrifuge to remove drops from the inside of the lid. Carefully apply the mixture to the QIAamp Mini spin column (in a 2 ml collection tube) without wetting the rim. Centrifuge at 6000 x g (8000 rpm) for 1 min. Place the QIAamp Mini spin column in a clean 2 ml collection tube and discard the tube containing the filtrate. Add 500 μ l Buffer AW1 without wetting the rim. Centrifuge at 6000 x g (8000 rpm) for 1 min. Place the QIAamp Mini spin column in a clean 2 ml collection tube, and discard the collection tube containing the filtrate. Add 500 μ l Buffer AW2 without wetting the rim. Centrifuge at full speed (20,000 x g; 14,000 rpm) for 3 min. Place the QIAamp Mini spin column in a new 2 ml collection tube and discard the old collection tube with the filtrate. Centrifuge at full speed for 1 min. Place the QIAamp Mini spin column in a clean 1.5 ml microcentrifuge tube, and discard the collection tube containing the filtrate. Add 200 μ l Buffer AE or distilled water.

RNA Extraction

Total RNA extraction was performed according to Qiagen kit protocol. For blood samples, buffy coat from 3-5 ml of EDTA blood was separated by centrifugation at 1,000 x g for 10 minutes. Remove plasma and transfer buffy coat to a new 15-ml tube. Add 10 ml Buffer EL and mix thoroughly. Incubate for 10–15 min on ice. Mix by vortexing briefly 2 times during incubation. Centrifuge at 400 x g for 10 min at 4°C, and completely remove and discard supernatant. Add 10 ml Buffer EL to the cell pellet. Resuspend cells by vortexing briefly. Centrifuge at 400 x g for 10 min at 4°C, and completely remove and discard supernatant. Add 600 μ l Buffer RLT to pelleted leukocytes. For lymphoblastoid cell line,

harvest 10 ml of lymphoblastoid cell line with cell density of 1×10^6 cells /ml. Pellet the cells by centrifuging for 5 min at 300 x g in a centrifuge tube. Carefully remove all supernatant by aspiration. Disrupt cells by adding 600 μ l Buffer RLT. Pipet lysate directly into a QIAshredder spin column in a 2 ml collection tube (provided) and centrifuge for 2 min at maximum speed to homogenize. Discard QIAshredder spin column and save homogenized lysate. Transfer lysate to new 1.5-ml tube. Disrupt cells by adding 600 μ l Buffer RLT. Transfer each cell lysate after adding buffer ALT into a QIAshredder spin column in a 2 ml collection tube and centrifuge for 2 min at maximum speed to homogenize. Discard QIAshredder spin column and save homogenized lysate. Add 1 volume 600 μ l of 70% ethanol to the homogenized lysate and mix by pipetting. Do not centrifuge. Carefully pipet sample, including any precipitate which may be formed, into a new QIAamp spin column in a 2 ml collection tube without moistening the rim. Centrifuge for 15 s at 8000 x g (10,000 rpm). Transfer the QIAamp spin column into a new 2 ml collection tube. Apply 700 μ l Buffer RW1 to the QIAamp spin column and centrifuge for 15 s at 8000 x g (10,000 rpm) to wash. Place QIAamp spin column in a new 2 ml collection tube. Pipet 500 μ l of Buffer RPE into the QIAamp spin column and centrifuge for 15 s at 8000 x g (10,000 rpm). Carefully open the QIAamp spin column and add 500 μ l of Buffer RPE. Close the cap and centrifuge at full speed (20,000 x g, 14,000 rpm) for 3 min. Place the QIAamp spin column in a new 2 ml collection tube and discard the old collection tube with the filtrate. Centrifuge at full speed for 1 min. Transfer QIAamp spin column into a 1.5 ml microcentrifuge tube and pipet 30–50 μ l of RNase-free water directly onto the QIAamp membrane. Centrifuge for 1 min at 8000 x g (10,000 rpm) to elute. Repeat this step once.

Reverse Transcription PCR

Reverse transcription PCR was performed using the SuperScript III First-Strand Synthesis System for RT-PCR (Invitrogen) from total RNA extracted from peripheral blood and EBV transformed lymphoblastoid cell line. Prepare RNA/primer mixture, total RNA of 1 pg to 5 μ g was mixed with 2.5 μ M oligo and 0.5 mM dNTPs to make a total volume of 10 μ l. Incubate at 65°C for 5 min, then place on ice for at least 1 min. Prepare the following cDNA

Synthesis Mix, add 1xRT buffer, 5mM MgCl₂, 10 μM DTT, 40 units RNasOUT™, 200 units Superscript™III RT each consecutively. Add 10 μl of cDNA Synthesis Mix to each RNA/primer mixture, mix gently, and collect by brief centrifugation. Incubate at 50°C for 50 minutes followed by 85°C for 5 minutes to terminate the reactions. Chill on ice. Collect the reactions by brief centrifugation. Add 1 μl of RNase H to each tube and incubate for 20 min at 37°C. cDNA synthesis reaction can be stored at -20°C or used for PCR immediately.

Mutation analysis of the promoter sequence

PCR amplification of the promoter sequences of the *PTPRF* gene was performed using primers as shown in Table 8. The PCR reaction was performed in a total volume for 20 μl reaction mixture in 200 μM dNTPs, 1X Qiagen PCR buffer (contains 1.5 mM MgCl₂), 1X Q-Solution, 0.1 unit HotStarTaq (QIAGEN), 0.2 μM of each primer and 50 ng of genomic DNA. The PCR amplification was performed as follows: initial denaturation at 95°C for 15 minute, followed by 35 cycles of denaturation at 95°C for 45 seconds, annealing at 60°C for 45 seconds, extension at 72°C for 1 minute and a final extension at 72°C for 10 minutes. PCR products were treated with ExoSAP-IT (USP Corporation, Cleveland, OH) at 37°C for 40 minutes followed by inactivation at 80°C for 20 minutes. PCR products were sent out for direct sequencing (Macrogen Inc., Seoul, Korea).

Mutation analysis of the coding sequence

PCR amplification of the entire coding sequences and flanking intronic sequences of the *PTPRF* gene was performed using set of primers and parameters as shown in Table 8. We used 50 ng of genomic DNA, 1XPCR buffer (Fermentas Inc., Maryland), 1.5 mM MgCl₂, 0.2 mM dNTPs, 0.2 μM of each primer and 0.5 U Taq DNA polymerase (Fermentas Inc., Maryland) in a total volume of 20 μl. The PCR amplification was performed as follows: initial denaturation at 95°C for 5 minute, followed by 35 cycles of denaturation at 95°C for 45 seconds, annealing was performed at optimal annealing temperature (Ta) for each specific primer (Table 8.) for 45 seconds, extension at 72°C for 1 minute and a final extension at 72°C for 10 minutes. The PCR products were treated with ExoSAP-IT (USP Corporation,

Cleveland, OH) at 37°C for 40 minutes followed by inactivation at 80°C for 20 minutes. The PCR products were sent out for direct sequencing (Macrogen Inc., Seoul, Korea).

Detection of abnormal splicing fragment by amplification of complementary DNA

Amplification of the whole complementary DNA *PTPRF* would help detection of splicing defect. PCR amplification was performed using set of primers and parameters as shown in Table 9. We used 100 ng of complementary DNA, 1XPCR buffer (Fermentas Inc., Maryland), 1.5 mM MgCl₂, 0.2 mM dNTPs, 0.2 μM of each primer and 0.5 U Taq DNA polymerase (Fermentas Inc., Maryland) in a total volume of 20 μl. The PCR amplification was performed as follows: initial denaturation at 95°C for 2 minute, followed by 40 cycles of denaturation at 95°C for 45 seconds, annealing was performed at optimal annealing temperature (Ta) for each specific primer (Table 9.) for 45 seconds, extension at 72°C for 1 minute 30 seconds and a final extension at 72°C for 10 minutes. The PCR products were treated with ExoSAP-IT (USP Corporation, Cleveland, OH) at 37°C for 40 minutes followed by inactivation at 80°C for 20 minutes. The PCR products were sent out for direct sequencing (Macrogen Inc., Seoul, Korea).

DNA sequence analysis

Sequence data were analyzed using Sequencher (version 4.2; Gene Codes Corporation, Ann Arbor, MI) and were aligned with nucleotide BLAST program from www.ncbi.nlm.nih.gov/BLAST.

ศูนย์วิทยทรัพยากร
จุฬาลงกรณ์มหาวิทยาลัย

Table 8. List of primers for amplification of *PTPRF* genomic DNA

Primer Name	Primer sequence (5'-3')	Annealing temperature (°C)	Amplicon size (bp)
Promoter_LAR-F2	TTG ATC TGG GAA TGG GAG AGC	60	948
Promoter_LAR-R2	TGG ACT AGC GGG GAG GGC AAG G		
LAR-EX3-F	CTG GAT GGT CAG TGA GGA TG	57	560
LAR-EX3-R	TCT GCA ACA GTG CAC ACA GC		
LAR-EX4-5-F	TGA ACA GTG CCT GGC ACA TA	57	750
LAR-EX4-5-R	TCC ACC ACT GAC TTT CAC TG		
LAR-EX6-F	TGC CTC TCA GAC CTG GAA AC	61	700
LAR-EX6-R	CAC CAC ACT GGC ACA TCA CA		
LAR-EX7-F	CGT TGG TTC TAG ACA GGA GG	57	630
LAR-EX7-R	GCA CAT ACA CCA AGA AGT CG		
LAR-EX8-F	GGC CTC AGT TTC CTA GGC TA	63	792
LAR-EX8-R	CTA GCA TGA TGT CTC CCA CC		
LAR-EX9-F1	CCT TCA GAG GTC ACC ATA AG	63	922
LAR-EX9-R1	CCT AAC CTC ACA CCC TTA TC		
LAR-EX10-11-F	TGT GTG GTC AGT TGG GAT GT	58	1040
LAR-EX10-11-R	AGT TCG GTT TGG CCA GCA GA		
LAR-EX12-F	CAG CAC CTA AGG GGT AGC CT	61	652
LAR-EX12-R	CTT CTC CCA TCT TAG CCT GT		
LAR-EX13-F	CAG GGA CAG ATG ATC TAA GG	60	486
LAR-EX13-R1	AGC ATC TCG GGT CTC ACA AC		
LAR-EX14-F	TCA GAG CAT CTG TAG CTG CT	57	540
LAR-EX14-R	CTG CTC GAC AGG CAA GAA GT		
LAR-EX15-16-F	TCC TCT CCA GCA GAG GCC AC	61	1054
LAR-EX15-16-R	TTG GAG GTC ACA CAC CAG AG		

Name	Primer sequence (5'-3')	Annealing temperature (°C)	Amplicon size (bp)
LAR-EX17-19-F	CTT GGT ACT CTG CAG CCA TC	57	947
LAR-EX17-19-R	TGA GAG TCA CTG GGA CAG TG		
LAR-EX20-21-F	GGG CTC TGA CAC GGA AGG TG	61	958
LAR-EX20-21-R	GGG TCC AGG ATG CAA GGC TG		
LAR-EX22-F	GGG GCA GTA GGA GGA CAG AG	59	301
LAR-EX22-R	CCT GCA GAA CAG ACC CAC AG		
LAR-EX23-F	GTG CTC CAT GGT CAC ACA TG	59	280
LAR-EX23-R	CTA GGA CAG GAC AGG AGC TG		
LAR-EX24-25-F	TGG CTG GCA CCA CGA GAT AG	57	720
LAR-EX24-25-R	AGC GAC TTC CTC CAC AGA AG		
LAR-EX26-27-F	GGT GAC ATA GCT TGA GGACC	60	840
LAR-EX26-27-R	GCA GGA CAC GGG CTC AGC TT		
LAR-EX28-29-F	ACT GCA GGT GAG AGG GTA CA	59	770
LAR-EX28-29-R	CCC TCT CTG GTC TTC TAG GC		
LAR-EX30-31-F	TAG AGC AGT GAG GAC TTC CT	57	693
LAR-EX30-31-R	CTT GAG CTA AGG TAC CAT GC		
LAR-EX32-33-F	CAT GGT ACT ACC CTG GTC TA	57	640
LAR-EX32-33-R	GGT AGG ACC ATA AGC ACA CA		
LAR-EX34-F	CTA ACT CCA TGG CTG CAG TG	57	269
LAR-EX34-R	CCA GTG ACA GCA TCT GCG TA		

Table 9. List of primers for amplification of *PTPRF* complementary DNA

Fragment	Primer Name	Primer sequence (5'-3')	Annealing temp (°C)	Amplicon size (bp)
Fragment 1.1	PTPRF-mRNA-F1	TGG ATA GGC GGA AGG AGT GG	60	993
	LAR-mRNA-R2	CTC CAG GAC GTT GCG GCC AA		
Fragment 1.2	LAR-mRNA-F2	TGC TCG AAG AGG AAC AGC TG	60	760
	PTPRF-mRNA-R1	CCA ATG CTG TAG CGG GTG GT		
Fragment 2	PTPRF-mRNA-F2.1	CAG CGT GAA CCT GAC ATG CG	60	1298
	PTPRF-mRNA-R2	ACT CCG TCC ACT TCT CCA GG		
Fragment 3	PTPRF-F2171	CAG AAG GTG ATG TGT GTG AG	60	1050
	PTPRF-R3220	GCT GTT GAT GTC TCG GAA C		
Fragment 4	PTPRF-mRNA-F4.1	TCG AGA AGG AGA TCA GGA CC	60	1280
	PTPRF-mRNA-R4.1	TGG GTG GTC TCG CAT ACC TG		
Fragment 5	PTPRF-mRNA-F5.1	CCC TAC TCG GAT GAG ATC GT	52	1330
	PTPRF-mRNA-R5.1	GCA GAC ACA CAC GGG TCA AT		
Fragment 6	PTPRF-mRNA-F6	GGA GCG GAT GAA GCA CGA GA	60	1456
	PTPRF-mRNA-R6	CAA CCC CTA CAG TGG CCC AT		
Fragment 7	PTPRF-mRNA-F7	GTA CCT CGG CAG CTT TGA CC	60	1570
	PTPRF-mRNA-R7	CAG CAC TAG CAT CCA CAA GG		

Quantitative Real-Time PCR

Gene expression was quantified by StepOnePlus™ Real-Time PCR Systems (Applied Biosystems, CA). Total RNA extracted from peripheral blood and EBV transformed lymphoblastoid cell line was converted to cDNA and used for this experiment. We quantified gene expression using primers and probes for GAPDH (Table 13.) as well as the Assay-On-Demand products for PTPRF (Hs00160858_m1), PTPRF (Hs00892984_m1) (Table 12.). The Assay-On-Demand products and universal master mix were commercially purchased (Applied Biosystems). Each probe was run in a separate tube, triplication. The components

of each reaction were shown in Tables 10-11. The total volume was 20 μ l. The real-time PCR program started with a 2-minute UNG activation step at 50°C, followed by a 10-minute denaturation at 95°C, during which the hot start AmpliTaqGold DNA polymerase was fully activated. This was followed by 40 cycles of 15 seconds of denaturation at 95°C and 1 minute of annealing/elongation at 60°C. For relative quantification, the following arithmetic formula was used: $2^{-\Delta\Delta Ct}$, where the amount of target gene was normalized to GAPDH and the relative expression of *PTPRF* gene was calculated in relation to the mean value of target gene expression in the healthy control group.

Table 10. Real-Time PCR Components for *PTPRF* expression analysis

Component	Volume/Reaction
TaqMan Gene Expression Assay (20x)	1 μ l
cDNA template + H ₂ O	9 μ l
TaqMan Universal PCR Master Mix (2x) (with AmpErase UNG)	10 μ l

Table 11. Real-Time PCR Components for *GAPDH*

Component	Volume/Reaction
10 μ M GAPDH-F85	0.4 μ l
10 μ M GAPDH-R191	0.4 μ l
10 μ M GAPDH-P121 (HEX)	0.2 μ l
cDNA template + H ₂ O	9 μ l
TaqMan Universal PCR Master Mix (2x) (with AmpErase UNG)	10 μ l

Table 12. List of TaqMan Probes in Quantitative Real-Time PCR experiment

Gene	Position	Name	Fluorescence Label	Amplicon Size
<i>PTPRF</i>	Exons 5-6	Hs00160858_m1	FAM	60
<i>PTPRF</i>	Exons 32-33	Hs00892984_m1	FAM	71
<i>GAPDH</i>	Exons 2-3	GAPDH-P121	HEX	107

Table 13. Description of Taqman Probes for GAPDH in Quantitative RT-PCR

Name	Sequence 5'-3'	Position (mRNA) NM_002046
GAPDH-F85	5'-gtgaaggctcggagtcacacgg-3'	85-104
GAPDH-R191	5'-tcaatgaaggggtcattgatgg-3'	121-140
GAPDH-P121	HEX-cgcctggtcaccagggctgc-BHQ1	191-170

Western Blot Analysis

Harvest 20 ml of lymphoblastoid cell line with cell density of 1×10^6 cells/ml. Wash cell pellet twice with PBS and centrifuge at 1,000 g for 10 minutes. Transfer the cell suspension into a 1.5 ml centrifuge tube. Add ice-cold RIPA lysis buffer with Halt protease inhibitor cocktail (Pierce) approximately 100 μ l per sample. Lysed cells were incubated on ice for 30 minutes, and sonicated with an ultrasonic sonicator at 80% power output for 10 seconds twice on ice. Lysates were centrifuged at 12,000 g for 10 minutes. The supernatant was collected and the protein concentrations was determined using the BCA protein assay reagent (Pierce). Protein extract of 100 μ g was treated with 6x SDS sample buffer and heated at 95°C for 5 minutes. Protein was electrophoresed through an 8% SDS polyacrylamide gel electrophoresis (SDS-PAGE) at 100 V for 2 hours. Transfer protein to PVDF membrane (GE Healthcare) at 100 V for 3 hours. Blotted PVDF membrane was blocked in freshly prepared Tris buffer saline (TBS) with 0.01 % Tween 20™ and 5% nonfat dry milk (TBST-M) for 1 hour at room temperature with constant agitation. Blocked membranes were incubated with (1:100 in TBST-M) anti-LAR (BD Transduction Laboratory) overnight at 4°C with constant agitation. The PVDF membrane was washed three times with agitation in Tris buffer saline (TBS) with 0.01 % Tween 20™ (TBST) for 5 minutes and then incubated with secondary antibody (1:1000 in TBST-M) goat anti-mouse IgG-HRP conjugated (sc-2005) (Santa Cruz Biotechnology) for anti-LAR, for 1 hour at room temperature with agitation. Wash the PVDF membrane three times for 5 minutes with TBST. LAR proteins were detected by using SuperSignal West Pico Chemiluminescent

Substrate™ (Pierce). In brief, two substrate components were mixed at a 1:1 ratio to prepare the substrate working solution. The working solution was then added directly to PVDF blot and incubated for 5 minutes at room temperature. The excess substrate was removed, and the membranes were covered with plastic wrap. The protected membrane was placed in a film cassette with the protein side faced up and exposed to X-ray film (Kodak). Exposure time may be varied to achieve optimal results. To determine GAPDH for protein normalization, the membrane was stripped with 0.2 M NaOH for 30 minutes. Wash three times with agitation in Tris buffer saline (TBS) with 0.01 % Tween 20™ (TBST) for 5 minutes and block with 5% nonfat dry milk (TBST-M) for 1 hour at room temperature with constant agitation. GAPDH was determined using (1:1000 in TBST-M) anti-GAPDH antibody (Trevigen) and (1:1000 in TBST-M) goat anti-rabbit IgG-HRP sc-2030 HRP conjugated (Santa Cruz Biotechnology), respectively.

Haplotype analysis

Panel 1 and 2 of the ABI Prism Linkage Mapping Set version 2.5 (Applied Biosystems, Foster City, CA) were amplified. These two panels consist of 31 tandem repeat markers on chromosome 1 that define a 10 cM resolution human index map (Table 15). Each panel consists of a group of markers that were fluorescently labeled with FAM, HEX, or NED. Amplifications were carried out as single reactions in 96 well plates, according to the manufacturer's protocol. An additional four microsatellite markers selected from Mapviewer, NCBI (D1S3721, D1S2645, D1S2713, D1S3728) were used (Table 14.). These markers were amplified in a 20 µl reaction mixture containing 50 ng DNA, 0.2 µM of each primer, 0.2 mM dNTPs, 11XPCR buffer (Fermentas Inc., Maryland), 1.5 mM MgCl₂ and 0.5 U Taq DNA polymerase (Fermentas Inc., Maryland). PCR condition was performed as follows: initial denaturation at 95°C for 5 minutes, followed by 35 cycles of denaturation at 95°C for 45 seconds, annealing was performed at 60°C for 45 seconds, extension at 72°C for 45 minutes and a final extension at 72°C for 10 minutes. After PCR-amplification of genomic DNA samples, amplified fragments were resolved on an ABI PRISM 3100 Genetic Analyzer (Applied Biosystems) together with ROX-500 size standard (Applied Biosystems). The

resulting genotype data were analysed using GeneScan Analysis (Applied Biosystems). Allele numbers were assigned for each marker based on the size of the amplified fragment.

Table 14. List of microsatellite Markers selected from Mapviewer

Locus	UniSTS	Forward Primer 5'-3'	Reverse Primer 5'-3'
D1S3721	11903	FAM-AGAGAACGGAACCAACAGAA	GGTCTCTTACCTGGCAGACA
D1S2645	78397	FAM-TTC CCC ACA TTG GTG TAT AG	CTG GCT TGA GTG TAG ACT CG
D1S2713	26158	FAM-CAG CCC CCA ACA CAT AC	CCT TAG GAG TCT ACA GAC GCC
D1S3728	56029	FAM-GTAACCTTGCCCAAAACAGA	AAGAGGTTAAGAATAAAGGCTGC

Table 15. List of microsatellite Markers for chromosome 1

Locus	Dye Label	Variation type	Heterozygosity	Position
D1S468	VIC	Dinucleotide	0.76	3.5 M
D1S214	NED	Dinucleotide	0.78	6.8 M
D1S450	FAM	Dinucleotide	0.81	9.5 M
D1S2667	VIC	Dinucleotide	0.82	11.4 M
D1S2697	VIC	Dinucleotide	0.7	16.3 M
D1S199	FAM	Dinucleotide	0.83	19.8 M
D1S234	FAM	Dinucleotide	0.81	25.0 M
D1S255	VIC	Dinucleotide	0.75	37.4 M
D1S3721	FAM	Tetranucleotide	-	41.5 M
D1S2645	FAM	Dinucleotide	-	42.0 M
D1S2713	FAM	Dinucleotide	-	44.2 M
D1S2797	FAM	Dinucleotide	0.74	46.7 M
D1S2890	VIC	Dinucleotide	0.81	57.6 M
D1S3728	FAM	Tetranucleotide	-	59.5 M
D1S230	VIC	Dinucleotide	0.78	60.7 M
D1S2841	VIC	Dinucleotide	0.78	68.3 M
D1S207	FAM	Dinucleotide	0.84	82.3 M
D1S2868	FAM	Dinucleotide	0.76	93.1 M

D1S206	NED	Dinucleotide	0.82	101.4 M
D1S2726	NED	Dinucleotide	0.75	110.9 M
D1S252	VIC	Dinucleotide	0.81	117.3 M
D1S498	NED	Dinucleotide	0.82	149.5 M
D1S484	VIC	Dinucleotide	0.64	159.0 M
D1S2878	NED	Dinucleotide	0.84	163.6M
D1S196	VIC	Dinucleotide	0.74	165.8 M
D1S218	NED	Dinucleotide	0.83	172.7 M
D1S238	FAM	Dinucleotide	0.86	186.4 M
D1S413	FAM	Dinucleotide	0.76	196.8 M
D1S249	FAM	Dinucleotide	0.87	203.9 M
D1S425	NED	Dinucleotide	0.81	210.1 M
D1S213	NED	Dinucleotide	0.86	221.8 M
D1S2800	FAM	Dinucleotide	0.77	232.5 M
D1S2785	VIC	Dinucleotide	0.76	238.9 M
D1S2842	NED	Dinucleotide	0.76	240.9 M
D1S2836	NED	Dinucleotide	0.79	244.9 M

PTPRF Gene Phylogeny

Analyses of coding sequences were searched from human *PTPRF* orthologues sequences at <http://www.ensembl.org>. Multiple sequence alignment was achieved using ClustalW. Molecular Evolutionary Genetics Analysis (MEGA) Software Version 4.0 (108) was used for phylogenetic and molecular evolutionary analyses based on the Neighbor-Joining (NJ) and maximal parsimony methods. Sequences selected for the phylogenetic tree are listed in Table 16.

Table16. List of *PTPRF* cDNA sequence from NCBI and ensembl

Species	NCBI ID/Ensemble ID
Cow	ENSBTAT00000024046
C.elegans	C09D8.1d
Dog	ENSCAFT00000008256
Guinea Pig	ENSCPOT00000010432
Ciona intestinalis	ENSCINT00000015315
Ciona savignyi	ENSCSAVT00000010989
Danio rerio	ENSDART00000065586
D.melanogaster DLar-RA	FBtr0081260
D.melanogaster DLar-RB	FBtr0112800
Horse	ENSECAT00000015281
Species	NCBI ID/Ensemble ID
Stickleback	ENSGACT00000003944
Chicken	ENSGALT00000016337
Macaque	ENSMMUT00000017492
Wallaby	ENSMEUT00000016188
Mouse	ENSMUST00000049074
Platypus	ENSOANT00000010223
Medaka	ENSORLT00000003985
Chimpanzee	ENSPTRT00000049482
Orangutan	ENSPPYT00000001727
RAT	ENSRNOT00000027271
Zebra Finch	ENSTGUT00000007709
Fugu	ENSTRUT00000022538
Tetraodon	ENSTNIT00000018672
Dolphin	ENSTTRT00000002379
Xenopus	ENSXETT00000004794

Lizard	ENSACAT00000014201
Human	ENST00000359947
Aedes aegypti	XM_001650582.1
Anopheles gambiae	XM_319248.3

Identification of other submicroscopic chromosomal imbalances

We performed SNP array for genome wide genotyping using Illumina Human 1M Beadchip. In brief, the patient DNA was extracted using Qiagen kit according to the instruction. DNA sample of 1 μ g was assayed for over 1,000,000 SNP loci. DNA was amplified overnight; the amplified product was then fragmented by a controlled enzymatic process. After alcohol precipitation and resuspension of the DNA, the BeadChip was prepared for hybridization in the capillary flow-through chamber; samples were applied to BeadChips and incubated overnight. The amplified and fragmented DNA samples annealed to locus-specific 50-mers (covalently linked to one of over 1,000,000 beadtypes) during the hybridization step. One bead type corresponds to each allele per SNP locus. After hybridization, allelic specificity is conferred by enzymatic base extension. Products were subsequently fluorescently stained. The intensities of the beads' fluorescence were detected by the Illumina BeadArray Reader, and were in turn analyzed using Bead Studio software for automated genotype.

Statistical Analysis

Statistical significance was determined according to an independent sample t-test using the SPSS program version 11.5 as specified.

CHAPTER IV

RESULTS

Chromosomal translocation in the proband and family members

We performed chromosome analysis of the proband and her family members on the metaphase spreads. The results showed an apparently reciprocal balanced translocation in our patient.

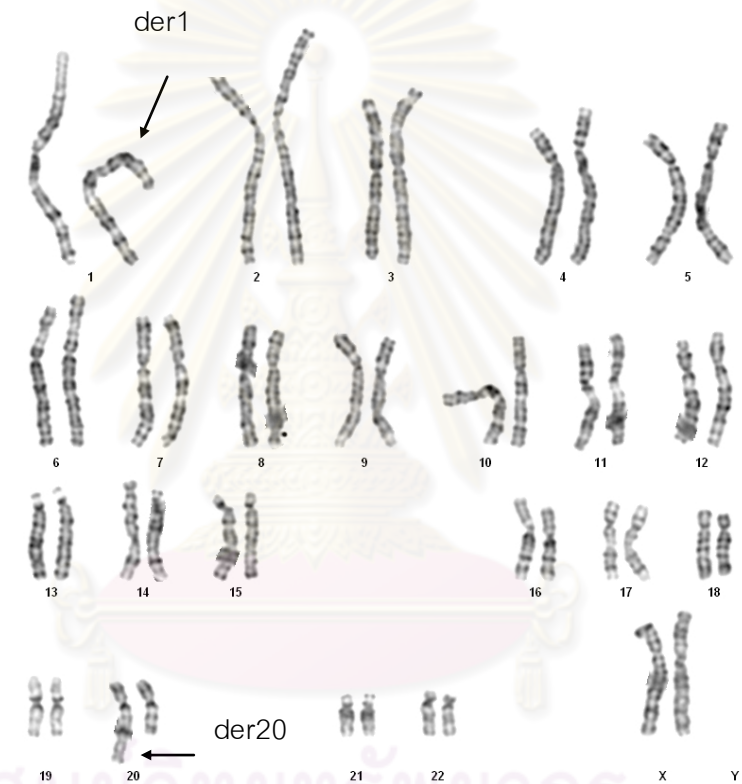


Figure 14. Chromosome analysis of the proband showing 46XX, t(1;20)(p34.1;q13.13).

This similar translocation was also present in her unaffected mother and other unaffected family members (Figure 14-17) but not in her elder brother (Figure 18). The pedigree of this family was shown in Figure 19.

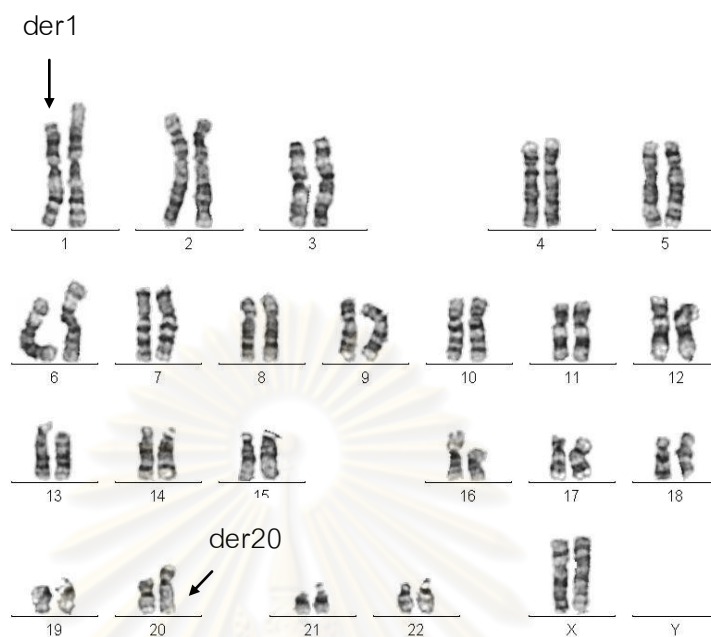


Figure 15. Chromosome analysis of the younger sister showing 46XX, t(1;20)(p34.1;q13.13).



Figure 16. Chromosome analysis of the elder sister showing 46XX, t(1;20)(p34.1;q13.13).

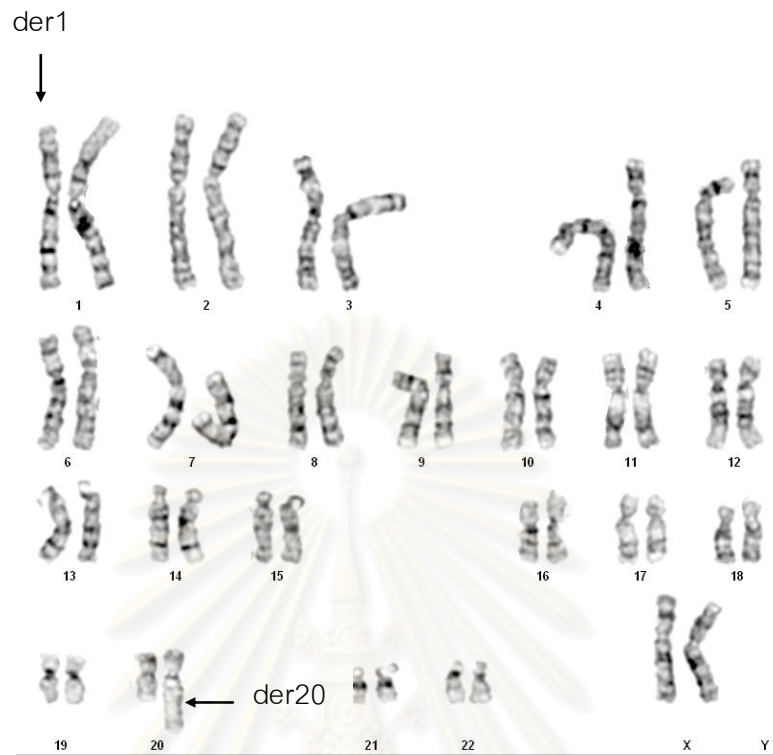


Figure 17. Chromosome analysis of the mother showing 46XX, t(1;20)(p34.1;q13.13).

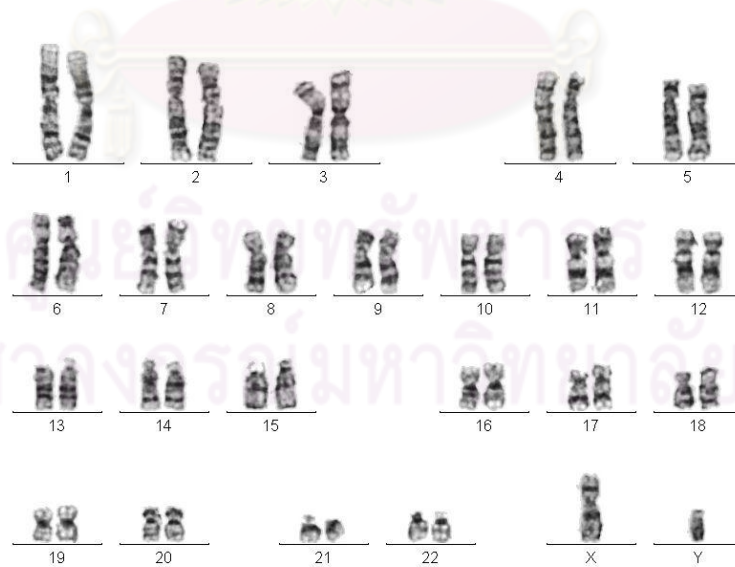


Figure 18. Chromosome analysis of the elder brother showing normal 46XY.

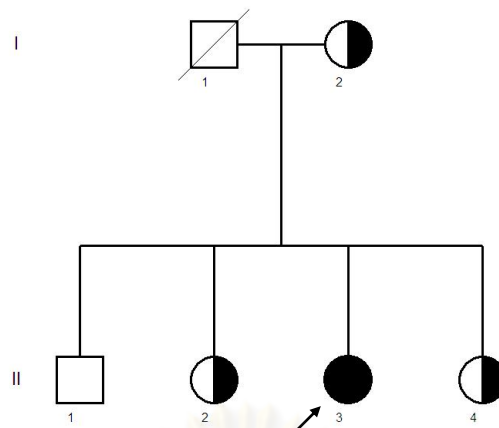


Figure 19. Pedigree of the family members showed that the patient, the unaffected mother and both unaffected sisters carried the balanced translocation of 46XX, t(1;20)(p34.1;q13.13). (black circle = proband, half filled circle = unaffected members with balanced translocation)

Familial, reciprocal autosomal translocation segregating with a specific phenotype, although rare, has proved useful for characterizing disease genes. A familial and apparently silent reciprocal translocation is occasionally observed in a phenotypically abnormal proband. From a theoretical viewpoint, such cases may result from mere chance, or reflect autosomal recessive inheritance, where one allele is disrupted by the translocation and the other allele by an intragenic mutation (67).

FISH analysis with breakpoint spanning clones

In order to characterize the translocation breakpoints, sequential FISH analysis was performed with BAC- and PAC-clones with inserts derived from 1p31 to 1p34 and 20q11 to 20q13 (Table 6). As shown in Figure 19, one of these PAC probes, RP5-1029K14, produced a FISH signal on both derivatives at 1p34.1 and 20p13.13, indicating that RP5-1029K14 encompasses the translocation breakpoint (Figure 19). The 126 kb genomic insert of the PAC contains the *PTPRF* gene in its telomeric portion (Figure 21). Whereas chromosome 20, three clones were spanning the translocation (RP1-73E16, RP11-347D21, RP5-991B18) (Figure 20). However, these three clones do not contain any known genes. We further narrow down the critical region, using approximately 10-kb probes created by a long range PCR technique and the RP5-1029K14 clone as template. One subfragment probe that gave a split signal was spanning from intron 8 to intron 12 of *PTPRF* gene (Figure 21).

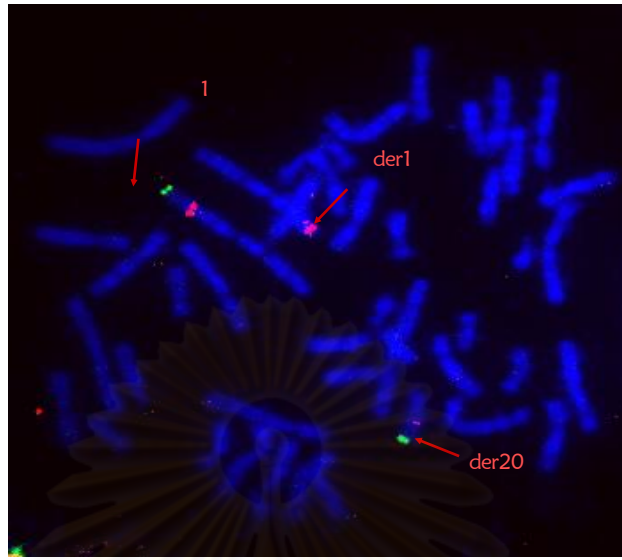


Figure 20. Fluorescence in situ hybridization of RP5-1029K14 giving split signals on chromosome 1. RP5-1029K14 spanning the 1p34.1 breakpoint is indicated by red signal. Hybridisation signals are found on both derivative chromosomes. The 1p subtelomeric probes labeled in green is served as a control.

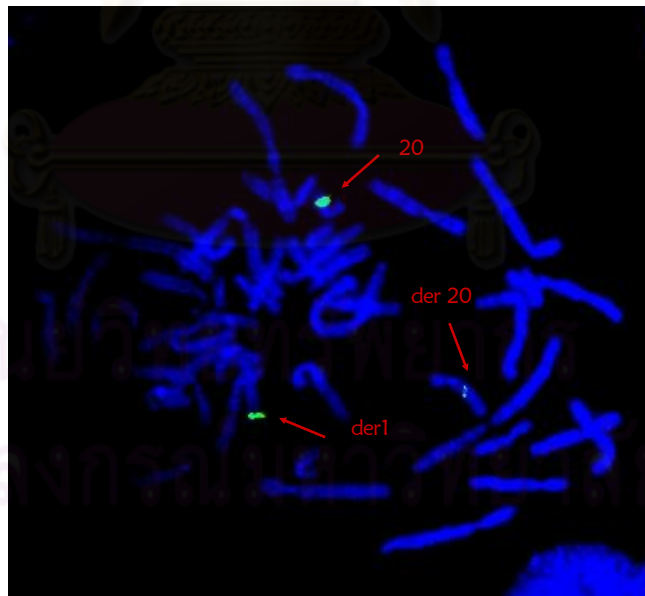


Figure 21. Fluorescence in situ hybridization of RP5-991B18 giving a split signal on chromosome 20. RP5-991B18 spanning the 20q13.13 breakpoint is indicated by green signal. Hybridisation signals are found on both derivative chromosomes.

Table 17. Summary of FISH results on chromosome 1

BAC/PAC clone	Location	Results
RP11-329N22	1p34.3	1p, der20
RP5-1066H13	1p34.2	1p, der20
RP11-282K6	1p34.1	1p, der20
RP1-92O14	1p34.1	1p, der20
RP11-506B15	1p34.1	1p, der20
RP5-1029K14	1p34.1	Split signal
RP11-184I16	1p34.1	1p, der1
RP11-570P14	1p34.1	1p, der1
RP11-30D7	1p34.1	1p, der1
RP11-69J16	1p34.1	1p, der1
RP11-291L19	1p34.1	1p, der1
RP11-322N21	1p34.1	1p, der1
RP11-49P4	1p33.0	1p, der1
RP11-346M5	1p33.0	1p, der1
RP11-330M19	1p33.0	1p, der1
RP11-329A14	1p33.0	1p, der1
RP11-428D12	1p33.0	1p, der1
RP11-296A18	1p32.3	1p, der1
RP11-334A14	1p32.3	1p, der1
RP11-109I2	1p32.3	1p, der1
RP11-243M12	1p32.2	1p, der1
RP11-470E16	1p32.1	1p, der1
RP11-32I17	1p31.3	1p, der1

Table 18. Summary of FISH results on chromosome 20

BAC/PAC clone	Location	Results
RP4-614O4	20q11.22	20q, der20
RP11-425M5	20q11.23	20q, der20
RP5-1123D4	20q12	20q, der20
RP4-753D4	20q13.11	20q, der20
RP1-47A22	20q13.11	20q, der20
RP3-453C12	20q13.12	20q, der20
RP5-1050K3	20q13.12	20q, der20
RP4-569M23	20q13.13	20q, der20
RP1-73E16	20q13.13	Split signal
RP11-347D21	20q13.13	Split signal
RP1-66N13	20q13.13	20, der1
RP5-991B18	20q13.13	Split signal
RP5-1164I10	20q13.13	20q, der1
RP4-791K14	20q13.13	20q, der1
RP5-1114A1	20q13.2	20q, der1
RP11-80K6	20q13.2	20q, der1
RP4-749H19	20q13.31	20q, der1
RP5-1018E9	20q13.32	20q, der1
RP4-719C8	20q13.32	20q, der1
RP11-157P1	20q13.33	20q, der1

Table 19. Summary of FISH results from subfragment probe on chromosome 1 and 20

BAC/PAC Subfragment	Location	Results
RP5-1029K14-F1/R2	1p34.1	1p, der20
RP5-1029K14-F2/R3	1p34.1	Split signal
RP5-1029K14-F3/R4	1p34.1	1p, der1
RP11-347D21-F2/R1	20q13.13	20q, der20
RP11-347D21-F3/R2	20q13.13	20q, der20
RP11-347D21-F4/R3	20q13.12	Split signal
RP11-347D21-F5/R4	20q13.13	20q, der1
RP11-347D21-F6/R5	20q13.13	20q, der1

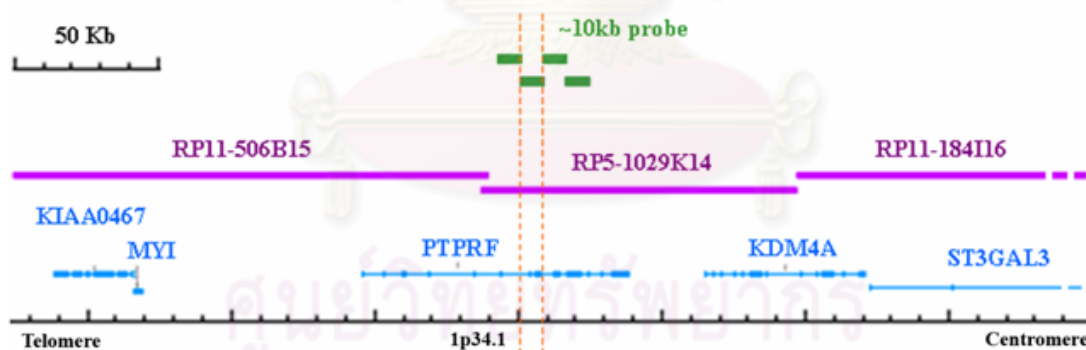
Schematic of the breakpoint and *PTPRF* gene

Figure 22. Schematic representation of the breakpoint and *PTPRF* on chromosome 1 modified from the NCBI Map Viewer (www.ncbi.nlm.nih.gov/mapview). 10 kb probes are shown in green, BAC/PAC contigs covering the 1p34.1 breakpoint are shown in purple. The orange lines indicate the critical region.

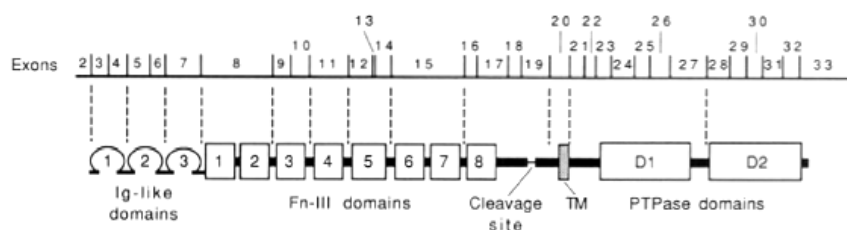


Figure 23. Schematics of the *PTPRF* gene including 33 exons encoding two tandem phosphatase domains which dominate its intracellular sequence, three immunoglobulin-like domains and eight fibronectin-type III domains in its extracellular E-subunit (68)

PTPRF, also known as Leukocyte Common Antigen-Related molecule (LAR), is a member of the protein tyrosine phosphatase (PTP) family. This PTP contains extracellular domain of three immunoglobulin-like domains in combination with eight fibronectin type-III-like repeats, a single transmembrane domain, and two intracellular tyrosine phosphatase domains. The *PTPRF* gene spans 92 kb, contains 34 exons, with an open reading frame of 5,724 bp, encoding 1,907 amino-acid protein.

To substantiate the role of *PTPRF* in human mammary gland development and to search for differences between the affected proband and her unaffected mother and sisters, we studied the its RNA levels by quantitative real-time analysis (qRT) and protein level by western blot analysis using RNA and protein extracted from the EBV-transformed lymphoblastoid cell lines, respectively.

Quantitative RT-PCR of *PTPRF* expression

We performed relative quantification of *PTPRF* RNA using both proximal and distal probes. GAPDH was used for normalization. Relative expression analysis revealed that both proximal (before the breakpoint) and distal *PTPRF* expressions of the proband were significantly decreased ($p < 0.01$) compared with those of her mother, elder sister and unaffected control (Figure 24) The higher RNA levels detected in the mother and elder sister

using the 5' probe than that using the 3' probe are speculated to be due to a feedback mechanism to increase transcription of both *PTPRF* alleles.

But because of the breakpoint, the level of the intact *PTPRF* RNA, representing by the RNA level determined by the 3' probe was lower. As expected, the *PTPRF*'s RNA level in the mother determined by the 3' probe was approximately half of that of control. However, the reasons that *PTPRF*'s RNA level in the sister was much higher than that of control remain to be elucidated.

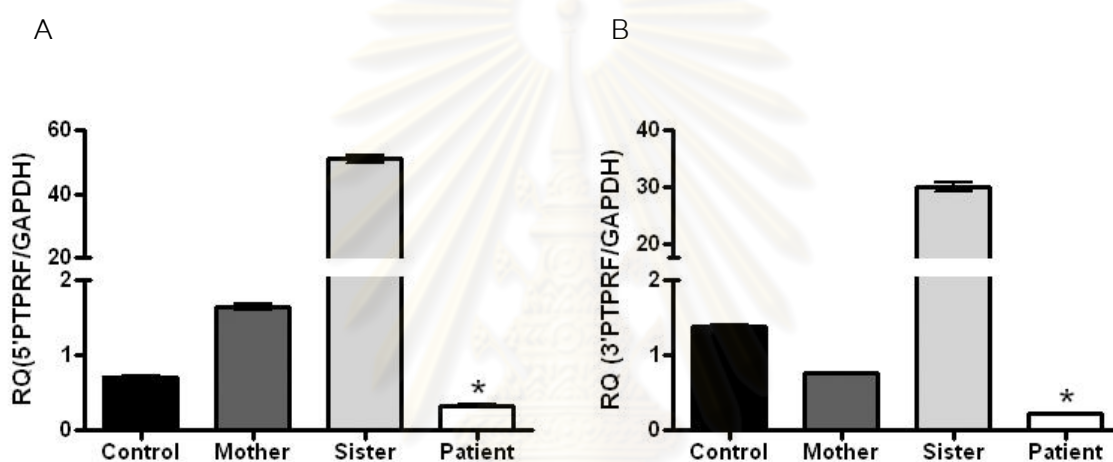


Figure 24. Quantitative real-time PCR results. (A) Relative quantification of 5' *PTPRF* probe (proximal to the breakpoint) showed that the expression level in the patient was significantly decreased compared with control, mother and sister. (B) Similarly, relative quantification of the 3' *PTPRF* probe (distal to the breakpoint) showed a significant decreased expression in the patient. Data represent means \pm SEM. * indicates $P < 0.01$ (independent 1-tailed t-test).

Absence of protein expression in the proband

The results showed almost absence of *PTPRF* expression in the proband while that of her unaffected mother and elder sister did have a significant ($p < 0.05$) remaining level of *PTPRF* protein (Figure 25). These experiments on *PTPRF* expression clearly showed

differences between the proband and her unaffected mother and elder sister, although they harbored the same balanced chromosome.

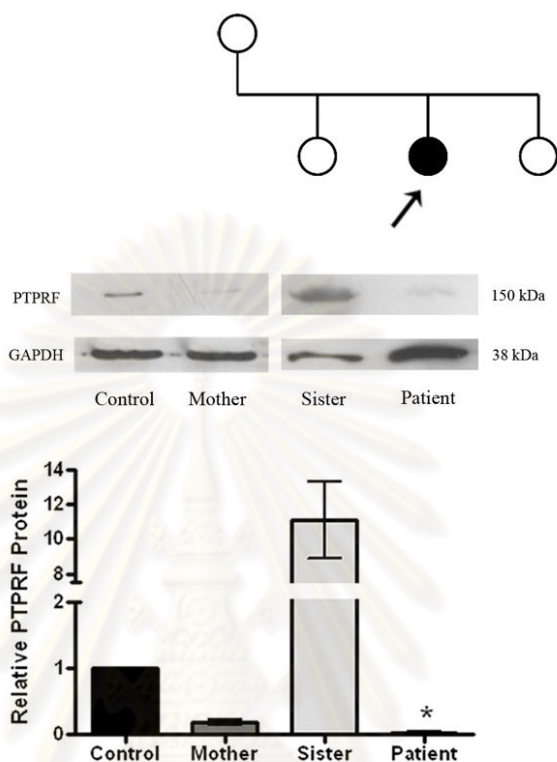


Figure 25. Western blot analysis of PTPRF protein of the patient showed a decreased level of the PTPRF compared with that in the mother, sister and unaffected control. Data represent means \pm SEM. * indicates $P < 0.05$ (independent 1-tailed t-test).

Mutation analysis of the *PTPRF* gene

We then attempted to find the pathogenic mutation in the other allele of PTPRF of the proband. Moreover, genomic DNA from patients of the Netherlands and Chile was also included. PCR-sequencing of its entire coding regions and its promoter (-654 to + 294) (109), although revealed many polymorphisms (Table 20) did not show any pathogenic mutations. Reverse transcribed – PCR (RT-PCR) using only Thai patient's RNA obtained from peripheral leukocytes found no aberrant splicing.

Table 20. Summary of polymorphism found in three patients

Location	Reference SNP	Variation class	Thai	Netherlander	Chilean
Intron 5	rs2842185	SNP	TT	CT	TT
Intron 5	rs2842186	SNP	AG	AA	AA
Exon 6	rs1065771	SNP	CC	CT	TT
Intron 6	rs943513	SNP	GG	GA	GG
Intron 6	g.39009delG	Deletion	GG	GG	(-/G)
Intron 6	rs11210874	SNP	TC	TC	TT
Intron 9	rs2304353	SNP	GG	AG	GG
Intron 9	g.60814G>T	SNP	GG	GT	GG
Intron 10	rs7540068	SNP	GT	GT	TT
Intron 10	rs7553297	SNP	AG	AG	GG
Exon 11	rs3828151	SNP	CA	CA	AA
Intron 14	rs12023161	SNP	AG	AG	GG
Intron 17	rs17371903	SNP	AA	AG	AA
Exon 19	rs631248	SNP	GA	AA	AA
Exon 20	rs1065772	SNP	CT	CT	TT
Exon 20	rs10890266	SNP	CT	CT	TT
Intron 20	rs539096	SNP	AG	GG	GG
Intron 23	rs603542	SNP	CT	CC	CC
Intron 23	rs571862	SNP	CT	TT	TT
Exon 25	rs641365	SNP	TC	CC	CC
Exon 25	rs641351	SNP	GA	AA	AA
Exon 27	rs1143701	SNP	CT	TT	TT
Intron 30	rs568639	SNP	TC	CC	CC
Exon 33	rs1143702	SNP	CT	TT	TT

Table 21. Summary results of our patient, her family members and unrelated patients

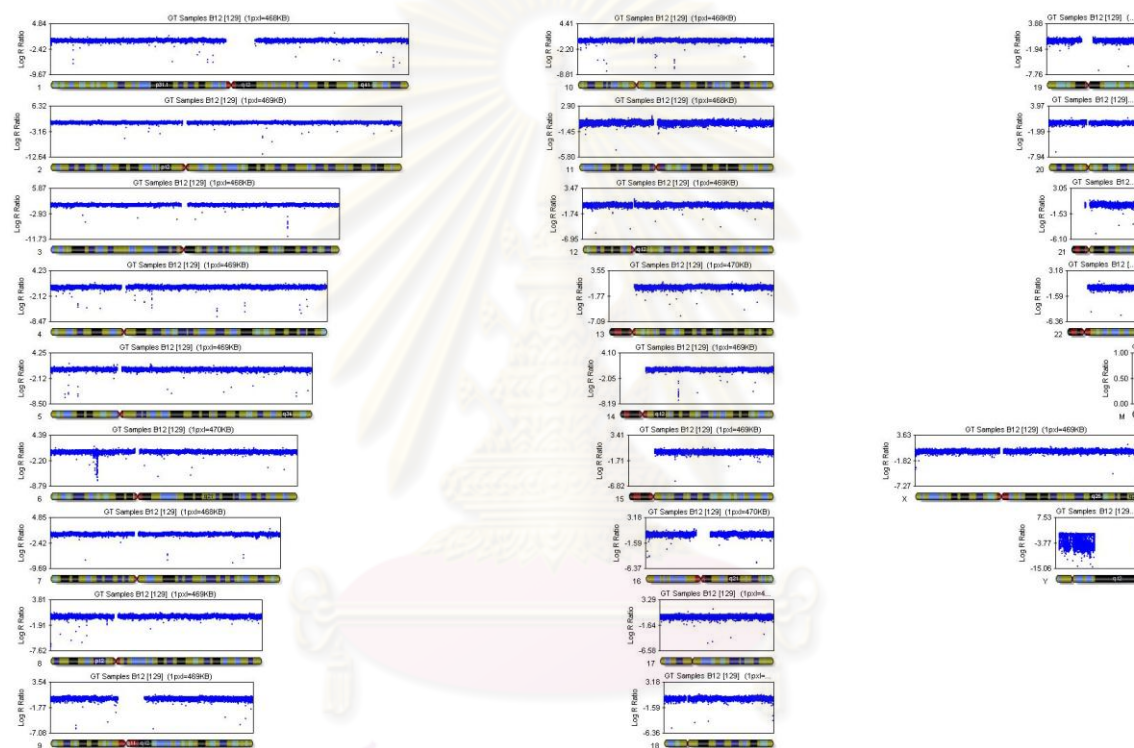
Sample	Phenotype	Chromosome	DNA analysis		RNA analysis
			Promoter	CDS	cDNA
Thai Proband	Bilateral amastia with ectodermal dysplasia	t(1;20)(p34.1;q13.13)	+92delGGCTCC ¹	Normal	Normal
Thai Mother	Normal	t(1;20)(p34.1;q13.13)	Normal	-	-
Thai Elder Sister	Normal	t(1;20)(p34.1;q13.13)	Normal	-	-
Thai Younger Sister	Normal	t(1;20)(p34.1;q13.13)	+92delGGCTCC ¹	-	-
Thai Elder Brother	Normal	Normal	+92delGGCTCC ¹	-	-
Chilean Proband ²	Bilateral amastia with hypohydrotic ectodermal	Normal	+92insGGCTCC ¹	Normal	-
Netherlander Proband ³	Bilateral amastia with hypohydrotic ectodermal	Normal	+23insGGCGGC	Normal	-
Netherlander Father	-	-	Normal	-	-
Netherlander Mother	-	-	Normal	-	-

CDS = coding sequence, cDNA = complementary DNA

No overlapping chromosomal aberrations in three patients

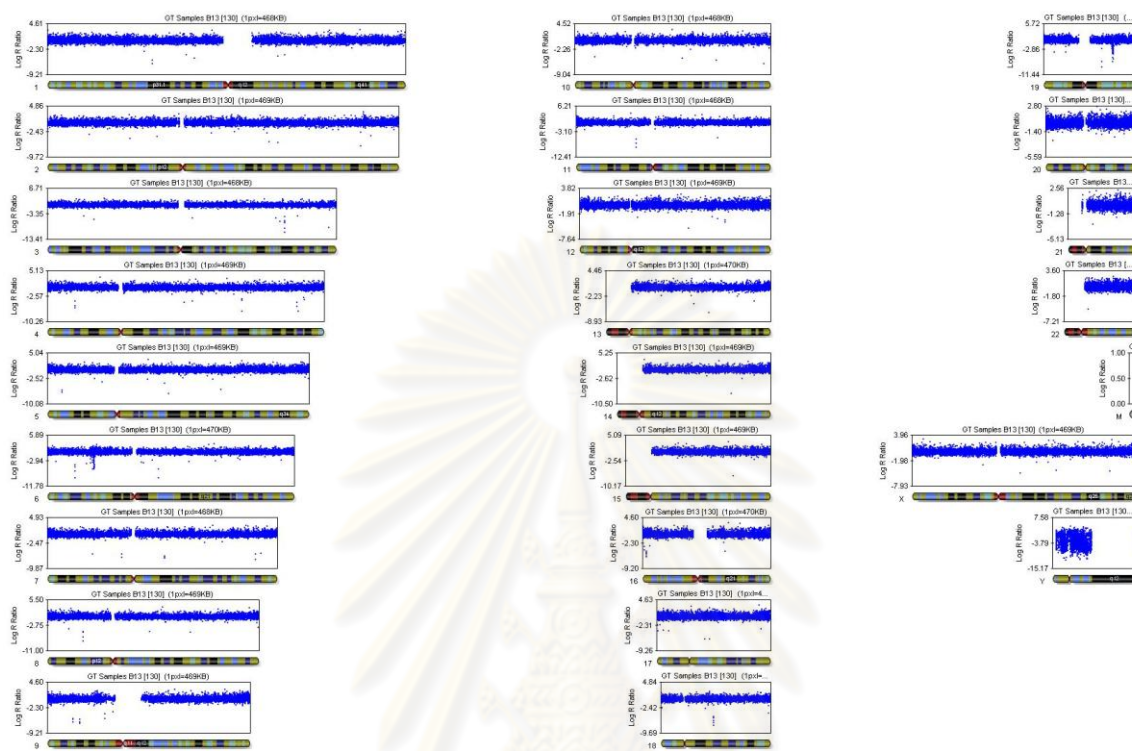
Measurement of both DNA copy number and allelic ratios in three patients using high-density SNP genotyping array did not show evidence of overlapping deletions or duplications (Figure 26-28).

Figure 26. 1M SNP Array result of the Thai patient.



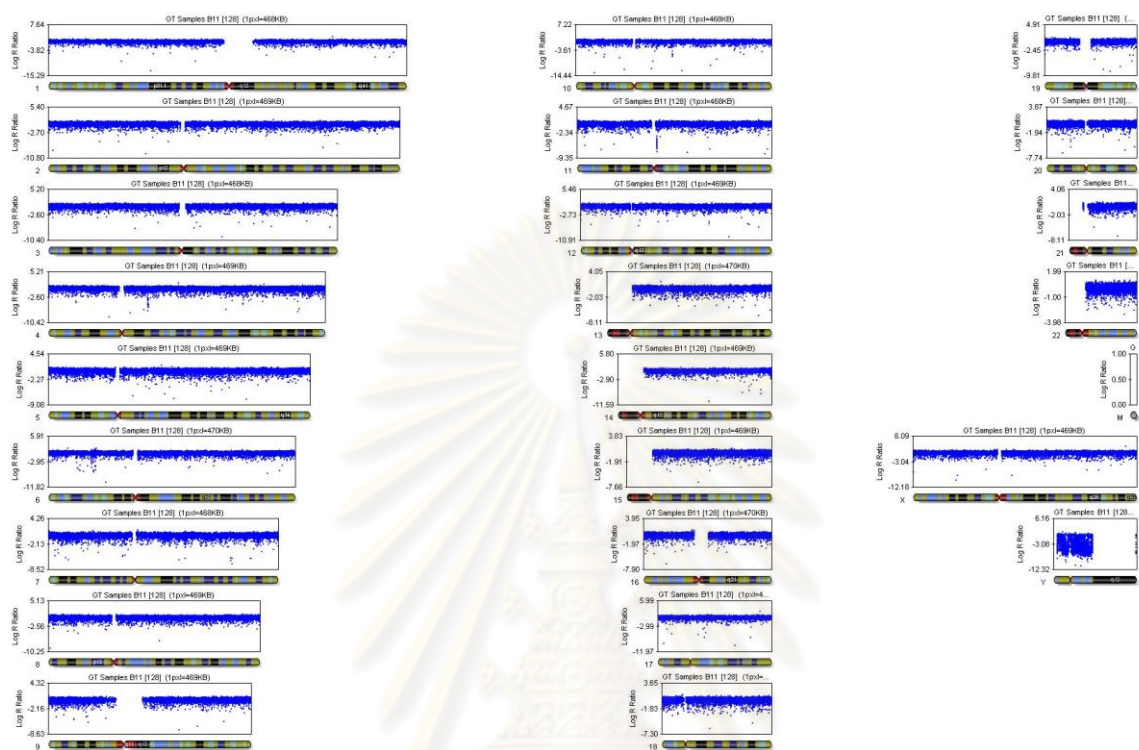
ศูนย์วิทยุทรัพยากร
จุฬาลงกรณ์มหาวิทยาลัย

Figure 27. 1M SNP Array result of the patient from Chile.



ศูนย์วิทยุทรัพยากร
จุฬาลงกรณ์มหาวิทยาลัย

Figure 28.1M SNP Array result of the patient from Netherlands.



ศูนย์วิทยุทรัพยากร
จุฬาลงกรณ์มหาวิทยาลัย

Haplotype analysis

Microsatellite analysis of chromosome 1 revealed that the proband and her sisters although harbored the same balanced translocation, inherited a different paternal chromosome (Figure 29).

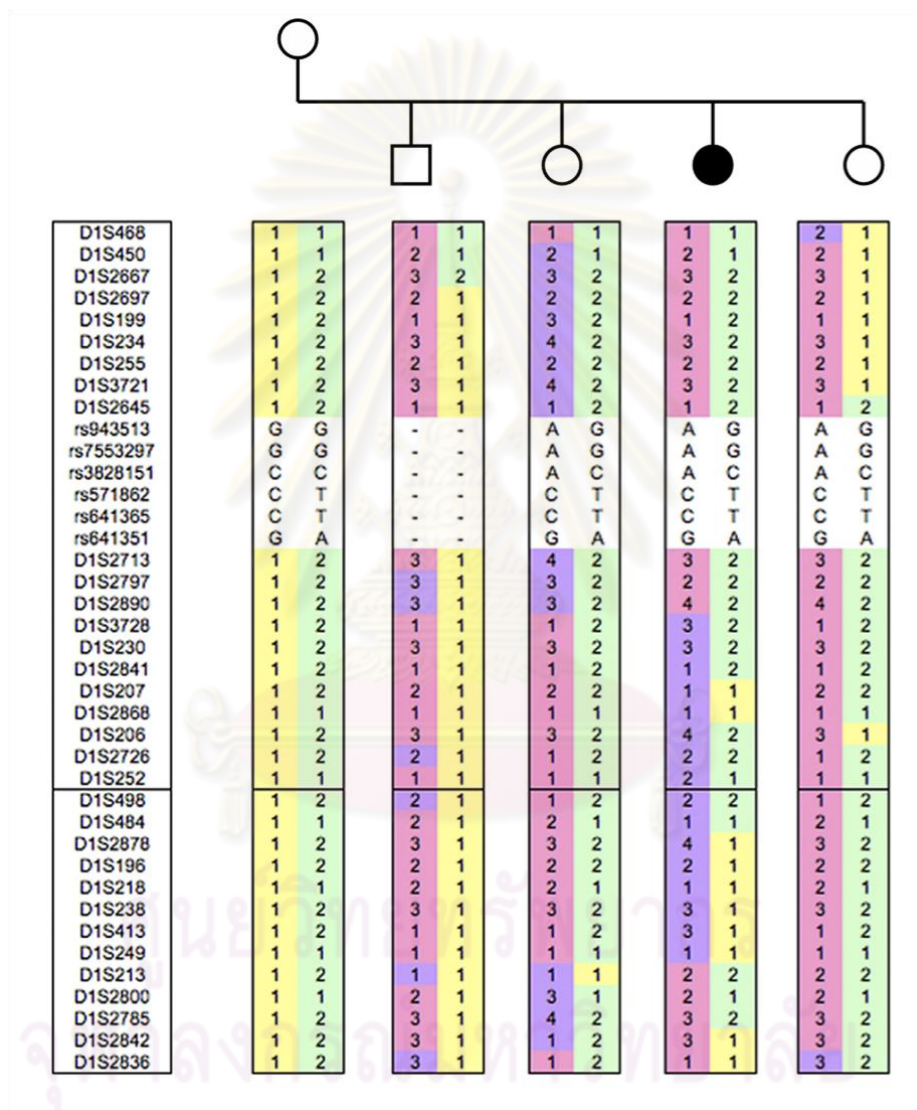


Figure 29. Haplotype analysis of chromosome 1 of family members. Two square vertical boxes on each row indicate the border of 1p and 1q, respectively. Region with transparent background indicate uninformative intragenic SNP. Haplotype of each member was imputed. Colors of each row represent the inherited haplotype.

PTPRF gene phylogeny in mammals and non mammals

A nearly complete cDNA of *PTPRF* genes in 29 species were used for phylogenetic analysis. Phylogenetic trees were constructed by the neighbor-joining method and maximum parsimony. Results showed that branching pattern of mammals are separated from non-mammals. Platypus, the only mammals that lay eggs, is the first branch that classified mammals out of non-mammals. We provide evidence that *PTPRF* may have a role in evolution of mammals. However, its presence in non-mammals indicated that the gene may not only involve in mammary gland development but also has other functions.

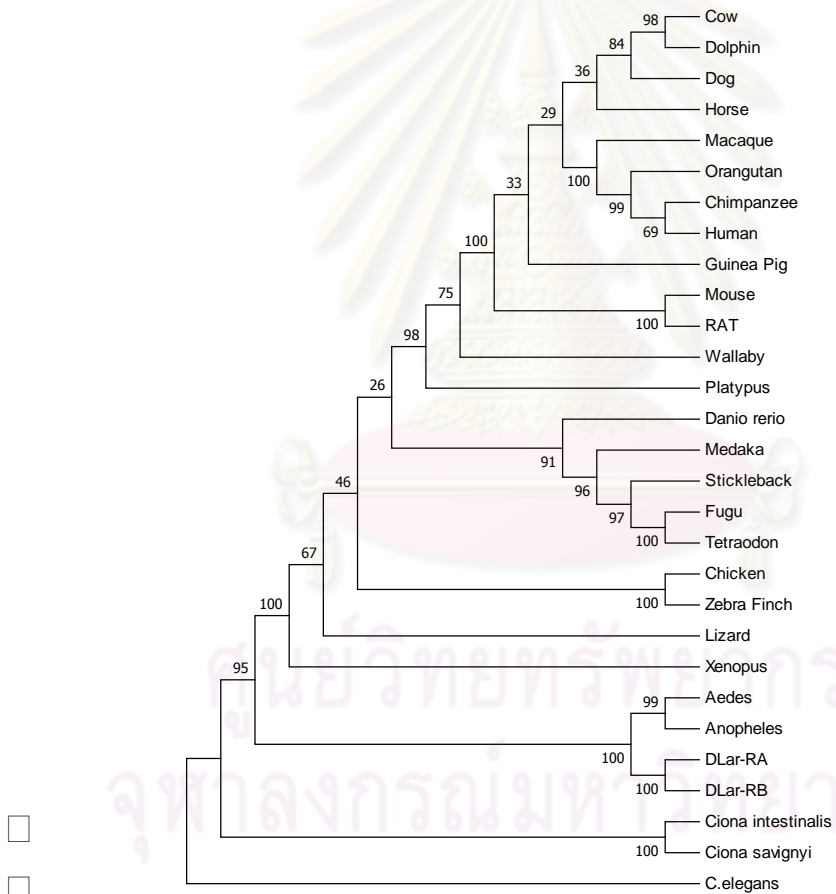


Figure 30. Evolutionary relationships of 29 taxa using neighbor Joining model (110). The evolutionary history was inferred using the Neighbor-Joining method. The optimal tree with the sum of branch length = 2.69166874 was shown. The percentage of replicate trees in which the associated taxa clustered together in the bootstrap test (1000 replicates) was

shown next to the branches (111). The evolutionary distances were computed using the Maximum Composite Likelihood method (112) and were in the units of the number of base substitutions per site. All positions containing gaps and missing data were eliminated from the dataset (Complete deletion option). There were a total of 1518 positions in the final dataset. Phylogenetic analyses were conducted in MEGA4 (108).

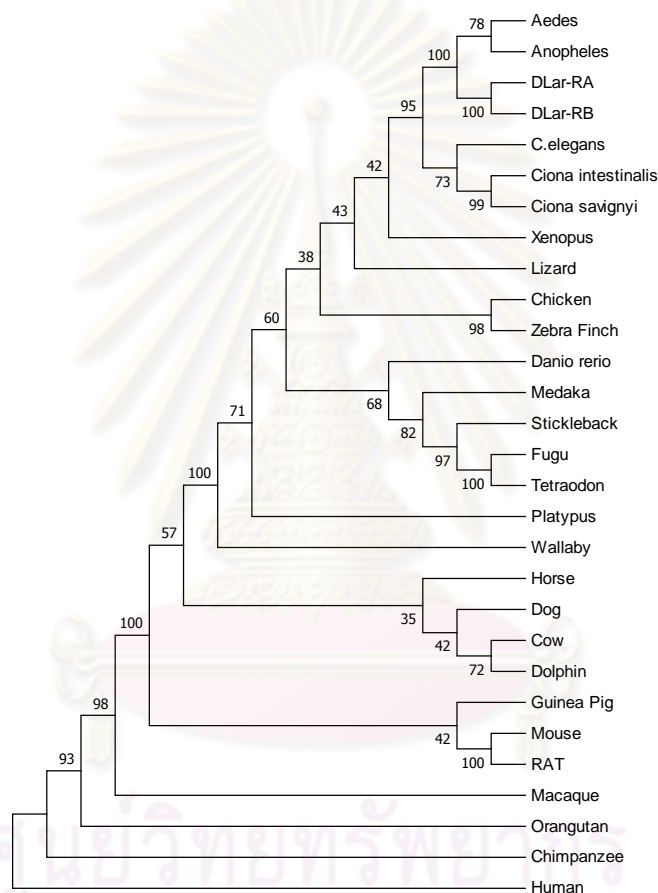


Figure 31. Evolutionary relationships of 29 taxa using Maximum Parsimony model (113). The evolutionary history was inferred using the Maximum Parsimony method. Tree #1 out of 3 most parsimonious trees (length = 4093) was shown. The consistency index is (0.394018), the retention index is (0.535757), and the composite index is 0.228151 (0.211098) for all sites and parsimony-informative sites (in parentheses). The percentage of replicate trees in which the associated taxa clustered together in the bootstrap test (1000 replicates) was shown next to the branches (111). The MP tree was obtained using the Close-Neighbor-

Interchange algorithm with search level 3 (111, 114) in which the initial trees were obtained with the random addition of sequences (10 replicates). The codon positions included were 1st+2nd+3rd+Noncoding. All positions containing gaps and missing data were eliminated from the dataset. There were a total of 1518 positions in the final dataset, out of which 791 were parsimony informative. Phylogenetic analyses were conducted in MEGA4 (108).



ศูนย์วิทยทรัพยากร
จุฬาลงกรณ์มหาวิทยาลัย

CHAPTER V

DISCUSSION

Mammary gland makes mammals different from other organisms. Although excellent progress has recently been made in defining the signaling pathways that are involved in the mammary gland development in mice (25), current knowledge about human mammary gland development is very restricted. Patients with absence of breast provide a way to identify genes involved in human breast development. But the fact that maintaining our human species relies on mammary gland development may lie behind the reason of the very rare incidence of bilateral amastia, with only 53 patients reported in the literature (Table 2).

Although strictly speaking, athelia refers to absence of the nipple, and amastia refers to absence of the breast, these terms have been used interchangeably (13). The term congenital breast absence is a separate entity from hypoplasia of the breast. Complete breast absence is defined by the absence of the nipple, whereas nipples are present in hypoplasia of the breast (48). However, there were no cases reported with amastia having normal nipples (13). Conversely, many cases have been reported with absence or hypoplasia of nipples but the mammary tissue remains (115, 116). This is consistent with the embryology of the breast in which the development of mammary gland occurs before that of the nipples.

Syndromes associated with the absence of breast and nipple include ectodermal dysplasia of the tricho-odonto-onychial type (3), congenital amastia with polywhorls and webbed fingers (5), acral-renal-ectodermal-dysplasia-lipoatrophic-diabetes (AREDYLD syndrome) (6, 7), bilateral amastia with ureteral triplication and dysmorphism (8), amastia with vaginal agenesis (9) and the scalp-ear-nipple syndrome (SEN or Finlay-Marks syndrome) (10, 11, 13-18). The latter is the most associated syndrome. Additionally, renal involvement has been reported in some cases of scalp-ear-nipple syndrome (16, 17). The structural ear malformation is presented in this disorder but not all patients had hearing impairments.

The most overlapping features in all associated syndromes in patients with absence of breast and nipple are the defects in ectoderm. It is possible that the disease

gene may underlie etiology behind both ectodermal tissue and breast development. The wide range of associated features presented in the patients may contribute to different entity. On the other hand, those syndromes may literally be the same disorder with variable expressivity.

The features in our case include complete absence of both breasts and nipples along with ectodermal dysplasia and unilateral renal agenesis. The entire features resemble the scalp-ear-nipple syndrome. However, the scalp-ear-nipple syndrome appears to be inherited as an autosomal dominant trait. In contrast, other syndromic and isolated forms of amastia and athelia may be sporadic occurrences, or be inherited mainly in either an autosomal dominant or autosomal recessive pattern. Our case is sporadic forms of amastia. Surprisingly, her cytogenetic analysis revealed an apparently reciprocal balanced translocation of $t(1;20)(p34.1;q13.13)$. The chromosomal aberration together with very rare prevalence of the amastia itself made our patient an invaluable case to determine the causative gene. To our knowledge the $t(1;20)(p34.1;q13.13)$ has not been observed in amastia patient or reported in any case. It is very likely that the underlying gene for bilateral amastia could be interrupted by the breakpoint. However, cytogenetic analyses of her family members revealed that the unaffected mother and both unaffected sisters carried the same balanced translocation. Hence, the translocation in the patient is not *de novo*, raising the possibility of autosomal recessive trait.

Although, this balanced translocation was also detected in her unaffected mother and sisters, a possibility of a gene interrupted by a breakpoint remains. The first example of a gene responsible for an autosomal recessive disorder identified by a chromosomal balanced translocation was the *ALMS1* gene for Alström syndrome (67). The gene was found to be interrupted by a breakpoint in a translocated chromosome, while the other allele had an intragenic mutation. We therefore determined to find out whether there were any genes interrupted by the breakpoints in our patient.

Fluorescence in situ hybridization technique (FISH) was performed on metaphase spreads with BAC/PAC as probes. We found that the breakpoints on chromosomes 1 were in the RP5-1029K14 clone containing a gene, Protein Tyrosine

Phosphatase Receptor type F (*PTPRF*). The breakpoint on chromosome 20 was obtained from three clones (RP1-73E16, RP11-347D21, RP5-991B18) giving a split signal. Nevertheless, regions covering these three clones did not contain any known gene.

We further narrowed down the critical region, using approximately 10-kb probes created by a long range PCR technique and the RP5-1029K14 clone as template. One subfragment probe that gave a split signal was spanning from intron 8 to intron 12 of the *PTPRF* gene. We analysed the repetitive sequence elements in the vicinity of the breakpoint region and found that they were Alu, MIR (mammalian interspersed repeat), LINE-L2, ERVL-MaLRs (endogenous Retrovirus; Transposable Element - mammalian apparent LTR-retro-transposon). It is tempting to speculate that these transposable sequence elements have promoted this translocation. This situation is similar to other reported familial germline translocations which are also localized in regions rich in repetitive sequences (117).

PTPRF, also known as Leukocyte Common Antigen-Related molecule (*LAR*), is a member of the protein tyrosine phosphatase (PTP) family. This PTP contains extracellular domain of three immunoglobulin-like domains in combination with eight fibronectin type-III-like repeats, a single transmembrane domain, and two intracellular tyrosine phosphatase domains (68). *PTPRF* spans 92 kb, contains 34 exons, with an open reading frame of 5,724 bp, encoding a 1,907 amino-acid protein.

In humans, *PTPRF* is known to be a tumor suppressor gene. Its somatic mutations were identified in 9 % of breast cancer (89). *PTPRF* was shown to increase expression markedly in human breast cancers (85). Although the fact that *Ptprf* knockout mice were incapable of delivering milk due to a defect in mammary glands (84) links the gene to mammary glands' development, *PTPRF* is not known to play a role in organ development in humans.

To substantiate the role of *PTPRF* in human mammary gland development and to search for differences between the affected proband and her unaffected mother and sisters, we studied the *PTPRF*'s RNA levels by quantitative real-time analysis (qRT) and protein level by western blot analysis using RNA and protein extracted from EBV-

transformed lymphoblastoid cell lines. Relative expression analysis revealed that both proximal and distal PTPRF expressions of the proband were significantly decreased ($p < 0.01$) compared with those of her mother, elder sister and the unaffected control. Western blot analysis showed almost absence of PTPRF expression in the proband while that of her unaffected mother and elder sister, although harbored the same balanced chromosome, did have a significant ($p < 0.05$) remaining level of PTPRF protein. The higher RNA level detected in the mother and sister than that of the control could be a feedback mechanism to increase transcription. But because of the breakpoint, the level of the intact PTPRF RNA in the mother, represented by the RNA level of the 3' probe was lower than that in the control and in proportion to its protein level. However, the reasons that PTPRF's RNA level in the sister was much higher than that of control remain to be elucidated.

We then attempted to find the pathogenic mutation in other two unrelated patients. First is the Netherlander patient with AREDYLD syndrome (6) and second is the Chilean patient presented with bilateral amastia and ectodermal dysplasia (20). Besides, the other allele of PTPRF of the proband was also investigated.

PCR-sequencing of its entire coding regions and its promoter, although revealed many polymorphisms did not show any pathogenic mutations. Interestingly, we found novel heterozygous promoter variant, +23insGGCGGC, in the Netherlander patient. This variant has never been reported and was not found in her parents indicating *de novo*. The possibility of being a pathogenic mutation remains elusive. Functional study is required to confirm a causative effect. However, we hypothesized that this is a recessive trait so the possibility of being pathogenic is unlikely.

Measurement of both DNA copy number and allelic ratios using high-density SNP genotyping array in all patients did not show evidence of overlapping deletions or duplications. We hypothesized that abnormal splicing could be an underlying determinant in our Thai patient. We then performed reverse transcribed – PCR using RNA from peripheral leukocytes as template. Unfortunately, no aberrant splicing was found.

Microsatellite analysis showed that the proband and her sisters inherited a different paternal chromosome. To identify which part of the different inherited paternal chromosome causes this disorder can be very difficult because the genomic regions containing cis -acting regulatory elements such as enhancers or repressors can stretch as much as 1 Mb in 5' - or 3' direction (118). An approach for the detection of such long range regulatory elements may arise from the study of highly conserved regions between evolutionary diverged species (118).

The reasons for the decreased expression of the *PTPRF* gene in the patient despite a lack of mutation in the other allele remains to be elucidated, but it could be due to increased methylation of the 5' CpG island of the *PTPRF* gene. The decreased expression may be due to modification of mRNA after transcription or regulation of mRNA expression by miRNA. Another possibility is the post transcription modification, recently, it was found that EGFR-induced cleavage could lead to degradation of the catalytic LAR-phosphatase subunit, thereby resulting in a significantly reduced overall cellular phosphatase activity of PTP-LAR (119) . In a context of different paternal allele, the transcriptional control or the alteration of chromatin structure can be disturbed in our patient. Whatever the reasons, one possibility is that the proband's paternal gene harbored a pathogenic mutation, when combined with the maternal translocated chromosome, resulting in severely deficient *PTPRF*'s RNA and an absence of *PTPRF* protein.

Phylogenic study of *PTPRF* gene in 29 species showed that branching pattern of mammals are separated from non-mammals. Its presence of *PTPRF* in non-mammals indicated that the gene may not only involve in mammary gland development but also has other functions. Yet, the role of *PTPRF* in human mammary gland development can not be ruled out. *PTPRF* may be one of the important genes in signaling pathways in breast development.

These findings should encourage further investigations, including the mutational screening of *PTPRF* in a large group of patients with bilateral amastia and ectodermal dysplasia. *PTPRF* Promoter might epigenetically silence the gene or leads to down regulation of its level of expression. Since *PTPRF* is known to be a tumor suppressor

gene, evaluation of the methylation status of *PTPRF* promoter might be another option to clarify an association with this pathology and its potential role in breast development.

We, for the first time, present evidences that *PTPRF* plays an important role in human breast development. This finding could have implications on evolution of mammals, developmental biology of human mammary glands and malignancy of breast cancer.



ศูนย์วิทยทรัพยากร
จุฬาลงกรณ์มหาวิทยาลัย

REFERENCES

- [1] Merlob P. Congenital malformations and developmental changes of the breast: a neonatological view. J Pediatr Endocrinol Metab. 16(4)(Apr-May 2003): 471-85.
- [2] Trier WC. Complete breast absence. Case report and review of the literature. Plast Reconstr Surg. 36(4)(October 1965): 431-9.
- [3] Tsakalagos N, Jordaan FH, Taljaard JJ, Hough SF. A previously undescribed ectodermal dysplasia of the tricho-odonto-onychial subgroup in a family. Arch Dermatol. 122(9)(September 1986): 1047-53.
- [4] Klinger M, Caviggioli F, Banzatti B, Fossati C, Villani F. Ectodermal dysplasia with amastia: a case of one-step reconstruction. Case Report Med. 2009;(2009): 927354.
- [5] Nelson MM, Cooper CK. Congenital defects of the breast - an autosomal dominant trait. S Afr Med J. 20;61(12)(March 1982): 434-6.
- [6] Breslau-Siderius EJ, Toonstra J, Baart JA, Koppeschaar HP, Maassen JA, Beemer FA. Ectodermal dysplasia, lipoatrophy, diabetes mellitus, and amastia: a second case of the AREDYLD syndrome. Am J Med Genet. 1;44(3)(October 1992): 374-7.
- [7] Pinheiro M, Freire-Maia N, Chautard-Freire-Maia EA, Araujo LM, Liberman B. AREDYLD: a syndrome combining an acrorenal field defect, ectodermal dysplasia, lipoatrophic diabetes, and other manifestations. Am J Med Genet. 16(1)(September 1983): 29-33.
- [8] Rich MA, Heimler A, Waber L, Brock WA. Autosomal dominant transmission of ureteral triplication and bilateral amastia. J Urol. 137(1)(January 1987): 102-5.
- [9]. Amesse L, Yen FF, Weisskopf B, Hertweck SP. Vaginal uterine agenesis associated with amastia in a phenotypic female with a de novo 46,XX,t(8;13)(q22.1;q32.1) translocation. Clin Genet. 55(6)(June 1999): 493-5.
- [10] Sobreira NL, Brunoni D, Cernach MC, Perez AB. Finlay-Marks (SEN) syndrome: a sporadic case and the delineation of the syndrome. Am J Med Genet A. 1;140(3)(February 2006):300-2.

- [11] Le Merrer M, Renier D, Briard ML. Scalp defect, nipples absence and ears abnormalities: an other case of Finlay syndrome. Genet Couns. 2(4)(1991): 233-6.
- [12] Tuffli GA, Laxova R. Brief clinical report: new, autosomal dominant form of ectodermal dysplasia. Am J Med Genet. 14(2)(February 1983): 381-4.
- [13] Baris H, Tan WH, Kimonis VE. Hypothelia, syndactyly, and ear malformation--a variant of the scalp-ear-nipple syndrome?: Case report and review of the literature. Am J Med Genet A. 15;134A(2)(April 2005): 220-2.
- [14] Edwards MJ, McDonald D, Moore P, Rae J. Scalp-ear-nipple syndrome: additional manifestations. Am J Med Genet. 15;50(3)(April 1994): 247-50.
- [15] Finlay AY, Marks R. An hereditary syndrome of lumpy scalp, odd ears and rudimentary nipples. Br J Dermatol. 99(4)(October 1978): 423-30.
- [16] Picard C, Couderc S, Skojaei T, Salomon R, de Lonlay P, Le Merrer M, et al. Scalp-ear-nipple (Finlay-Marks) syndrome: a familial case with renal involvement. Clin Genet. 56(2)(August 1999): 170-2.
- [17] Plessis G, Le Treust M, Le Merrer M. Scalp defect, absence of nipples, ear anomalies, renal hypoplasia: another case of Finlay-Marks syndrome. Clin Genet. 52(4)(October 1997): 231-4.
- [18] Al-Gazali L, Nath R, Iram D, Al Malik H. Hypotonia, developmental delay and features of scalp-ear-nipple syndrome in an inbred Arab family. Clin Dysmorphol. 16(2)(April 2007): 105-7.
- [19] Greenberg F. Choanal atresia and athelia: methimazole teratogenicity or a new syndrome? Am J Med Genet. 28(4)(December 1987): 931-4.
- [20] Ligia AD, Lay-Son GR, Sanz PC, C TS. Hypohydrotic ectodermal dysplasia, a clinical case and review of the literature. Rev Chil Pediatr. 76(2)(April 2005): 166-72.
- [21] Chu EY, Hens J, Andl T, Kairo A, Yamaguchi TP, Brisken C, et al. Canonical WNT signaling promotes mammary placode development and is essential for initiation of mammary gland morphogenesis. Development. 131(19)(October 2004): 4819-29.

- [22] Eblaghie MC, Song SJ, Kim JY, Akita K, Tickle C, Jung HS. Interactions between FGF and Wnt signals and Tbx3 gene expression in mammary gland initiation in mouse embryos. J Anat. 205(1)(July 2004): 1-13
- [23] Veltmaat JM, Van Veelen W, Thiery JP, Bellusci S. Identification of the mammary line in mouse by Wnt10b expression. Dev Dyn. 229(2)(February 2004): 349-56.
- [24] Mailleux AA, Spencer-Dene B, Dillon C, Ndiaye D, Savona-Baron C, Itoh N, et al. Role of FGF10/FGFR2b signaling during mammary gland development in the mouse embryo. Development. 129(1)(January 2002):53-60.
- [25] Robinson GW. Cooperation of signalling pathways in embryonic mammary gland development. Nat Rev Genet. 8(12)(December 2007): 963-72.
- [26] Bamshad M, Lin RC, Law DJ, Watkins WC, Krakowiak PA, Moore ME, et al. Mutations in human TBX3 alter limb, apocrine and genital development in ulnar-mammary syndrome. Nat Genet. 16(3)(July 1997): 311-5.
- [27] Davenport TG, Jerome-Majewska LA, Papaioannou VE. Mammary gland, limb and yolk sac defects in mice lacking Tbx3, the gene mutated in human ulnar mammary syndrome. Development. 130(10)(May 2003): 2263-73.
- [28] Veltmaat JM, Mailleux AA, Thiery JP, Bellusci S. Mouse embryonic mammogenesis as a model for the molecular regulation of pattern formation. Differentiation. 71(1)(January 2003): 1-17.
- [29] van Genderen C, Okamura RM, Farinas I, Quo RG, Parslow TG, Bruhn L, et al. Development of several organs that require inductive epithelial-mesenchymal interactions is impaired in LEF-1-deficient mice. Genes Dev. 15;8(22)(November 1994): 2691-703.
- [30] Chen J, Zhong Q, Wang J, Cameron RS, Borke JL, Isaacs CM, et al. Microarray analysis of Tbx2-directed gene expression: a possible role in osteogenesis. Mol Cell Endocrinol. 25;177(1-2)(May 2001): 43-54.
- [31] Cho KW, Kim JY, Song SJ, Farrell E, Eblaghie MC, Kim HJ, et al. Molecular interactions between Tbx3 and Bmp4 and a model for dorsoventral positioning of mammary gland development. Proc Natl Acad Sci USA. 7;103(45)(November 2006): 16788-93.

- [32] Phippard DJ, Weber-Hall SJ, Sharpe PT, Naylor MS, Jayatalake H, Maas R, et al. Regulation of Msx-1, Msx-2, Bmp-2 and Bmp-4 during foetal and postnatal mammary gland development. Development. 122(9)(September 1996): 2729-37.
- [33] Satokata I, Ma L, Ohshima H, Bei M, Woo I, Nishizawa K, et al. Msx2 deficiency in mice causes pleiotropic defects in bone growth and ectodermal organ formation. Nat Genet. 24(4)(April 2000): 391-5.
- [34] Foley J, Dann P, Hong J, Cosgrove J, Dreyer B, Rimm D, et al. Parathyroid hormone-related protein maintains mammary epithelial fate and triggers nipple skin differentiation during embryonic breast development. Development. 128(4)(February 2001):513-25.
- [35] Wysolmerski JJ, Philbrick WM, Dunbar ME, Lanske B, Kronenberg H, Broadus AE. Rescue of the parathyroid hormone-related protein knockout mouse demonstrates that parathyroid hormone-related protein is essential for mammary gland development. Development. 125(7)(April 1998): 1285-94.
- [36] Dunbar ME, Dann PR, Robinson GW, Hennighausen L, Zhang JP, Wysolmerski JJ. Parathyroid hormone-related protein signaling is necessary for sexual dimorphism during embryonic mammary development. Development. 126(16)(August 1999): 3485-93.
- [37] Hens JR, Wysolmerski JJ. Key stages of mammary gland development: molecular mechanisms involved in the formation of the embryonic mammary gland. Breast Cancer Res. 7(5)(2005): 220-4.
- [38] Hennighausen L, Robinson GW. Signaling pathways in mammary gland development. Dev Cell. 1(4)(October 2001): 467-75.
- [39] Hovey RC, Trott JF, Vonderhaar BK. Establishing a framework for the functional mammary gland: from endocrinology to morphology. J Mammary Gland Biol Neoplasia. 7(1)(January 2002): 17-38.
- [40] Heckman BM, Chakravarty G, Vargo-Gogola T, Gonzales-Rimbau M, Hadsell DL, Lee AV, et al. Crosstalk between the p190-B RhoGAP and IGF signaling pathways is required for embryonic mammary bud development. Dev Biol. 1;309(1)(September 2007): 137-49.

- [41] Chakravarty G, Hadsell D, Buitrago W, Settleman J, Rosen JM. p190-B RhoGAP regulates mammary ductal morphogenesis. Mol Endocrinol. 17(6)(June 2003): 1054-65.
- [42] Burck U, Held KR. Athelia in a female infant - heterozygous for anhidrotic ectodermal dysplasia. Clin Genet. 19(2)(February 1981): 117-21..
- [43] Wilson MG, Hall EB, Ebbin AJ. Dominant inheritance of absence of the breast. Humangenetik. 15(3)(1972): 268-70.
- [44] Perez Aznar JM, Urbano J, Garcia Laborda E, Quevedo Moreno P, Ferrer Vergara L. Breast and pectoralis muscle hypoplasia. A mild degree of Poland's syndrome. Acta Radiol. 37(5)(September 1996): 759-62.
- [45] Tawil HM, Najjar SS. Congenital absence of the breasts. J Pediatr. 73(5)(November 1968): 751-3.
- [46] Mathews J. Bilateral absence of breasts. N Y State J Med. 74(1)(January 1974): 87-9.
- [47] Kowlessar M, Orti E. Complete breast absence in siblings. Am J Dis Child. 115(1)(January 1968): 91-2.
- [48] Lin KY, Nguyen DB, Williams RM. Complete breast absence revisited. Plast Reconstr Surg. 106(1)(July 2000): 98-101.
- [49] Iamin MT, Kumar VP. Complete absence of breasts in a 24-year-old woman associated with ectodermal dysplasia. Plast Reconstr Surg. 111(2)(February 2003): 959-61.
- [50] Martinez-Chequer JC, Carranza-Lira S, Lopez-Silva JD, Mainero-Ratchelous F, Zenteno JC. Congenital absence of the breasts: a case report. Am J Obstet Gynecol. 191(1)(July 2004): 372-4.
- [51] Tommerup N. Mendelian cytogenetics. Chromosome rearrangements associated with mendelian disorders. J Med Genet. 30(9)(September 1993): 713-27.
- [52] Wirth J, Nothwang HG, van der Maarel S, Menzel C, Borck G, Lopez-Pajares I, et al. Systematic characterisation of disease associated balanced chromosome rearrangements by FISH: cytogenetically and genetically anchored YACs

- identify microdeletions and candidate regions for mental retardation genes. J Med Genet. 36(4)(April 1999): 271-8.
- [53] Bugge M, Bruun-Petersen G, Brondum-Nielsen K, Friedrich U, Hansen J, Jensen G, et al. Disease associated balanced chromosome rearrangements: a resource for large scale genotype-phenotype delineation in man. J Med Genet. 37(11)(November 2000): 858-65.
- [54] Warburton D. De novo balanced chromosome rearrangements and extra marker chromosomes identified at prenatal diagnosis: clinical significance and distribution of breakpoints. Am J Hum Genet. 49(5)(November 1991): 995-1013.
- [55] Erdogan F, Chen W, Kirchhoff M, Kalscheuer VM, Hultschig C, Muller I, et al. Impact of low copy repeats on the generation of balanced and unbalanced chromosomal aberrations in mental retardation. Cytogenet Genome Res. 115(3-4)(2006): 247-53
- [56] Lindenbaum RH, Clarke G, Patel C, Moncrieff M, Hughes JT. Muscular dystrophy in an X; 1 translocation female suggests that Duchenne locus is on X chromosome short arm. J Med Genet. 16(5)(October 1979): 389-92.
- [57] Cross I, Delhanty J, Chapman P, Bowles LV, Griffin D, Wolstenholme J, et al. An intrachromosomal insertion causing 5q22 deletion and familial adenomatous polyposis coli in two generations. J Med Genet. 29(3)(March 1992): 175-9.
- [58] Davison EV, Gibbons B, Aherne GE, Roberts DF. Chromosomes in retinoblastoma patients. Clin Genet. 15(6)(June 1979): 505-8.
- [59] Puissant H, Azoulay M, Serre JL, Piet LL, Junien C. Molecular analysis of a reciprocal translocation t(5;11) (q11;p13) in a WAGR patient. Hum Genet. 79(3)(July 1988): 280-2.
- [60] Puliti A, Caridi G, Ravazzolo R, Ghiggeri GM. Teaching molecular genetics: chapter 4-positional cloning of genetic disorders. Pediatr Nephrol. 22(12)(December 2007): 2023-9.
- [61] McKusick VA, Amberger JS. The morbid anatomy of the human genome: chromosomal location of mutations causing disease. J Med Genet. 30(1)(January 1993): 1-26.

- [62] Naritomi K, Hyakuna N, Suzuki Y, Orii T, Hirayama K. Zellweger syndrome and a microdeletion of the proximal long arm of chromosome 7. Hum Genet. 80(2)(October 1988): 201-2.
- [63] Naritomi K, Izumikawa Y, Ohshiro S, Yoshida K, Shimozawa N, Suzuki Y, et al. Gene assignment of Zellweger syndrome to 7q11.23: report of the second case associated with a pericentric inversion of chromosome 7. Hum Genet. 84(1)(December 1989): 79-80.
- [64] Buhler EM. Unmasking of heterozygosity by inherited balanced translocations. Implications for prenatal diagnosis and gene mapping. Ann Genet. 26(3)(1983): 133-7.
- [65] Pentao L, Lewis RA, Ledbetter DH, Patel PI, Lupski JR. Maternal uniparental isodisomy of chromosome 14: association with autosomal recessive rod monochromacy. Am J Hum Genet. 50(4)(April 1992): 690-9.
- [66] Fannemel M, Riise R, Lofterod B, Tommerup N. High-resolution chromosome analysis in autosomal recessive disorders: Laurence-Moon-Bardet-Biedl syndrome. Clin Genet. 43(2)(February 1993): 111-2..
- [67] Hearn T, Renforth GL, Spalluto C, Hanley NA, Piper K, Brickwood S, et al. Mutation of ALMS1, a large gene with a tandem repeat encoding 47 amino acids, causes Alstrom syndrome. Nat Genet. 31(1)(May 2002): 79-83.
- [68] O'Grady P, Krueger NX, Streuli M, Saito H. Genomic organization of the human LAR protein tyrosine phosphatase gene and alternative splicing in the extracellular fibronectin type-III domains. J Biol Chem. 7;269(40)(October 1994): 25193-9.
- [69] Streuli M, Krueger NX, Ariniello PD, Tang M, Munro JM, Blattler WA, et al. Expression of the receptor-linked protein tyrosine phosphatase LAR: proteolytic cleavage and shedding of the CAM-like extracellular region. Embo J. 11(3)(March 1992): 897-907.
- [70] Chagnon MJ, Uetani N, Tremblay ML. Functional significance of the LAR receptor protein tyrosine phosphatase family in development and diseases. Biochem Cell Biol. 82(6)(December 2004): 664-75.

- [71] Serra-Pages C, Saito H, Streuli M. Mutational analysis of proprotein processing, subunit association, and shedding of the LAR transmembrane protein tyrosine phosphatase. J Biol Chem. 23;269(38)(September 1994): 23632-41.
- [72] Aicher B, Lerch MM, Muller T, Schilling J, Ullrich A. Cellular redistribution of protein tyrosine phosphatases LAR and PTPsigma by inducible proteolytic processing. J Cell Biol. 11;138(3)(August 1997): 681-96.
- [73] Guan KL, Dixon JE. Evidence for protein-tyrosine-phosphatase catalysis proceeding via a cysteine-phosphate intermediate. J Biol Chem. 15;266(26)(September 1991): 17026-30.
- [74] Streuli M, Krueger NX, Thai T, Tang M, Saito H. Distinct functional roles of the two intracellular phosphatase like domains of the receptor-linked protein tyrosine phosphatases LCA and LAR. Embo J. 9(8)(August 1990): 2399-407.
- [75] Yu Q, Lenardo T, Weinberg RA. The N-terminal and C-terminal domains of a receptor tyrosine phosphatase are associated by non-covalent linkage. Oncogene. 7(6)(June 1992): 1051-7.
- [76] Tsujikawa K, Ichijo T, Moriyama K, Tadotsu N, Sakamoto K, Sakane N, et al. Regulation of Lck and Fyn tyrosine kinase activities by transmembrane protein tyrosine phosphatase leukocyte common antigen-related molecule. Mol Cancer Res. 1(2)(December 2002): 155-63.
- [77] Muller T, Choidas A, Reichmann E, Ullrich A. Phosphorylation and free pool of beta-catenin are regulated by tyrosine kinases and tyrosine phosphatases during epithelial cell migration. J Biol Chem. 9;274(15)(April 1999): 10173-83.
- [78] Streuli M, Krueger NX, Hall LR, Schlossman SF, Saito H. A new member of the immunoglobulin superfamily that has a cytoplasmic region homologous to the leukocyte common antigen. J Exp Med. 1;168(5)(November 1988): 1523-30.
- [79] O'Grady P, Thai TC, Saito H. The laminin-nidogen complex is a ligand for a specific splice isoform of the transmembrane protein tyrosine phosphatase LAR. J Cell Biol. 29;141(7)(June 1998): 1675-84.

- [80] Serra-Pages C, Kedersha NL, Fazikas L, Medley Q, Debant A, Streuli M. The LAR transmembrane protein tyrosine phosphatase and a coiled-coil LAR-interacting protein co-localize at focal adhesions. Embo J. 15;14(12)(June 1995): 2827-38.
- [81] Kypta RM, Su H, Reichardt LF. Association between a transmembrane protein tyrosine phosphatase and the cadherin-catenin complex. J Cell Biol. 134(6)(September 1996): 1519-29.
- [82] Kulas DT, Goldstein BJ, Mooney RA. The transmembrane protein-tyrosine phosphatase LAR modulates signaling by multiple receptor tyrosine kinases. J Biol Chem. 12;271(2)(January 1996): 748-54.
- [83] Zhang WR, Li PM, Oswald MA, Goldstein BJ. Modulation of insulin signal transduction by eutopic overexpression of the receptor-type protein-tyrosine phosphatase LAR. Mol Endocrinol. 10(5)(May 1996): 575-84..
- [84] Schaapveld RQ, Schepens JT, Robinson GW, Attema J, Oerlemans FT, Franssen JA, et al. Impaired mammary gland development and function in mice lacking LAR receptor-like tyrosine phosphatase activity. Dev Biol. 1;188(1)(August 1997): 134-46.
- [85] Yang T, Zhang JS, Massa SM, Han X, Longo FM. Leukocyte common antigen-related tyrosine phosphatase receptor: increased expression and neuronal-type splicing in breast cancer cells and tissue. Mol Carcinog. 25(2)(June 1999): 139-49.
- [86] Chang C, Yu TW, Bargmann CI, Tessier-Lavigne M. Inhibition of netrin-mediated axon attraction by a receptor protein tyrosine phosphatase. Science. 2;305(5680)(July 2004): 103-6.
- [87] Jirik FR, Harder KW, Melhado IG, Anderson LL, Duncan AM. The gene for leukocyte antigen-related tyrosine phosphatase (LAR) is localized to human chromosome 1p32, a region frequently deleted in tumors of neuroectodermal origin. Cytogenet Cell Genet. 61(4)(1992): 266-8.
- [88] Harder KW, Saw J, Miki N, Jirik F. Coexisting amplifications of the chromosome 1p32 genes (PTPRF and MYCL1) encoding protein tyrosine phosphatase LAR and L-myc in a small cell lung cancer line. Genomics. 10;27(3):552-3.

- [89] Wang Z, Shen D, Parsons DW, Bardelli A, Sager J, Szabo S, et al. Mutational analysis of the tyrosine phosphatome in colorectal cancers. Science. 21;304(5674)(May 2004): 1164-6.
- [90] Konishi N, Tsujikawa K, Yamamoto H, Ishida E, Nakamura M, Shimada K, et al. Overexpression of leucocyte common antigen (LAR) P-subunit in thyroid carcinomas. Br J Cancer. 22;88(8)(April 2003): 1223-8.
- [91] Levea CM, McGary CT, Symons JR, Mooney RA. PTP LAR expression compared to prognostic indices in metastatic and non-metastatic breast cancer. Breast Cancer Res Treat. 64(2)(November 2000): 221-8.
- [92] Ahmad F, Considine RV, Goldstein BJ. Increased abundance of the receptor-type protein-tyrosine phosphatase LAR accounts for the elevated insulin receptor dephosphorylating activity in adipose tissue of obese human subjects. J Clin Invest. 95(6)(June 1995): 2806-12.
- [93] Ahmad F, Goldstein BJ. Effect of tumor necrosis factor-alpha on the phosphorylation of tyrosine kinase receptors is associated with dynamic alterations in specific protein-tyrosine phosphatases. J Cell Biochem. 64(1)(January 1997): 117-27.
- [94] Kulas DT, Zhang WR, Goldstein BJ, Furlanetto RW, Mooney RA. Insulin receptor signaling is augmented by antisense inhibition of the protein tyrosine phosphatase LAR. J Biol Chem. 10;270(6)(February 1995): 2435-8.
- [95] Mooney RA, Kulas DT, Bleye LA, Novak JS. The protein tyrosine phosphatase LAR has a major impact on insulin receptor dephosphorylation. Biochem Biophys Res Commun. 27;235(3)(June 1997): 709-12.
- [96] Li PM, Zhang WR, Goldstein BJ. Suppression of insulin receptor activation by overexpression of the protein-tyrosine phosphatase LAR in hepatoma cells. Cell Signal. 8(7)(November 1996): 467-73.
- [97] Ren JM, Li PM, Zhang WR, Sweet LJ, Cline G, Shulman GI, et al. Transgenic mice deficient in the LAR protein-tyrosine phosphatase exhibit profound defects in glucose homeostasis. Diabetes. 47(3)(March 1998): 493-7.

- [98] Zabolotny JM, Kim YB, Peroni OD, Kim JK, Pani MA, Boss O, et al. Overexpression of the LAR (leukocyte antigen-related) protein-tyrosine phosphatase in muscle causes insulin resistance. Proc Natl Acad Sci U S A. 24;98(9)(April 2001): 5187-92.
- [99] Zhang JS, Longo FM. LAR tyrosine phosphatase receptor: alternative splicing is preferential to the nervous system, coordinated with cell growth and generates novel isoforms containing extensive CAG repeats. J Cell Biol. 128(3)(February 1995): 415-31.
- [100] Zhang JS, Honkaniemi J, Yang T, Yeo TT, Longo FM. LAR tyrosine phosphatase receptor: a developmental isoform is present in neurites and growth cones and its expression is regional- and cell-specific. Mol Cell Neurosci. 10(5-6)(April 1998): 271-86.
- [101] Yeo TT, Yang T, Massa SM, Zhang JS, Honkaniemi J, Butcher LL, et al. Deficient LAR expression decreases basal forebrain cholinergic neuronal size and hippocampal cholinergic innervation. J Neurosci Res. 1;47(3)(February 1997): 348-60.
- [102] Krueger NX, Van Vactor D, Wan HI, Gelbart WM, Goodman CS, Saito H. The transmembrane tyrosine phosphatase DLAR controls motor axon guidance in *Drosophila*. Cell. 23;84(4)(February 1996): 611-22.
- [103] Bernabeu R, Yang T, Xie Y, Mehta B, Ma SY, Longo FM. Downregulation of the LAR protein tyrosine phosphatase receptor is associated with increased dentate gyrus neurogenesis and an increased number of granule cell layer neurons. Mol Cell Neurosci. 31(4)(April 2006): 723-38.
- [104] Honkaniemi J, Zhang JS, Yang T, Zhang C, Tisi MA, Longo FM. LAR tyrosine phosphatase receptor: proximal membrane alternative splicing is coordinated with regional expression and intraneuronal localization. Brain Res Mol Brain Res. 18;60(1)(September 1998): 1-12.
- [105] Xie Y, Yeo TT, Zhang C, Yang T, Tisi MA, Massa SM, et al. The leukocyte common antigen-related protein tyrosine phosphatase receptor regulates regenerative neurite outgrowth in vivo. J Neurosci. 15;21(14)(July 2001): 5130-8.

- [106] Van der Zee CE, Man TY, Van Lieshout EM, Van der Heijden I, Van Bree M, Hendriks WJ. Delayed peripheral nerve regeneration and central nervous system collateral sprouting in leucocyte common antigen-related protein tyrosine phosphatase-deficient mice. Eur J Neurosci. 17(5)(March 2003): 991-1005.
- [107] Johnson KG, McKinnell IW, Stoker AW, Holt CE. Receptor protein tyrosine phosphatases regulate retinal ganglion cell axon outgrowth in the developing *Xenopus* visual system. J Neurobiol. 5;49(2)(November 2001): 99-117.
- [108] Tamura K, Dudley J, Nei M, Kumar S. MEGA4: Molecular Evolutionary Genetics Analysis (MEGA) software version 4.0. Mol Biol Evol. 24(8)(August 2007): 1596-9.
- [109] Miscio G, Tassi V, Coco A, Soccio T, Di Paola R, Prudente S, et al. The allelic variant of LAR gene promoter -127 bp T-->A is associated with reduced risk of obesity and other features related to insulin resistance. J Mol Med. 82(7)(July 2004): 459-66.
- [110] Saitou N, Nei M. The neighbor-joining method: a new method for reconstructing phylogenetic trees. Mol Biol Evol. 4(4)(July 1987): 406-25.
- [111] Felsenstein J. Confidence limits on phylogenies: An approach using the bootstrap. Evolution. 39(4)(1985): 783-91.
- [112] Tamura K, Nei M, Kumar S. Prospects for inferring very large phylogenies by using the neighbor-joining method. Proc Natl Acad Sci U S A. 27;101(30)(July 2004): 11030-5.
- [113] Eck R, Dayhoff M. Atlas of Protein Sequence and Structure. National Biomedical Research Foundation, Silver Springs, Maryland; 1996.
- [114] Nei M, Kumar S. Molecular Evolution and Phylogenetics. New York: Oxford University Press; 2000: 333.
- [115] Ishida LH, Alves HR, Munhoz AM, Kaimoto C, Ishida LC, Saito FL, et al. Athelia: case report and review of the literature. Br J Plast Surg. 58(6)(September 2005): 833-7.
- [116] Alcon Saez JJ, Elia Martinez MA, Elia Martinez I, Pont Colomer M, Lurbe Ferrer E. [Amastia and athelia as an exceptional presentation of hypohydrotic ectodermal

- dysplasia in an adolescent female]. An Pediatr (Barc). 69(3)(September 2008): 289-90.
- [117] Podolski J, Byrski T, Zajaczek S, Druck T, Zimonjic DB, Popescu NC, et al. Characterization of a familial RCC-associated t(2;3)(q33;q21) chromosome translocation. J Hum Genet. 46(12)(2001): 685-93.
- [118] Kleinjan DA, van Heyningen V. Long-range control of gene expression: emerging mechanisms and disruption in disease. Am J Hum Genet. 76(1)(January 2005): 8-32.
- [119] Ruhe JE, Streit S, Hart S, Ullrich A. EGFR signaling leads to downregulation of PTP-LAR via TACE-mediated proteolytic processing. Cell Signal. 18(9)(September 2006): 1515-27.



ศูนย์วิทยทรัพยากร
จุฬาลงกรณ์มหาวิทยาลัย



APPENDICES

ศูนย์วิทยทรัพยากร
จุฬาลงกรณ์มหาวิทยาลัย

APPENDIX A
BUFFER AND REAGENT

1. LB Agar

Agar	15	g
<input type="checkbox"/> Tryptone	10	g
<input type="checkbox"/> Yeast extract	5	g
<input type="checkbox"/> NaCl	10	g
<input type="checkbox"/> Chloramphenicol (200mg/ml)	62.5	μl
or Kanamycin (200mg/ml)	125	μl
Distilled water to volume	1,000	ml

Sterilize the solution by autoclaving and store at 4°C.

2. LB Broth

Tryptone	10	g
<input type="checkbox"/> Yeast extract	5	g
<input type="checkbox"/> NaCl	10	g
<input type="checkbox"/> Chloramphenicol (200mg/ml)	62.5	μl
or Kanamycin (200mg/ml)	125	μl
Distilled water to volume	1,000	ml

Sterilize the solution by autoclaving and store at 4°C

3. P1 Solution

Glucose	9.008	g
<input type="checkbox"/> Tris base	3.03	g
<input type="checkbox"/> EDTA.2H ₂ O	3.72	g

Dissolve in distilled water and adjusted pH to 8.0 with 1M NaOH

Distilled water to volume	1000	ml
---------------------------	------	----

Sterilize the solution by autoclaving

Add RNase (100mg/ml)	1	ml
----------------------	---	----

Store at 4°C

4. P2 Solution

NaOH	8	g
SDS	1	g
Distilled water to volume	1000	ml

Sterilize the solution by autoclaving and store at room temperature.

5. P3 Solution

5 M potassium acetate	60.0	ml
<input type="checkbox"/> Glacial acetic acid	11.5	ml
Distilled water to volume	100	ml

Sterilize the solution by autoclaving and store at 4°C.

6. 20X SSC

NaCl	175.2	g
<input type="checkbox"/> Sodium Citrate	88.2	g
<input type="checkbox"/> Dissolve in distilled water and adjusted pH to 7.4		
Distilled water to volume	1000	ml

Sterilize the solution by autoclaving and store at room temperature

7. 5% Tween 20

TWEEN 20	5	ml
Distilled water to volume	100	ml

Mix the solution and store at room temperature.

8. 2X SSC

20X SSC	50	ml
Distilled water to volume	500	ml

Mix the solution and store at room temperature.

9. 2X SSC/0.05% Tween 20

20X SSC	50	ml
<input type="checkbox"/> 5 % TWEEN 20	5	ml

Distilled water to volume	500	ml
---------------------------	-----	----

Mix the solution and store at room temperature.

10. 0.4X SSC

20X SSC	10	ml
---------	----	----

Distilled water to volume	500	ml
---------------------------	-----	----

Mix the solution and store at room temperature.

11. DAPI Working

4,6-Diamino-2-Phenylene (DAPI)	100	μ l
--------------------------------	-----	---------

Antifade	200	μ l
----------	-----	---------

Distilled water to volume	1	ml
---------------------------	---	----

Mix the solution and store at at -20°C .

12. Antifade

DABCO (1,4 diazabicyclo(2.2.2) octane)	0.233	g
--	-------	---

<input type="checkbox"/> 87% Glycerol	9	ml
---------------------------------------	---	----

<input type="checkbox"/> Tris-HCl pH 8.0	200	μ l
--	-----	---------

<input type="checkbox"/> Distilled water	800	μ l
--	-----	---------

Mix the solution and store at at -20°C .

13. 3M NaOAc

Sodium Acetate $3\text{H}_2\text{O}$	408.3	g
--------------------------------------	-------	---

Dissolve in distilled water and adjusted pH to 7.0

Distilled water to volume	1000	ml
---------------------------	------	----

Sterilize the solution by autoclaving and store at room temperature.

14. Hybridization solution

Drextane sulfate	1	g
------------------	---	---

Formamide	5	ml
-----------	---	----

<input type="checkbox"/> 20X SSC	1	ml
----------------------------------	---	----

Distilled water to volume	10	ml
---------------------------	----	----

Filtered through a 0.45- μm and stored at 4 °C

15. Lysis I buffer

Sucrose	109.54	g
1 M Tris-HCl (pH 7.5)	10	ml
1M MgCl ₂	5	ml
Triton X-100	10	ml
Distilled water to volume	1,000	ml

Sterilize the solution by autoclaving and store at 4°C.

16. 1 M Tris-HCl (pH 7.5)

Tris base	12.11	g
-----------	-------	---

Dissolve in distilled water and adjusted pH to 7.5 with HCl (conc)

Distilled water to volume	100	ml
---------------------------	-----	----

Sterilize the solution by autoclaving and store at room temperature.

17. 1 M MgCl₂

MgCl ₂ .6H ₂ O	20.33	g
Distilled water to volume	100	ml

Sterilize the solution by autoclaving and store at room temperature.

18. Proteinase K

Proteinase K	20	mg
Distilled water to volume	1	ml

Mix the solution and store at -20°C.

19. 10X TBE buffer

Tris-base	108	g
Boric acid	55	g
0.5 M EDTA (pH 8.0)	40	ml
Distilled water to volume	1,000	ml

Mix the solution and store at room temperature.

20. 6X loading dye

Ficoll 400	15	g
Bromphenol blue	0.25	g
Xylene cyanol	0.25	g
1 M Tris (pH 8.0)	1	ml
Distilled water to volume	100	ml

Mix well and store at room temperature.

21. RIPA lysis Buffer

1M Tris-HCl (pH 8.8)	25	ml
1M NaCl	75	ml
100% Nonidet-P40	5	ml
10% Sodium Deoxycholate	25	ml

Mix the solution and store at at 4°C.

22. 6X Sample buffer

1M Tris-HCl (pH 6.8)	3	ml
SDS	1.2	g
100% Glycerol	6	ml
Bromphenol Blue	0.03	g
Distilled water to volume	10	ml

Mix the solution and store at at 4°C.

Before use add 24% 2-mercaptoethanol (Stock is 14.2 M, Working is 864 mM) or add 30 μ l in 6X Sample buffer stock 470 μ l

23. 10X PBS

NaCl	80	g
Na ₂ HPO ₄	2	g

KCl	14.4	g
KH ₂ PO ₄	2.4	g
Distilled water to volume	1,000	ml

Mix to dissolve and adjust pH to 7.4

Sterilize the solution by autoclaving and store at room temperature.

24. 10X TBS

Tris base	61	g
NaCl	90	g
Distilled water to volume	1,000	ml

Mix to dissolve and adjust pH to 7.6

Sterilize the solution by autoclaving and store at room temperature.

25. 8% SDS polyacrylamide gel electrophoresis (SDS-PAGE)

Resolving gel (10 ml)

40% Acrylamide:Bis (37.5:1)	2	ml
1 M Tris-HCl (pH 8.8)	2.5	ml
10% SDS	0.1	ml
10% (NH ₄) ₂ S ₂ O ₈	0.1	ml
TEMED	0.01	ml
Distilled water	5.29	ml

Stacking gel (10 ml)

40% Acrylamide:Bis (37.5:1)	1	ml
0.5 M Tris-HCl (pH 6.8)	2.5	ml
10% SDS	0.1	ml
10% (NH ₄) ₂ S ₂ O ₈	0.1	ml
TEMED	0.01	ml
Distilled water	4.29	ml

26. 1 M Tris-HCl (pH 8.8)

Tris base	12.11	g
-----------	-------	---

Dissolve in distilled water and adjusted pH to 8.8 with HCl (conc)

Distilled water to volume	100	ml
---------------------------	-----	----

Sterilize the solution by autoclaving and store at room temperature.

27. 0.5 M Tris-HCl (pH 6.8)

Tris base	6.055	g
-----------	-------	---

Dissolve in distilled water and adjusted pH to 6.8 with HCl (conc)

Distilled water to volume	100	ml
---------------------------	-----	----

Sterilize the solution by autoclaving and store at room temperature.

28. 10X Tris-glycine (pH 8.3)

Tris base	6.055	g
-----------	-------	---

Glycine	147.1372	g
---------	----------	---

Dissolve in distilled water and adjusted pH to 8.3

Distilled water to volume	1,000	ml
---------------------------	-------	----

Sterilize the solution by autoclaving and store at room temperature.

29. Running Buffer

10X Tris-glycine (pH 8.3)	100	ml
---------------------------	-----	----

10% SDS	10	ml
---------	----	----

Distilled water	890	ml
-----------------	-----	----

Mix the solution and store at room temperature.

30. Transfer buffer

10X Tris-glycine (pH 8.3)	100	ml
---------------------------	-----	----

Methanol	200	ml
----------	-----	----

Distilled water	800	ml
-----------------	-----	----

Mix the solution and store at room temperature.

31. % Non Fat Dry Milk (NFDM)

Non Fat Dry Milk	2.5	g
------------------	-----	---

Adjust with 0.01% TBST to	50	ml
---------------------------	----	----

Mix well and store at 4°C

32. 10% SDS solution

Sodium dodecyl sulfate	10	g
Distilled water to volume	100	ml

Mix the solution and store at room temperature.

33. 10% Ammoniumpersulphate ($(\text{NH}_4)_2\text{S}_2\text{O}_8$)

$(\text{NH}_4)_2\text{S}_2\text{O}_8$	1	g
Distilled water to volume	10	ml

Mix well and store at 4°C



ศูนย์วิทยทรัพยากร
จุฬาลงกรณ์มหาวิทยาลัย

APPENDIX B

GLOSSARY

Balanced chromosomal translocation: an exchange between part of nonhomologous chromosome where there is no gain or loss of genetic material.

Amastia: refers to a condition where breast tissue, nipple, and areola are absent, either congenitally or iatrogenically.

Athelia: is the congenital absence of one or both nipples. It is a rare condition. It sometimes occurs on one side in children with the Poland sequence and on both sides in certain types of ectodermal dysplasia.

Amazia: refers to a condition where mammary gland is absent while the nipple and areola remain present.

Ectodermal dysplasia: are described as "heritable conditions in which there are abnormalities of two or more ectodermal structures such as the hair, teeth, nails, sweat glands, cranial-facial structure, digits and other parts of the body.

Poland's syndrome: is a rare birth defect characterized by underdevelopment or absence of the chest muscle (pectoralis) on one side of the body and (but not always) webbing of the fingers (cutaneous syndactyly) of the hand on the same side (ipsilateral hand) mostly common on the right side of body and found more in males than females.

Finlay-Marks syndrome: In 1978, Finlay and Marks described the association of scalp defect, malformed ears, and absence of nipples in a family. The association is also known as scalp-ear-nipple syndrome.

Dentinogenesis Imperfecta: is a genetic disorder of tooth development. This condition causes teeth to be discolored (most often a blue-gray or yellow-brown color) and translucent. Teeth are also weaker than normal, making them prone to rapid wear, breakage, and loss.

BIOGRAPHY

Name	Ms.Surasawadee Ausavarat
Date of birth	November 14 th , 1983
Place of birth	Bangkok, Thailand

Education

She received her bachelor degree with a second class honor in Medical Technology from Faculty of Allied Health Science, Chulalongkorn University in 2003. She got a Royal Golden Jubilee (RGJ) Ph.D. Scholarship from the Thailand Research Fund (TRF) and participated in Interdepartment of Biomedical Sciences, Faculty of Graduate School, Chulalongkorn University since 2004.

Research Grants

1. 90's Anniversary Chulalongkorn University, Rachadaphisek Somphot Grants, Chulalongkorn University, Bangkok, Thailand.
2. The Royal Golden Jubilee Ph.D Program, Thailand Research Fund (TRF).

Publications

1. Absence of breast development and deficiency of PTPRF. Ausavarat S, Tongkobpetch S, Praphanphoj V, Mahatumarat C, Rojvachiranonda N, Snabboon T, Markello TC, Gahl WA, Suphapeetiporn K, Shotelersuk V. (manuscript in preparation)
2. Novel mutations in the STK11 gene in Thai patients with Peutz-Jeghers syndrome. Ausavarat S, Loeyklang P, Vejchapipat P, Chongsrisawat V, Suphapeetiporn K, Shotelersuk V. World J Gastroenterol. (accepted)
3. Two novel EBP mutations in Thai patients with Conradi-Hünemann-Happle syndrome. Ausavarat S, Tanpaiboon P, Tongkobpetch S, Suphapeetiporn K, Shotelersuk V. Eur J Dermatol. 2008 Jul-Aug;18(4):391-3.
4. A novel mutation in EFNB1, probably with a dominant negative effect, underlying craniofrontonasal syndrome. Shotelersuk V, Siriwan P, Ausavarat S. Cleft Palate Craniofac J. 2006 Mar;43(2):152-4.